A NON-ITERATIVE METHOD FOR URBAN TRAFFIC SIGNAL TIMING

Dissertation for the Degree of Ph. D.

MICHIGAN STATE UNIVERSITY

GAIL HAROLD GROVE

1977

This is to certify that the

thesis entitled

A Non-Iterative Method for Urban Traffic
Signal Timing

presented by

Gail Harold Grove

has been accepted towards fulfillment
of the requirements for
Doctor of Philosophy degree in Systems Science

John B. Kreer
Major professor

Date July 19, 1977

ABSTRACT

A NON-ITERATIVE METHOD
FOR URBAN TRAFFIC SIGNAL TIMING

By

Gail Harold Grove

The primary objective of this research was to improve the basic TRANSYT traffic network signal timing method by replacing Robertson's time consuming hill-climbing optimization process with a much faster and thus less costly running non-iterative split and offset calculation technique.

The TRANSYT/G splits were obtained by using differential calculus methods on the network objective function. This objective function was constructed of tractable approximations to the stops, uniform and random delay terms for each link within the network.

The TRANSYT/G offsets were determined from the Morgan and Little maximal bandwidth offsets modified so as to include: an improved apportionment of unequal directional bandwidths, queue growth and decay allowances by means of partial excess green shifts, and an application to networks.

Gail Harold Grove

Based upon the results of testing two data sets from Ft. Wayne, Indiana and Washington, D.C., it was concluded that:

1. This author's split estimation method is superior to Robertson's in terms of lower objective function and higher system speed values. This is true for its use in both TRANSYT/G for on-line control applications and in TRANSYT for more accurate off-line signal timing optimization studies, and,
2. TRANSYT/G's vastly improved computer running time versus TRANSYT makes it a potential candidate for an on-line signal timing control method.

A secondary result of this research was the development of a finite traffic queue dispersion model for use in off-line simulation studies requiring a more accurate model than the infinite queue version presently being used in TRANSYT.

A NON-ITERATIVE METHOD
FOR URBAN TRAFFIC SIGNAL TIMING

By

Gail Harold Grove

A DISSERTATION

Submitted to
Michigan State University
in partial fulfillment of the requirements
for the degree of

DOCTOR OF PHILOSOPHY

Department of Electrical Engineering and
Systems Science

1977

G1069964

ACKNOWLEDGEMENTS

I wish to thank my major Professor, Dr. John B. Kreer for his many helpful suggestions and guidance throughout my research and my committee members for their timely review of this dissertation.

A special thank you is to be extended to my wife Sandra for her patience and continual encouragement during the many months of this research effort.

TABLE OF CONTENTS

LIST OF TABLES

LIST OF FIGURES

Figure		Page

LIST OF SYMBOLS

F = the network objective function,

F_j = the objective function for the j^{th} link,

f_i = the objective function for the i^{th} node,

S_j = the vehicle stops per second on the j^{th} link,

D_j = the vehicular uniform delay on the j^{th} link,

R_j = the vehicular random delay on the j^{th} link,

W_j = the delay weighting factor on the j^{th} link,

K = the link stop penalty factor,

t_{gj} = the start of the green inverval for the j^{th} link,

t_{aj} = the start of the amber interval for the j^{th} link,

t_{rj} = the start of the red interval for the j^{th} link,

t_{ej} = the time when the queue length first decays to zero for the j^{th} link,

$i_j(t)$ = the arrival flow rate for the j^{th} link,

$o_j(t)$ = the departure flow rate for the j^{th} link,

G_j = the green interval saturation flow rate for the j^{th} link,

$I_j(t)$ = the cumulative number of arrivals at time t on the j^{th} link,

$O_j(t)$ = the cumulative number of departures at time t on the j^{th} link,

$Q_j(t)$ = the queue length at time t on the j^{th} link,

C = the cycle length,

A = the platoon dispersion or smoothing factor,

t = the travel time down a link,

t_{ave} = the average travel time,

$E(T)$ = the expected travel time,

X_j = the degree of saturation on the j^{th} link,

T_o = the oversaturation time allowed,

m_j = the random delay slope in the oversaturation region for the j^{th} link,

C_o = the optimum cycle length,

L = the total lost time per cycle,

L_A = the lost time for the primary phase,

Y_j = the ratio of maximum directional flow to saturation flow for the j^{th} phase,

$\bar{g}_j$ = the minimum green time for the j^{th} phase,

φ_j = the j^{th} phase,

s_i = the normalized signal split for the i^{th} node,

$\bar{s}_i$ = the integer valued signal split for the i^{th} node,

$\hat{s}_i$ = the near-optimum normalized split for the i^{th} node,

k_j = the bounds on the integer value split,

g_j = the sum of the amber and minimum green times for the j^{th} phase,

IN_j = the uniform arrival flow rate on the j^{th} link,

IN_{jk} = the uniform arrival flow rate on the j^{th} link during the k^{th} half cycle,

c_j = the capacity efficiency of the j^{th} link,

c_{jk} = the capacity efficiency of the j^{th} link during the k^{th} half cycle,

h_j = the ratio of total arrivals to G_jC on the j^{th} link,

ℓ_i = the number of links terminating at the i^{th} node

t_{ij} = the start of the i^{th} time interval for the j^{th} phase,

t_{ijk} = the start of the i^{th} time interval for the j^{th} phase during the k^{th} half cycle,

s_{ij} = the j^{th} phase split for the i^{th} node,

K_{1j}, K_{2j} = the random delay approximation constants for the j^{th} link,

$\overline{S}_i$ = the weighted sum of stops for the i^{th} node,

$\overline{D}_i$ = the weighted sum of uniform delays for the i^{th} node,

$\overline{R}_i$ = the weighted sum of random delays for the i^{th} node,

L_{kj} = the second partial derivatives of the f_i with respect to the s_{ij},

$\underline{S}_i$ = the phase split vector for the i^{th} node,

r_j = the red time for the j^{th} node,

$b(\bar{b})$ = the outbound (inbound) directional bandwidth,

x_j = the location of the j^{th} node downstream from the reference point,

$v_j(\bar{v}_j)$ = the outbound (inbound) vehicle speed along the j^{th} link,

$\tau_{ij}(\bar{\tau}_{ij})$ = the travel time from the i^{th} node to the j^{th} node in the outbound (inbound) direction,

θ_{ij} = the relative offset from the i^{th} node to the j^{th} node measured between the center of the red intervals of the two nodes,

g = the minimum green for the set of nodes along an arterial,

α_j = the offset shift of the j^{th} node for unequal directional bandwiths,

$p(\bar{p})$ = the outbound (inbound) platoon length,

$\bar{h}_j$ = the ratio of total arrivals to G_j on the j^{th} link,

B = the maximum equal bandwith,

β_{cj} = the queue clearance offset shift of the j^{th} node relative to the critical node,

$\gamma_{cj}(\bar{\gamma}_{cj})$ = the excess green to the right of the rear edge of the outbound (inbound) bandwidth for the j^{th} node relative to the critical node,

$\mu(\bar{\mu})$ = the outbound (inbound) average cumulative arrivals,

ϕ_{cj} = the TRANSYT/G offset for the j^{th} node relative to the critical node,

P_n = the steady state time-independent probability of n vehicles being in the system,

λ = the ratio of the queue arrival rate to the service rate,

N = the finite maximum number of vehicles in the queue,

$Z_n(\theta)$ = the probability generating function for the discrete distribution of a finite maximum allowable queue length,

$E(n)$ = the expected number of vehicles in the queue,

σ^2 = the variance of $E(n)$.

CHAPTER I

INTRODUCTION

1.1 Benefits of Improved Urban Traffic Flow

Modern society has become more time conscious in its day to day activities, especially when commuting between home, work, and recreation areas. As a result, man is intolerant of unnecessary delay in his travel. A significant portion of our population must contend with driving through urban areas having considerable congestion of vehicles. Thus, one of the primary duties of a transportation engineer or planner is to improve traffic flow through our cities by decreasing vehicle travel time.

In light of our energy shortage, it has become increasingly important to reduce the amount of vehicle stop and go movement which wastes so much of our dwindling fuel supply. Virginia engineers (CR1) claim a potential savings of 125,000 gallons per day for a computer controlled network of 400 signals in Washington, D.C. Based upon sixty cents per gallon, this savings could be $75,000/day in this area alone.

Increasing traffic densities in urban areas, limited space for additional roadways, and the escalating cost of roadway construction make it mandatory to undertake research which contributes to the efficient utilization of our existing urban roadway facilities. The research described in this thesis is directed towards increasing the efficient use of our existing urban street networks, while simultaneously providing improved service to the drivers. This has been accomplished by the development of a real-time algorithm for calculating traffic signal synchronizations which could be used for on-line computer control of an urban network of signalized intersections.

1.2 Previous Signal Timing Optimization Procedures

In Hillier's delay-difference method (HI1), he considered tree or ladder-type networks which could be simplified into a single link by combining links in parallel and in series. The objective was the minimization of delay in each link where flows were considered uniform. The delay on a link was assumed to be a function of the offsets of the two signals at the ends of this link and is independent of all other network offsets. This algorithm calçulates the sum of the two directional delays by varying the integer valued offsets and selects the offset minimizing the sum of the two delays. This method appears time consuming for calculating the offset for a single link but has the advantage that computations increase linearly with the number of links unlike most other models.

Allsop extended Hillier's work to general non-simplifiable grid networks (AL1) and later used a dynamic programming concept which minimizes the total delay and gives a global minimum (AL2). However, this technique is too slow to be used for real-time control of medium sized networks of approximately 50 intersections.

Inose, et al. (IN1) developed an algorithm applicable only to tree networks in which the common cycle time is selected as the maximum of the individual, ideal intersection cycle times assuming uniform arrivals at isolated intersections. Splits are then selected by minimization of delay while offsets are calculated as a function of the heavier of the directional vehicle volumes on the links connecting each pair of nodes. Inose, et al., assume no turning movements and no platoon dispersion. Any link which would form a closed loop of links within the network is not used in the offset calculations, thus restricting application to tree networks. This method is simple and effective provided that there are very few turning movements. It is unlikely that the total delay is minimized.

SIGOP (TR1) was the first systematic signal timing optimization program applicable to a general network. The length of each split phase for a signal is set proportional to the total or critical flow in each phase.

The total flow was considered to be the sum over all lanes and approaches while the critical flow was the maximum noted per lane through the given node. The optimization procedure determines the offset differences for each link and optimal offsets for the entire network. The objective function is a linear combination of stops and delays. An n by n matrix inversion is required, where n equals the number of nodes. Two deficiencies are apparent in SIGOP. First, the offset optimization procedure produces a local optimum rather than a global optimum. Second, since the stochastic effects on each link are ignored, the lower bound on cycle time is selected as the optimum especially whenever the capacities of the signalized intersections are approached.

Shortly, thereafter, Robertson (RO1) developed a more sophisticated model and more effective optimization process called TRANSYT. A detailed description will be found in Chapter II. TRANSYT has been field tested in London and Glasgow with favorable results.

Kaplan and Powers (KP1) presented a comparison of SIGOP and TRANSYT as applied in San Jose and Glasgow; each area having high signal density. They concluded that:

1. There is no measurable difference between SIGOP and TRANSYT for short cycle times,

2. Double cycled TRANSYT produced travel times which were 5 percent less than SIGOP and single cycled TRANSYT in the Glasgow network, and

3. The TRANSYT model appeared more accurate in predicting travel times.

For more details on these earlier algorithms, Munjal and Hsu's comparative study (MH1) is an excellent summary of the state-of-the-art circa 1972. Since this time, several other signal timing methods have appeared in the literature.

Messer et al. (MW1) have applied a variable sequence, multiphase, progression optimization program to the real-time control of a Dallas, Texas arterial. Good progressions were obtained and no apparent problems due to variable phase sequencing were experienced in this pilot study.

Gartner (GA1) confirmed by direct field observations on a major Toronto arterial that his microscopic flow pattern analysis reduced traffic delay.

Gartner and Little (GL1) presented a dynamic programming approach to obtain the splits and offsets of a general network. They extended Hillier's combination method to general networks. Actual field evaluations were being planned at the time of their article.

Lieberman and Woo's SIGOP II (LW1) is composed of a flow model and a dynamic programming methodology which minimizes an objective function composed of vehicle delay, stops, and excess queue length. Turning movements, lane channelization, multiphase control, signal split constraints, platoon disperson (from TRANSYT), and short term volume variations are included. SIGOP II is claimed to possess computational speed which varies linearly with the number of nodes and is somewhat slower than SIGOP but faster than TRANSYT. However, it appears that program tapes and the field validation are incomplete at this time.

Even though this review of previous contributions was brief, it should be noted that a vast amount of time and effort has been expended by many researchers and that many volumes are devoted to their results. However, one should proceed onward to the preview of this author's work.

1.3 Preview

Chapter II describes the objective function, the traffic flow model and the optimization procedure of the existing TRANSYT computer program. The variables utilized in the optimization of the objective function are the individual signal splits and the offsets between the signals comprising the network. Appendix A contains a derivation of the dispersion of traffic queues and an extension to finite queue lengths.

The main body of this author's research comprises Chapters III and V. Chapter III is a detailed derivation of the near-optimum split calculation employed in TRANSYT/G. Chapter IV is a brief description of arterial offsets, while Chapter V details the TRANSYT/G offset method. The offsets are determined from an extension of the Morgan-Little maximal bandwidth concept. Both splits and offsets are calculated in a non-iterative fashion, thus vastly reducing the computer run time and cost as compared to the existing TRANSYT model.

Portions of the Ft. Wayne, Indiana and the Washington, D.C. downtown areas were selected for a comparison of the improved TRANSYT/G program versus the TRANSYT program. Chapter VI contains the two network applications while Appendix B includes general computer program flow charts and listings.

Conclusions and suggested future research objectives are included in Chapter VII.

CHAPTER II

THE TRANSYT MODEL

The mathematical model characterizing traffic flow is composed of a set of expressions or equations representing the traffic dynamics and its ultimate control based upon the network's physical configuration and the behavior of the traffic operating within its boundaries.

For control purposes, we desire a model capable of providing information of significant detail for the calculation of the selected traffic signal timing variables. However, it must not be so detailed that it is incapable of real-time computer speeds encountered in on-line control situations.

The Traffic Network Study Tool (TRANSYT) developed by Robertson (RO1, RO2) is a method of optimizing traffic signal settings using an off-line computer model of the known network system conditions. It is composed of three main elements:

1. A network objective function for ranking different sets of signal settings,

2. A traffic flow model used solely for generating a value of the objective function for a given set of signal timings, vehicle flows and network geometry, and

3. A hill-climbing optimization process that alters the signal settings and determines if the objective function has been reduced or not.

Before proceeding further on this subject some terminology must be defined. In an urban traffic network which is being modeled, each signalized intersection will be represented by a node and each significant directional traffic stream leading into an intersection will be represented by a link. This concept of a link applies to special bus-only lanes, pedestrian crossings and heavy flow left turn lanes in addition to the normal through traffic lanes. In a network, one traffic signal is usually chosen as the reference signal. Then the phasing of any other network signal is determined by the time interval between the centers of the main street reds of the two signals under consideration. This interval ranges from zero up to the cycle length and is called the offset. The other parameter of interest is the split, defined as the ratio of the main street green and amber time intervals to the cycle length. The synchronization problem requires the specification of a split and offset for each signal in the network such that some predetermined objective will be achieved.

2.1 Objective Function

In TRANSYT, Robertson defined the overall network function, F, as

$$F = \sum_{j=1}^{\ell} F_j = \sum_{j=1}^{\ell} [KS_j + W_j(D_j + R_j)], \qquad (2.1)$$

where S_j = the vehicle stops per second on the j^{th} link,

K = the stop penalty common to all links in the network,

D_j = the vehicular uniform delay on the j^{th} link,

R_j = the vehicular random delay on the j^{th} link,

W_j = the delay weighting factor on the j^{th} link,

F_j = the objective function for the j^{th} link, and

ℓ = the number of links comprising the network.

A typical urban traffic stream is composed of many different types of vehicles, such as automobiles, various sized trucks, buses and pedestrians, each with their own average speeds. Thus, each link j is allowed to have its own delay weighting factor W_j. In general, most links are assigned unity weighting. However, it may be desirable to have non-unity delay weighting on certain links such as those containing bus-only traffic.

By use of the objective function different sets of signal timings, in this case splits and offsets, can now be compared. The set of timings having the smallest objective function is considered to be the best of those sets investigated.

If a network having n signalized intersections and ℓ links, the stop penalty K and the link delay weighting factors W_j, $j = 1,\ldots,\ell$ are given then the stops, S_j, the uniform and random delays, D_j and R_j respectively, for all ℓ links can be determined from a traffic flow model of the urban traffic network.

2.2 The TRANSYT Flow Model

The major characteristics of vehicular flow in a signalized network are represented in the TRANSYT flow model.

2.2.1 Basic Assumptions

The basic assumptions of the TRANSYT flow model are:

1. All major intersections of the network have traffic signals or are controlled by a priority rule,

2. All of the signals in the network have a common cycle time or one-half of it, commonly referred to as 'double cycling,'

3. Traffic enters the network at a constant specified rate on each approach, and

4. The percentage of vehicle volumes turning at each signalized intersection remains constant throughout the entire cycle.

2.2.2 Flow Histograms

All traffic behavior calculations required for the stops and delay terms are made by manipulation of three types of histograms and representation of individual vehicles is not required. These three flow histograms are:

1. Arrival - the traffic flow histogram that would arrive at the stop line at the end of the link if it were not impeded by a signal at the stop line,
2. Departure - the traffic flow histogram that departs from the stop line of a link, and
3. Saturation - the traffic flow histogram that would leave the stop line if there were enough flow to exceed the intersection's capacity.

The actual flow histogram for any link during any one cycle will vary from the average histogram due to the random nature of individual vehicles and is accounted for in the objective function's random delay term described later in this chapter. The general histogram form is illustrated in Figure 2.1 and is significantly more representative than uniform models such as Figure 2.2.

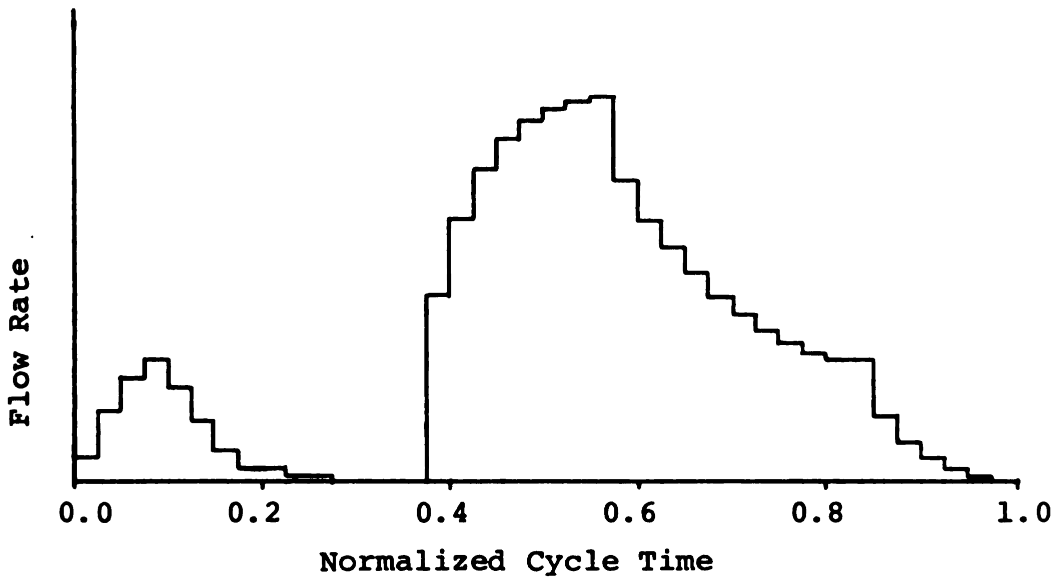

Figure 2.1 A Typical TRANSYT Flow Histogram

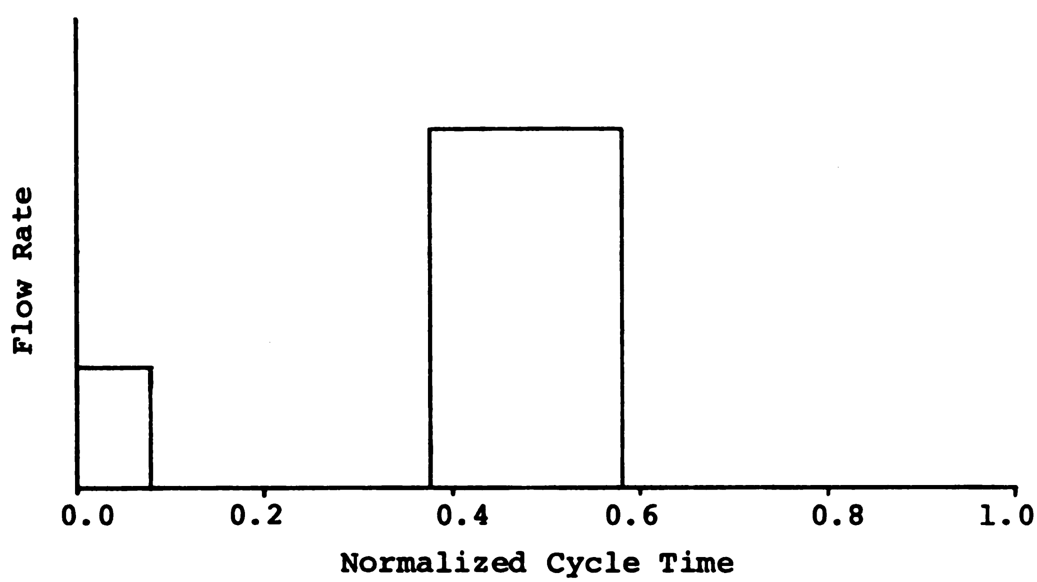

Figure 2.2 A Typical Uniform Flow Histogram

2.2.3 Traffic Queues

Before proceeding further, several definitions are required for the development of the basic queueing process used in the TRANSYT flow model. These definitions for the j^{th} link are:

$i_j(t)$ = the arrival flow rate from the arrival histogram (vehicles/hour),

$o_j(t)$ = the departure flow rate from the departure histogram (vehicles/hour),

G_j = the green interval saturation flow rate from the saturation histogram (vehicles/hour),

$I_j(t)$ = the cumulative number of arrivals at time t,

$O_j(t)$ = the cumulative number of departures at time t,

$Q_j(t)$ = the queue length at time t,

t_{gj} = the start of the green interval,

t_{aj} = the start of the amber interval,

t_{rj} = the start of the red interval,

t_{ej} = the time when the queue length decreases to zero, and

C = the cycle length.

The arrival flow rate for each link during each cycle length spans three different time intervals, namely; the green, the amber, and the red time intervals. Such a representation is illustrated in Figure 2.3, covering two cycle lengths.

The basic cumulative arrival and departure relations are defined as:

$$I_j(t) \equiv \int_{t_{rj}}^{t} i_j(\tau)d\tau, \tag{2.2}$$

and

$$O_j(t) \equiv \int_{t_{rj}}^{t} o_j(\tau)d\tau, \tag{2.3}$$

where $t_{rj} \leq t \leq t_{rj} + C$.

This traffic flow model assumes that the arrivals are periodic, that is; the same arrival histogram is repeated cycle after cycle, thus

$$i_j(t) = i_j(t - nC),\ n = 1,2,\ldots\ . \tag{2.4}$$

Several important requirements of this flow model are that the signalized intersection must not be saturated, namely;

$$I_j(t_{rj} + C) = \int_{t_{rj}}^{t_{rj}+C} i_j(\tau)d\tau < (t_{rj} + C - t_{gj})G_j, \tag{2.5}$$

and that the arrival rate during the green interval does not equal or exceed the saturation flow,

$$i_j(t) < G_j \quad \text{for} \quad t_{gj} \leq t < t_{aj} + C\ . \tag{2.6}$$

Based upon these assumptions, requirements and Figure 2.4, it can be shown that the vehicle flow entering a

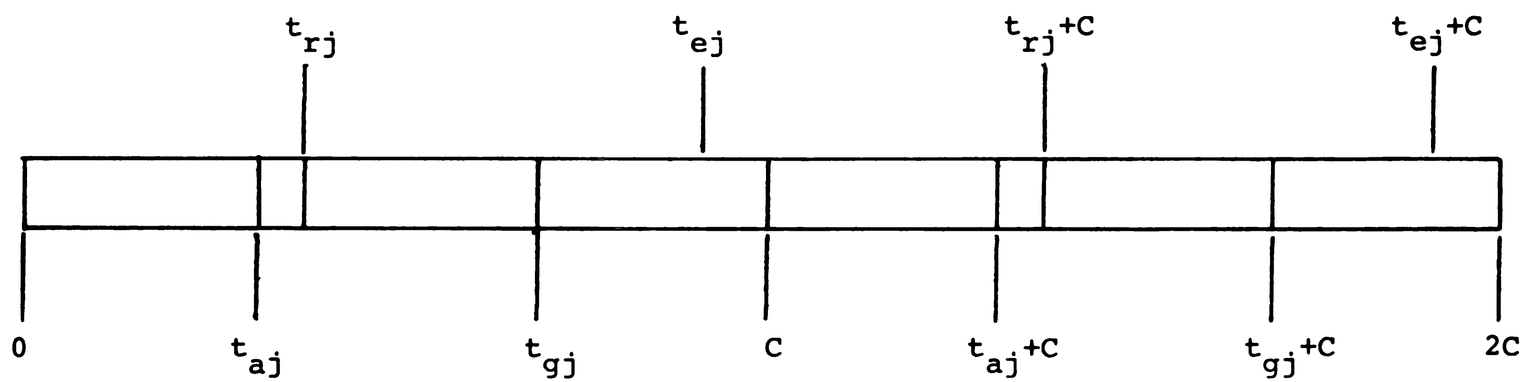

Figure 2.3 Green, Amber, and Red Time Intervals in a Cycle Length

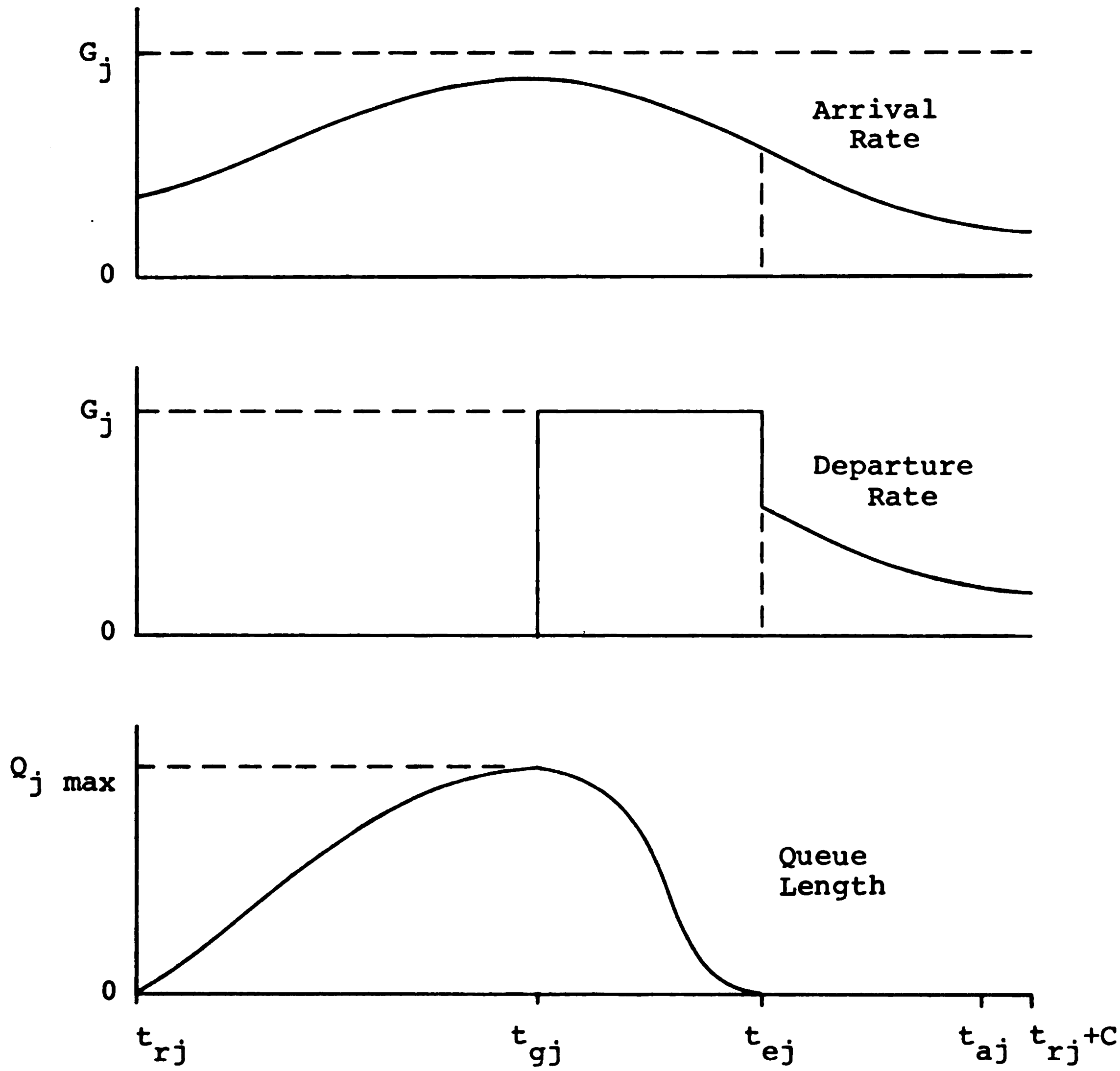

Figure 2.4 Departures and Queue Length for Non-Uniform Arrivals on the j^{th} Link

link also exits that link during a cycle length. Thus, since the queue must clear prior to the end of the green interval, we have

$$O_j(t_{rj} + C) = I_j(t_{rj} + C). \tag{2.7}$$

In a similar manner, all arrivals that have accumulated from the start of the red interval up until the time when the queue decays to zero must depart during the time from the start of the green to the same point when the queue clears. Thus,

$$O_j(t_{ej}) = I_j(t_{ej}) . \tag{2.8}$$

During the remainder of the cycle when there is no queue, the departures equal the arrivals at each point in time, i.e.,

$$o_j(t) = i_j(t) \quad \text{for} \quad t_{ej} \leq t < t_{rj} + C, \tag{2.9}$$

or

$$O_j(t_{rj} + C) - O_j(t_{ej}) = I_j(t_{rj} + C) - I_j(t_{ej}) \tag{2.10}$$

Over the total cycle length, the departure rate can be summarized as

$$o_j(t) = \begin{cases} 0 & \text{for} \quad t_{rj} \leq t < t_{gj} \\ G_j & \text{for} \quad t_{gj} \leq t < t_{ej} \\ i_j(t) & \text{for} \quad t_{ej} \leq t < t_{rj} + C . \end{cases} \tag{2.11}$$

The model requires the treatment of each link and its associated flow histograms for two successive cycle lengths before proceeding to the next link. The first cycle allows for proper development of queues and flow histograms while the second cycle length is used for the calculation of the stops and delays for the objective function. Due to the previously mentioned unsaturated flow assumptions and requirements, the queues will decay to zero and remain zero only once during any one green time interval. Thus the queue is always zero at t_{aj}. This is illustrated in Figure 2.4 and is represented mathematically by

$$Q_j(t) = I_j(t) - O_j(t) = \begin{cases} I_j(t) & t_{rj} \leq t \leq t_{gj} \\ I_j(t) - (t - t_{gj})G_j \quad \text{for} & t_{gj} \leq t \leq t_{ej} \\ 0 & t_{ej} \leq t < t_{rj} + C \end{cases} \tag{2.12}$$

The time at which a queue clears, t_{ej}, can be determined from

$$O_j(t_e) = I_j(t_e) - (t_{ej} - t_{gj})G_j = 0$$

$$\text{for} \quad t_{gj} < t_{ej} < t_{aj} + C \,. \tag{2.13}$$

2.2.4 Platoon Dispersion

The traffic flow into a link is obtained by using the appropriate fraction of the departure histograms representing the turning movement flows from the upstream feeder links. The on-off nature of traffic signal control tends to create moving queues or platoons of vehicles which tend to disperse as they travel away from the traffic signal; this dispersion being due to different individual vehicle speeds.

Based upon his field work, Robertson developed the following empirical platoon dispersion relation for the j^{th} link.

$$i_j(k + t) = Ao_j(k) + (1 - A)i_j(k - 1 + t) \quad (2.14)$$

subject to $Ai_j(k - 1 + t) \geq 1$,

where $o_j(k)$ = the departure flow magnitude of an upstream link during the k^{th} time interval,

$i_j(k + t)$ = the arrival flow magnitude during the $(k + t)$ time interval,

$$t = 0.8E(T), \quad (2.15)$$

$$A = \frac{1}{1 + 0.5t}, \quad (2.16)$$

and $E(T)$ = the expected travel time.

The side constraint on Robertson's equation is required to ensure that the magnitude of flow will decrease as the platoon disperses. If this constraint were violated the sequence $\{i_j(\cdot)\}$ would be monotonically increasing and thus would not be an accurate representation of the actual platoon dispersion phenomenon.

The smoothing factor A is bounded above and below by 1 and 0 respectively and decreases in a negative exponential manner as the travel time, t increases from zero. Thus, this so-called exponential smoothing is a function of the travel time down a link.

A statistical derivation of traffic queues and their dispersion is presented in detail in Appendix A.

As an example of platoon dispersion, consider a portion of an arterial represented by the node-link diagram of Figure 2.5. For the following case:

$i_1(t)$ = 1000 vehicles/hour, for all t

G_1 = 2000 vehicles/hour

t_{r1} = 0 seconds

t_{g1} = 25 seconds

t_{e1} = 50 seconds

C = 60 seconds

t = 5, 10, and 20 seconds.

The $o_1(t)$ departure pattern leaving stopline 1 and the $i_2(t)$ arrival histogram appearing at the downstream stopline 2 were calculated and plotted in Figure 2.6. It should be noted that as the travel time, t, increases, the maximum amplitude of $i_2(t)$ decreases and a longer time is required for $i_2(t)$ to decay to zero. This dispersion mechanism is a basic part of the TRANSYT flow model.

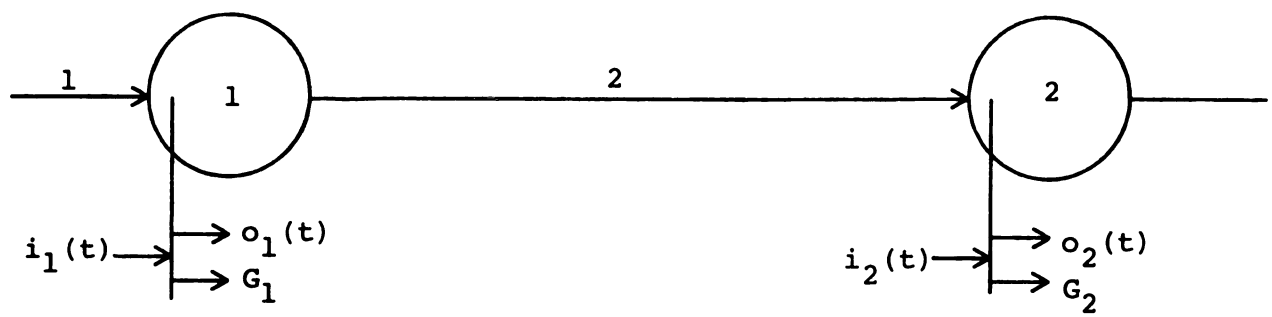

Figure 2.5 Node-Link Diagram and Stoplines

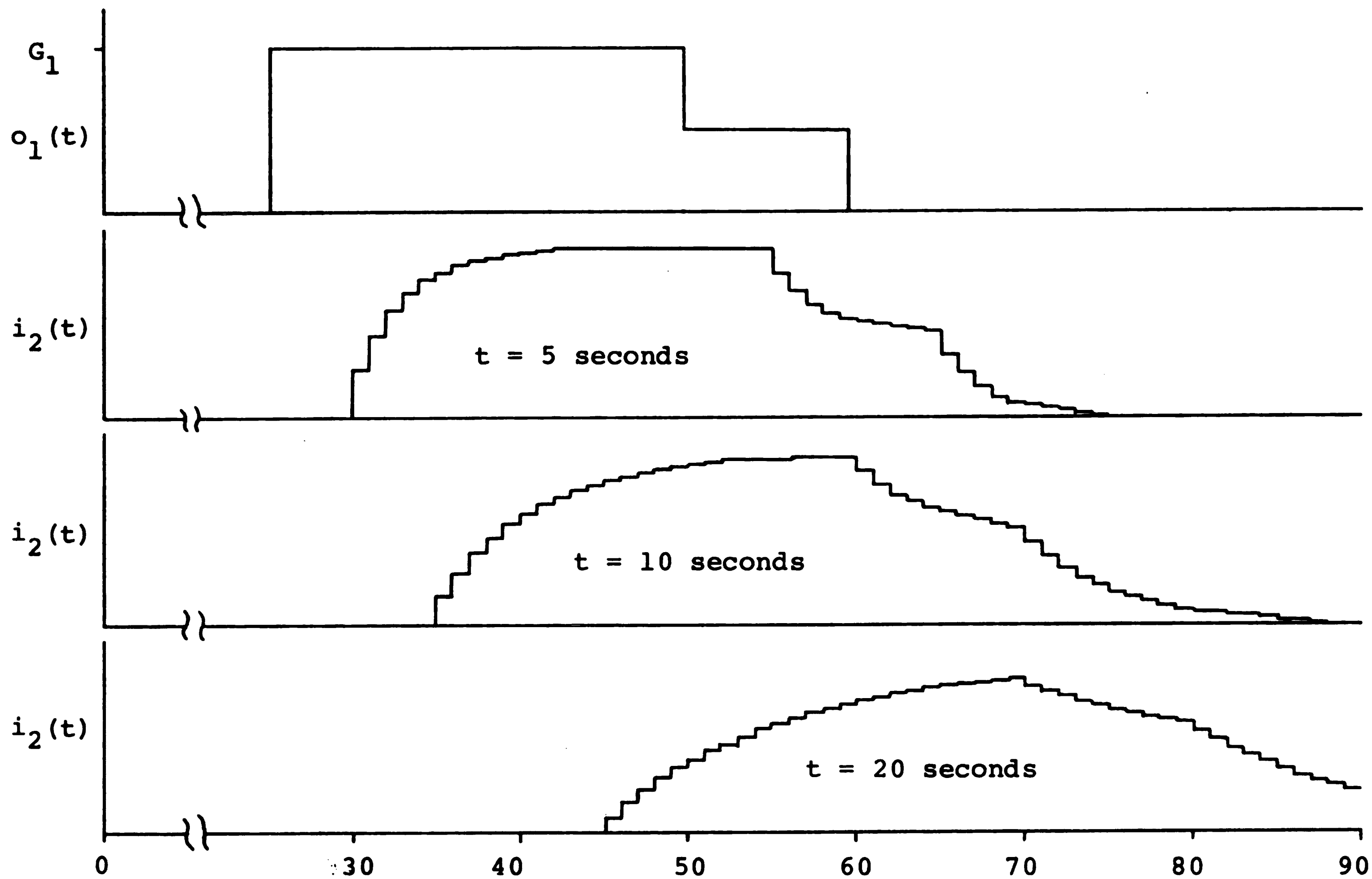

Figure 2.6 Platoon Dispersion as a Function of Travel Time

2.2.5 Stops, Uniform and Random Delays

Next, the general stops and delay relations can be written from the arrival queue length graphs illustrated in Figure 2.4.

The vehicle stops per second on the j^{th} link of the traffic network can be determined by considering the stops due to the vehicle queueing during a time interval dt to be $i_j(t)dt$. Thus the total vehicle stops per cycle for the j^{th} link is the area under the arrivals graph of Figure 2.4, namely;

$$S_j = \int_{t_{rj}}^{t_{ej}} i_j(t)dt = I_j(t_{ej}). \tag{2.17}$$

By use of equations 2.8-2.11, the stops equation can be written as

$$\begin{aligned} S_j &= O(t_{ej}) = \int_{t_{rj}}^{t_{ej}} o_j(t)dt \\ &= G_j(t_{ej} - t_{gj}). \end{aligned} \tag{2.18}$$

Similarly, the delay due to vehicle queueing during this same time interval dt is $Q_j(t)dt$, thus giving the total uniform delay per cycle for the j^{th} link as

$$D_j = \int_{t_{rj}}^{t_{ej}} Q_j(t)dt. \tag{2.19}$$

Then using the definitions of queue length and cumulative arrivals,

$$D_j = \int_{t_{rj}}^{t_{gj}} I_j(t)dt + \int_{t_{gj}}^{t_{ej}} [I_j(t) - (t - t_{gj})G_j]dt$$

$$= \int_{t_{rj}}^{t_{ej}} [\int_{t_{rj}}^{t} i_j(\tau)d\tau]dt - G_j(t_{ej} - t_{gj})^2/2 \ . \quad (2.20)$$

All TRANSYT flow calculations are made on the basis of average flow rates and queues that are expected to occur during each cycle unit. However, in real life situations, the random behavior of individual vehicles will tend to fluctuate about the average levels of the flow histograms. Robertson (RO1) observed in his field studies that a cycle time which is long enough to clear a queue during one green time period for uniform arrivals may not be sufficient for complete queue decay for random arrivals during every cycle. Thus an extra delay term, called the random delay, R_j, solely dependent upon the degree of saturation at the stop line on the j^{th} link, was added to the link's objective function, namely:

$$R_j = \frac{(X_j)^2}{4(1 - X_j)} \ , \quad (2.21)$$

where the j^{th} link's degree of saturation, X_j, is given by

$$X_j = \frac{1}{(t_{rj} + C - t_{gj})G_j} \int_{t_{gj}}^{t_{rj}+C} o_j(t)dt$$

$$= \frac{O_j(t_{rj} + C)}{(t_{rj} + C - t_{gj})G_j} \quad (2.22)$$

This also can be written in terms of the cumulative arrivals as

$$X_j = \frac{I_j(t_{rj} + C)}{(t_{rj} + C - t_{gj})G_j} \tag{2.23}$$

It should be noted that this saturation term is bounded within the unit interval, [0,1]. In a subsequent revision of TRANSYT, Robertson (RO2) presented a slightly more complex representation of the random delay, namely:

$$R_j = \sqrt{\left\{\frac{2(1 - X_j) + m_j X_j}{m_j(4 - m_j)}\right\}^2 + \frac{X_j^2}{m_j(4 - m_j)}} - \left\{\frac{2(1 - X_j) + m_j X_i}{m_j(4 - m_j)}\right\}, \tag{2.24}$$

where

$$m_j = \frac{2C}{(t_{rj} + C - t_{gj})G_j\ T_o} \tag{2.25}$$

T_o = the specified length of allowed oversaturation time in minutes.

This random delay employed in TRANSYT overcomes the discontinuity at the point of 100% saturation, $X_j = 1$, and the negative random delay values in the oversaturation region, $X_j > 1$. Both the original TRANSYT random delay model and that used in its revision are illustrated in Table 2.1 and Figure 2.7 for comparison.

2.2.6 Dummy Links

In a network comprised of links forming closed loops, it is necessary to estimate some departure

Table 2.1 Random Delay Values

X_j	Original TRANSYT R_j	Revised TRANSYT R_j $m_j = 0.0001$	$m_j = 0.001$	$m_j = 0.01$	$m_j = 0.1$
0.0	0.000	0.000	0.000	0.000	0.000
0.1	0.003	0.003	0.003	0.003	0.003
0.2	0.013	0.012	0.012	0.012	0.012
0.3	0.032	0.032	0.032	0.032	0.031
0.4	0.067	0.067	0.067	0.066	0.064
0.5	0.125	0.125	0.125	0.124	0.117
0.6	0.225	0.225	0.225	0.222	0.200
0.7	0.408	0.408	0.407	0.398	0.333
0.8	0.800	0.800	0.795	0.756	0.546
0.9	2.025	2.020	1.977	1.671	0.878
1.0	$\pm\infty$	49.751	15.565	4.762	1.365
1.1	-3.025	1002.493	102.429	12.001	2.007
1.2	-1.800	2001.249	201.239	21.155	2.769
1.3	-1.408	3000.833	300.830	30.799	3.610
1.4	-1.225	4000.625	400.623	40.608	4.501
1.5	-1.125	5000.500	500.499	50.490	5.423
1.6	-1.067	6000.417	600.416	60.410	6.365
1.7	-1.032	7000.357	700.357	70.353	7.320
1.8	-1.012	8000.312	800.312	80.309	8.285
1.9	-1.003	9000.278	800.278	90.275	9.256
2.0	-1.000	10000.250	1000.250	100.248	10.233

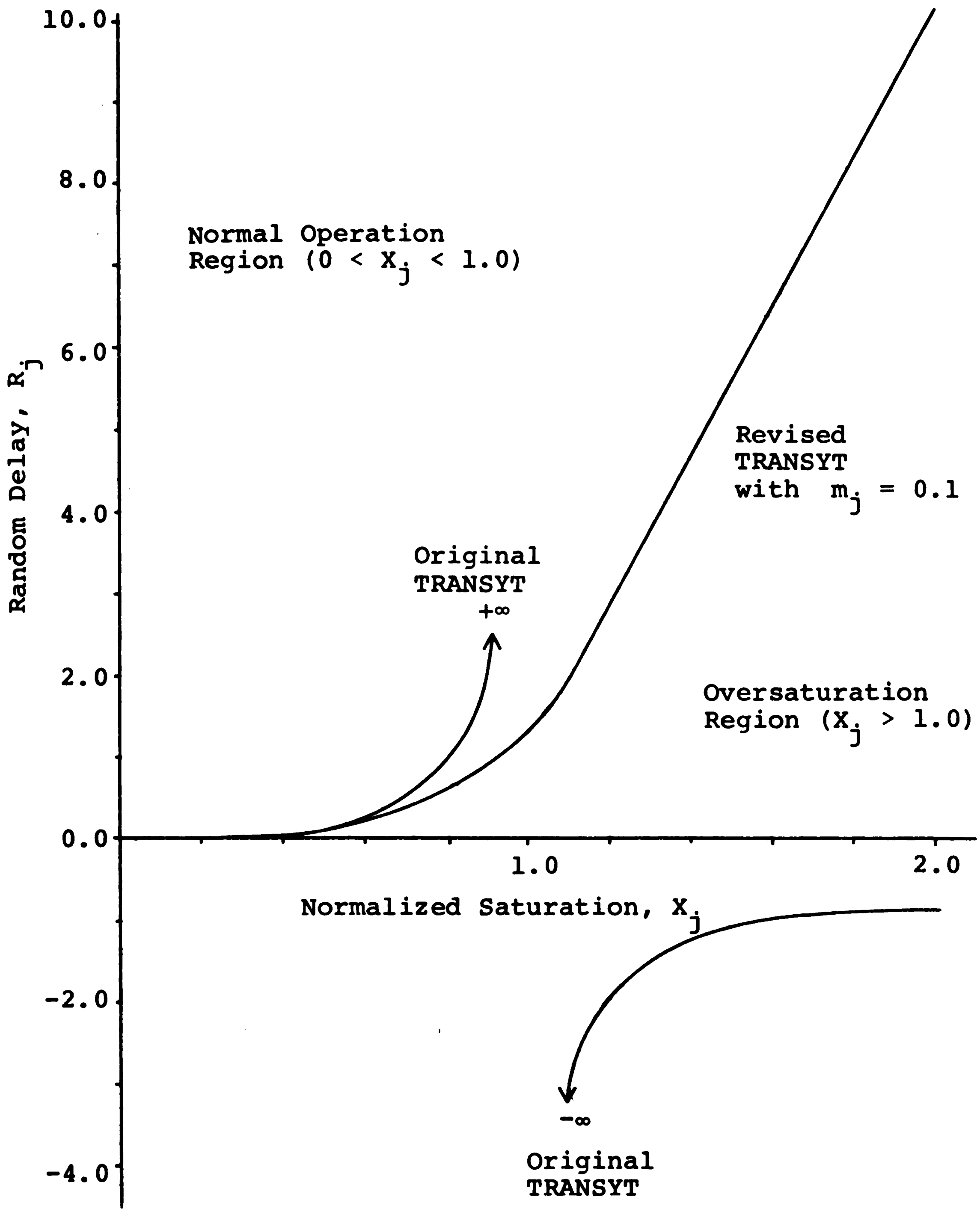

Figure 2.7 Random Delay Versus Normalized Saturation

patterns since each genuine link is processed only once in calculating the objective function. A so-called "dummy link" must be introduced in parallel with a genuine link to break any set of links forming a closed loop. This inserted dummy link has the same total flow as the genuine link but its arrival histogram is assumed to be uniform over the cycle length. The arrival pattern for the next downstream link in the loop is calculated from the appropriate percentage of the dummy link's departure pattern. Then the flow histograms for the remaining links comprising the closed loop are calculated in the normal solution sequence. The rules for dummy link inclusion are:

1. Every closed loop of links must be broken by a dummy link.
2. One dummy link can be used to break several closed loops provided that the loops have at least one common link.
3. The dummy link should be introduced at a node within a loop at which the degree of saturation of the corresponding link is high or the volume flow rate entering the downstream link is low.
4. Use as few dummy links as possible.

2.3 Optimization Procedure

The optimization portion of TRANSYT makes use of a special search procedure developed by Robertson to accomplish a hill-climbing process.

In Great Britain, where TRANSYT was conceived, most existing traffic signal equipment use 50 step control mechanisms. Thus Robertson's optimization increment sizes are based upon the 50 step cycles where each increment must be less than one half the number of steps in the cycle.

The hill-climbing process takes the first increment in the increment list and adjusts the offset of the first intersection or node in the node list for a local minimum of the network's objective functions. The offset of the second node is then adjusted in a similar manner and so on until the end of the node list is reached. At this point, the second increment is used and each node is reoptimized in turn. The process is considered complete when all the nodes have been optimized for all of the increments.

Robertson suggests the following two increment lists for a 50 step cycle:

a) 7, 20, 7, 20, 7, 1, 1 for offsets and

b) 7, 20, -1, 7, 20, 1, -1, 1 for splits and offsets.

The 7 step increments are used to find an approximate local minimum while the 20 step increments avoid getting trapped in that minimum. The positive unity steps are for fine-tuning the approximate offsets while the -1 steps allow adjustments of the splits.

If the number of steps in the cycle length differ from 50, then the 7 and 20 step increments should be adjusted proportionately.

Although Robertson's optimization procedure appears to give very good results, it has several drawbacks. First of all, the optimization process may produce a local optimum instead of the desired global optimum. The problem being that the objective function is not necessarily convex for the general case. A function F defined on an open interval (a,b) is said to be convex if for each $x,y \in (a,b)$ and each λ, $0 \leq \lambda \leq 1$, we have

$$F(\lambda x + (1 - \lambda)y) \leq \lambda F(x) + (1 - \lambda)F(y) \quad (2.26)$$

This definition and Figure 2.8 illustrates the concept of convexity.

The second drawback to Robertson's hill-climbing process is that the number of computations involved increase in the order of the square of the number of intersections and thus restricts its use to off-line applications.

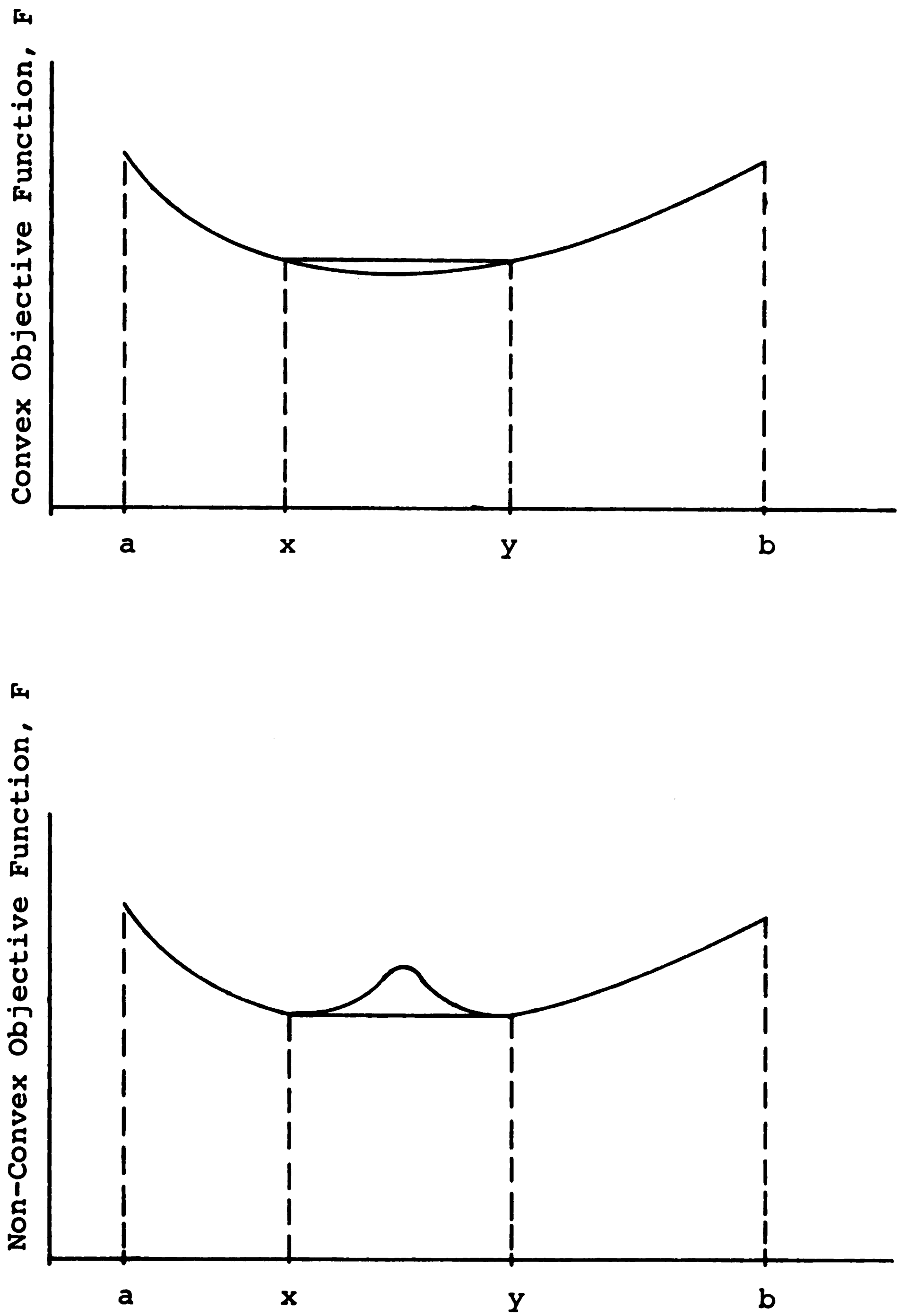

Figure 2.8 Convex and Non-Convex Objective Functions

CHAPTER III

TRANSYT/G NEAR-OPTIMUM SPLIT CALCULATION

The most widely known method of selecting a reasonably good split for a signalized intersection is that attributed to Webster, first published in his classic paper in 1958 (WE1). A very good summary and comparative evaluation of this technique was presented by Gerlough and Wagner in 1967 for an isolated intersection (GW1) and in 1969 for an arterial (WA1). Wagner et al. state that any systematic approach for determining the split must be at least as well defined as Webster's. Webster used a combination of Poisson arrival model theory and computer simulation in order to deduce his formula for average delay per vehicle at a signalized intersection. From this, he derived expressions for optimum cycle length and split that minimized his total delay relation at the i^{th} intersection. These were:

$$C_0 = \frac{1.5L + 5}{1 - \sum_{j=1}^{n} Y_j} , \qquad (3.1)$$

and

$$\hat{s}_i = \frac{C_o - r_A + 1.5L_A + \frac{5}{n}}{r_A - 1.5L_A - \frac{5}{n}} , \qquad (3.2)$$

where C_0 = the optimum cycle length,

r_A = the effective red for the primary phase A,

L = the total lost time per cycle,

L_A = the lost time for the primary phase A,

Y_j = the ratio of maximum directional flow to saturation flow for phase j, and

n = the number of signal phases.

It should be noted that the lost time includes the effect of the starting delay and reduced flow during the amber time. Webster's or some refinement of it is rapidly becoming the standard.

Before proceeding, several observations concerning Webster's split for a two-phase signal can be made for various levels of traffic flow density (GW1). These are:

1. For light flow - the split can be varied greatly from the optimum without producing an oversaturation effect on either phase, and

2. For medium flow - the split can be varied somewhat from the optimum before approaching oversaturation, and

3. For heavy flow - only a small variation in split can cause oversaturation.

The TRANSYT program contains an optional procedure for determining allocation of green times for two or multiphase signals based upon equalization of saturation on all phases. This technique is a refinement of

Webster's and appears to give a good initial starting point for iterative optimization schemes.

The philosophy and objective of this author's research was to develop a non-iterative signal timing algorithm. Thus, a near-optimum set of splits will be determined for our general traffic network on a single pass through the TRANSYT traffic flow model. The general method employed by this author was to write the objective function in terms of the network signal splits, and then calculate the optimum split set by calculus methods.

In developing these signal split relations, only two phase single cycle signals will be considered in the first portion of this chapter thus preventing the derivations from becoming overly complex and obscuring the technique at hand. Later, this method will be extended to the double cycling and multiphase cases.

3.1 Split Bounds

Of course, the loosest set of bounds on the signal split normalized with respect to the cycle length, would be $0 < s_i < 1$. System requirements however, dictate a somewhat tighter set; for example when considering the minimum green time per phase, we have:

$$0 < \frac{\bar{g}_A}{C} \leq s_i \leq 1 - \frac{\bar{g}_B}{C} < 1, \qquad (3.3)$$

where: $\bar{g}_A$ = minimum green time in cycle units for the primary phase (φ_A),

$\bar{g}_B$ = minimum green time in cycle units for the secondary phase (φ_B),

C = cycle length in cycle units.

A minimum green time is required to allow any queues to discharge and for pedestrians to cross the street. When considering the cumulative arrivals and departures at any given intersection, some additional quantities such as the ratio of arrivals to saturation flows can be introduced into the overall bounds on the split. These quantities may or may not be a tighter restriction, depending upon the given set of system conditions, thus use of minimum-maximum functions are required.

As previously shown in Figure 2.4, the total departures during the non-red time must equal the total arrivals during the entire cycle in order for the queue to clear prior to the start of the next red time interval. For link j, we have

$$I_j(t_{rj} + C) = \int_{t_{rj}}^{t_{rj}+C} o_j(t)dt = \int_{t_{gj}}^{t_{rj}+C} o_j(t)dt$$

$$\leq \int_{t_{g_j}}^{t_{rj}+C} G_j dt \; . \tag{3.4}$$

The split for a two-phase signal is the ratio of the primary phase A green and amber time intervals to the cycle length (cross-hatched in Figure 3.1). From this we have:

$$\begin{aligned} s_i &= (t_{rA} + C - t_{gA})/C \\ t_{gA} &= t_{rB} \\ t_{rA} &= t_{gB} \end{aligned} \tag{3.5}$$

Using the definition for the split from above, the phase cumulative arrival relations for Figure 3.1 become:

$$\begin{aligned} I_A(t_{rA} + C) &\leq G_A(t_{rA} + C - t_{gA}) = G_A(s_i)C, \\ I_B(t_{rB} + C) &\leq G_B(t_{rB} - t_{gB}) = G_B(1 - s_i)C. \end{aligned} \tag{3.6}$$

Then solving for the split, s_i, and combining produces the following bounds:

$$0 < \frac{I_A(t_{rA} + C)}{G_A C} \leq s_i \leq 1 - \frac{I_B(t_{rB} + C)}{G_B C} < 1. \tag{3.7}$$

As the link becomes more saturated, these bounds on the split become tighter.

In the computerized TRANSYT traffic flow model, the split is restricted to be an integer belonging to the closed interval [0,C], where C is the cycle length in cycle units. Therefore, the previously discussed normalized split, s_i, is scalar transformed to the integer split, $\bar{s}_i$, by:

$$\bar{s}_i = C \cdot s_i. \tag{3.8}$$

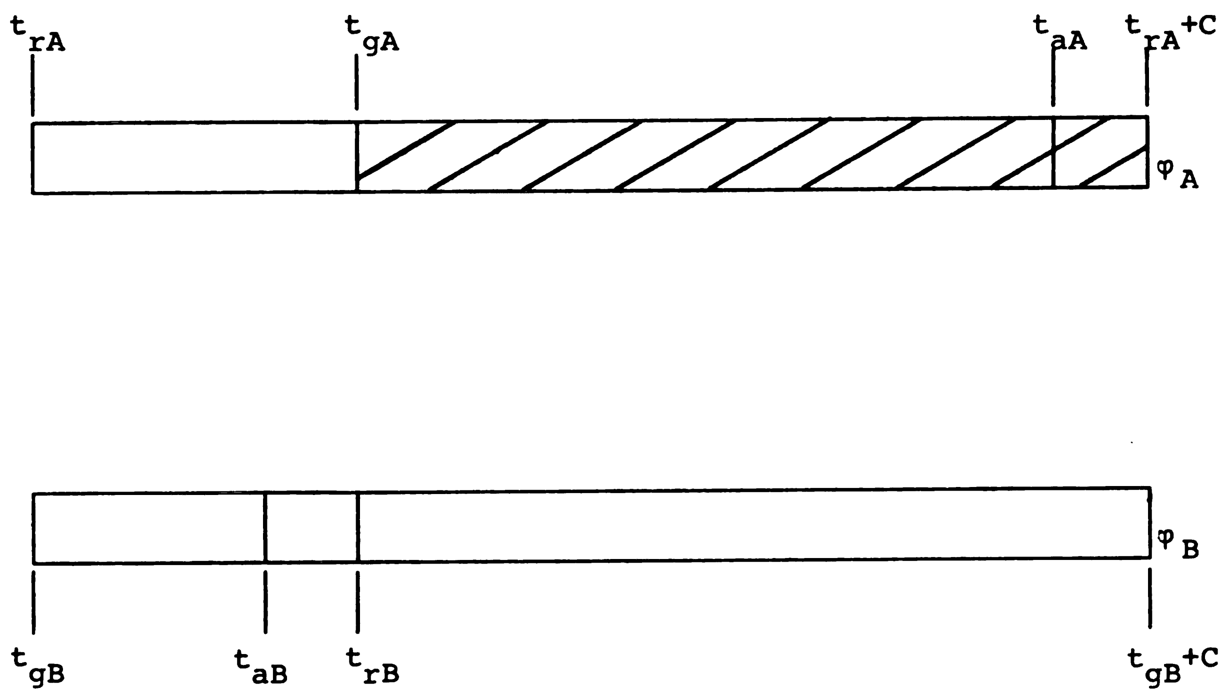

Figure 3.1 Phase A and B Time Interval Relationships

The unnormalized upper and lower bounds may not result in an integer value and thus must be restricted as such. Specifically, each real valued bound having a non-zero decimal part must be rounded up to the next highest integer. This may be accomplished by the use of two well defined mathematical functions, namely the 'greatest integer' and the 'signum' functions:

$[\bar{h}_j] \equiv$ the greatest integer less than or equal to $\bar{h}_j$,

and

$$\operatorname{sgn}(\bar{h}_j) \equiv \begin{cases} +1 & \text{if} \quad \bar{h}_j > 0 \\ 0 & \text{if} \quad \bar{h}_j = 0 \\ -1 & \text{if} \quad \bar{h}_j < 0 . \end{cases} \tag{3.9}$$

We then define

$$\bar{k}_j \equiv [\bar{h}_j] + \operatorname{sgn}(\bar{h}_j - [\bar{h}_j]), \tag{3.10}$$

where

$$\bar{h}_j = \frac{I_j(t_{rj} + C)}{G_j}, \; j = A,B. \tag{3.11}$$

Since we are setting up integer bounds on an integer valued split parameter, $\bar{s}_i$, where the $\bar{h}_j$ are real, the rounding of the $\bar{h}_j$ values must be done such that the $\bar{k}_j$ values will be within the $\bar{h}_j$ bounds. That is,

$$\bar{h}_A \leq \bar{k}_A \leq \bar{s}_i \leq C - \bar{k}_B \leq C - \bar{h}_B . \tag{3.12}$$

From this set of split bounds, it is required that

$$\sum_j \bar{k}_j \le C \tag{3.13}$$

to insure a valid split value. In the case of equality, $\bar{k}_A = \bar{s}_i = C - \bar{k}_B$, the split is uniquely determined by its bounds.

By denoting the sum of the minimum green plus amber time intervals for the j^{th} phase as g_j, we have the bounds on the integer split for the intersection of two one-way streets as:

$$\max(g_A, \bar{k}_A) \le \bar{s}_i \le C - \max(g_B, \bar{k}_B). \tag{3.14}$$

For the intersection of two bidirectional streets, the summation of the ratios of cumulative arrivals to the saturation flow rates per phase will govern the bounds calculation, thus

$$\sum_{j\in\varphi_A} \max(g_j, \bar{k}_j) \le \bar{s}_i \le C - \sum_{j\in\varphi_B} \max(g_j, \bar{k}_j), \tag{3.15}$$

where the link subscript $j = 1, 2, \ldots, \ell$.

3.2 Tractable Model of Stops and Uniform Delay

The least complicated signalized intersection that may occur in a general network is the corner intersection composed of two one-way streets, each having a uniform arrival rate as in Figure 3.2. After one complete cycle of simulation, the queues will have had sufficient time to develop properly. The general delay and stops equations from Section 2.2 can then be written easily from the rectangular area under the arrival rate curve and the triangular area under the queue length curve of Figure 3.2. Thus, since the input is constant at IN_j over the whole cycle length, we have for link j:

$$S_j = \int_{t_{rj}}^{t_{ej}} i_j(t)dt = IN_j(t_{ej} - t_{rj}) = G_j(t_{ej} - t_{gj}), \quad (3.16)$$

$$D_j = \int_{t_{rj}}^{t_{ej}} Q_j(t)dt = IN_j \int_{t_{rj}}^{t_{gj}} (t - t_{rj})dt$$

$$- (G_j - IN_j) \int_{t_{gj}}^{t_{ej}} (t - t_{ej})dt$$

$$= \frac{1}{2} IN_j(t_{gj} - t_{rj})^2 + \frac{1}{2} (G_j - IN_j)(t_{ej} - t_{gj})^2 \quad (3.17)$$

where the time at which the queue clears is

$$t_{ej} = t_{gj} + (t_{gj} - t_{rj})\left(\frac{IN_j}{G_j - IN_j}\right). \quad (3.18)$$

Substitution back into the stop and delay equations results in

$$S_j = (t_{gj} - t_{rj})c_j \quad (3.19)$$

and

$$D_j = \frac{1}{2}(t_{gj} - t_{rj})^2 c_j, \quad (3.20)$$

where

$$c_j = \frac{G_j \; IN_j}{G_j - IN_j} . \quad (3.21)$$

Most of the intersections comprising a general urban traffic network have many links with non-uniform arrival rates, thus the areas under the arrivals, $i_j(t)$, and queue length, $Q_j(t)$, curves (Figure 2.4) representing the stops and delay are not rectangular and triangular respectively as in the uniform case (Figure 3.2). Thus, by using the stops and delay equations based upon uniform arrivals, some degree of error will be introduced into the solution of the general network. But, since the goal is to achieve only near-optimum signal settings in a trade-off for real time operation, these uniform arrival stops and delay equations will be accepted as an accurate enough model.

3.3 Tractable Model of Random Delay

The revised TRANSYT random delay model described in Section 2.2.5 can be rewritten as:

$$R_j = \frac{1}{m_j(4 - m_j)}\{2\sqrt{1 - (2 - m_j)X_j + X_j^2} - 2 + (2 - m_j)X_j\}. \quad (3.22)$$

In order to write the random delay in terms of the normalized split, s_i, for the i^{th} intersection, we recall equation 2.23 from Chapter II for the degree of saturation of the j^{th} link. For a two phase signal this relation becomes:

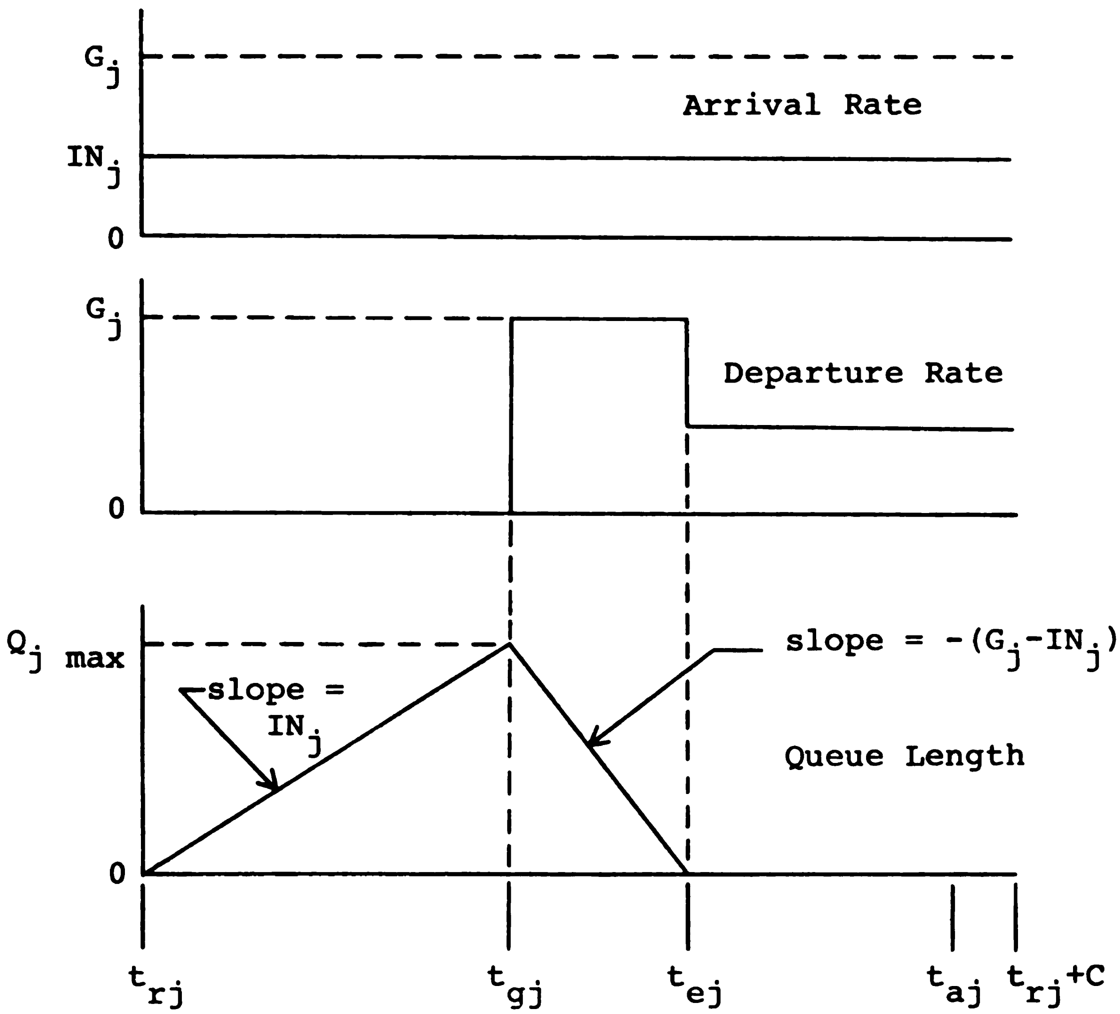

Figure 3.2 Departures and Queue Length for Uniform Arrivals on the j^{th} Link

$$X_j = \begin{cases} \dfrac{I_j(t_{rj} + C)}{G_j\ s_i C} = \dfrac{h_j}{s_i} & \text{for} \quad j \in \varphi_A \\ \\ \dfrac{I_j(t_{rj} + C)}{G_j(1 - s_i)C} = \dfrac{h_j}{1-s_i} & \text{for} \quad j \in \varphi_B, \end{cases} \tag{3.23}$$

where $h_j \equiv \dfrac{I_j(t_{rj} + C)}{G_j C}$. (3.24)

Now the derivative with respect to the split can be derived as:

$$\frac{dR_j}{ds_i} = \frac{\partial R_j}{\partial X_j} \cdot \frac{\partial X_j}{\partial s_i}$$

$$= \frac{1}{m_j(4-m_j)} \left\{ \frac{2X_j - (2-m_j)}{\sqrt{1-(2-m_j)X_j+X_j^2}} + (2-m_j) \right\} \cdot \frac{\partial X_j}{\partial s_i}, \tag{3.25}$$

where

$$\frac{\partial X_j}{\partial s_i} = \begin{cases} \dfrac{-I_j(t_{rj} + C)}{G_j C\ s_i^2} = \dfrac{-h_j}{s_i^2} = \dfrac{-X_j^2}{h_j} & \text{for} \quad j \in \varphi_A \\ \\ \dfrac{I_j(t_{rj} + C)}{G_j C(1 - s_i)^2} = \dfrac{h_j}{(1-s_i)^2} = \dfrac{X_j^2}{h_j} & \text{for} \quad j \in \varphi_B \end{cases} \tag{3.26}$$

It is observed that this form of the random delay and its derivative with respect to the normalized split leads to a very complicated form when attempting to derive the near-optimum split calculation equations. With the use of an appropriate approximation to the random delay derivative, a tractable answer will be shown to exist.

The random delay derivative with respect to the degree of saturation, X_j, was evaluated for several different values of m_j and is illustrated in Table 3.1. From this we can see that the first derivative, or slope, and m_j are reciprocals of each other in the oversaturation region ($X_j > 1.0$).

In order to decide upon an acceptable approximation of the random delay with respect to the split, first one must determine the range over which the approximation must hold. We see that

$$\frac{dR_j}{ds_i} \begin{cases} \leq 0 & \text{for} \quad j \in \varphi_A \\ \geq 0 & \text{for} \quad j \in \varphi_B \, . \end{cases} \tag{3.27}$$

The limits of this derivative are:

$$\lim_{s_i \to 0^+} \left(\frac{dR_j}{ds_i}\right) = \begin{cases} -\infty & \text{for} \quad j \in \varphi_A \\ \approx 0 & \text{for} \quad j \in \varphi_B , \end{cases} \tag{3.28}$$

$$\lim_{s_i \to 1^-} \left(\frac{dR_j}{ds_i}\right) = \begin{cases} \approx 0 & \text{for} \quad j \in \varphi_A \\ +\infty & \text{for} \quad j \in \varphi_B \, . \end{cases} \tag{3.29}$$

From Section 3.1, we found that the normalized split is constrained within the bounds:

$$s_i(\min) = \frac{\max(g_A, \bar{k}_A)}{C} \leq s_i \leq 1 - \frac{\max(g_B, \bar{k}_B)}{C} = s_i(\max) \, . \tag{3.30}$$

Table 3.1 Random Delay Derivative with Respect to Degree of Saturation

X_j	TRANSYT $\partial R_j/\partial X_j$ $m_j = 0.0001$	$m_j = 0.001$	$m_j = 0.01$	$m_j = 0.1$
0.0	0.000	0.000	0.000	0.000
0.1	0.059	0.059	0.059	0.058
0.2	0.141	0.141	0.140	0.138
0.3	0.260	0.260	0.259	0.249
0.4	0.444	0.444	0.441	0.412
0.5	0.750	0.749	0.740	0.659
0.6	1.312	1.309	1.279	1.045
0.7	2.526	2.514	2.397	1.667
0.8	5.991	5.915	5.261	2.651
0.9	24.589	23.237	15.328	4.061
1.0	5024.876	507.783	52.381	5.683
1.1	9975.211	976.946	86.194	7.092
1.2	9993.765	993.895	94.937	8.077
1.3	9998.225	997.254	97.511	8.698
1.4	9998.439	998.449	98.542	9.085
1.5	9999.000	999.005	99.048	9.331
1.6	9999.306	999.308	99.331	9.494
1.7	9999.490	999.491	99.504	9.606
1.8	9999.609	999.610	99.619	9.685
1.9	9999.691	999.692	99.698	9.744
2.0	9999.750	999.750	99.754	9.787

For the usual minimum green and amber time intervals in a 60 unit cycle length,

$$13 \leq \max(g_j, \bar{k}_j) \quad \text{for all} \quad j. \tag{3.31}$$

Thus the bounds on the normalized split for a 60 unit cycle length become:

$$0.217 \leq s_i \leq 0.783 \quad . \tag{3.32}$$

These bounds can be shown to remain reasonably constant for other cycle lengths. Thus our random delay approximation will be considered for split values between 0.2 and 0.8.

For a typical link having a 2000 vehicle/hour/lane saturation flow rate, the m_j term will commonly be in the 0.0001 to 0.1 range and the h_j term will be less than 1.0. Table 3.2 represents a tabulation of the dR_j/ds_i relations over the above m_j and h_j ranges. The following random delay approximation was selected:

$$\frac{dR_j}{ds_i} = \frac{h_j}{m_j} (K_{1j} s_i + K_{2j}) \quad . \tag{3.33}$$

From Table 3.2, the K_{1j} and K_{2j} constants were calculated to give:

$$\frac{dR_j}{ds_i} = \begin{cases} \dfrac{h_j}{m_j} (41.66 s_i - 33.33) \ , \ j \in \varphi_A \\ \\ \dfrac{h_j}{m_j} (41.66 s_i - 8.33) \ , \quad j \in \varphi_B \ , \end{cases} \tag{3.34}$$

Table 3.2 Random Delay Derivative with Respect to Split

h_A / m_A / s_i	Phase A: dR_A/ds_i					
h_A	0.5			1.0		
m_A	0.01	0.001	0.0001	0.01	0.001	0.0001
s_i						
0.2	-1,248.6	-12,498.6	-124,998.6	-2,499.6	-24,999.6	-249,999.6
0.3	- 552.5	- 5,552.4	- 55,552.4	-1,110.6	-11,110.6	-111,110.6
0.4	- 301.7	- 3,112.7	- 31,237.5	- 624.3	- 6,249.3	- 62,499.3
0.5	- 104.8	- 1,015.6	- 10,049.8	- 399.0	- 3,999.0	- 39,999.0
0.6	- 10.0	- 11.9	- 12.1	- 276.3	- 2,776.2	- 27.776.2
0.7	- 2.7	- 2.9	- 2.9	- 201.5	- 2,038.1	- 20,405.4
0.8	- 1.2	- 1.2	- 1.2	- 150.9	- 1,556.4	- 15,618.8

Note: For the phase B derivative, dR_B/ds_i, replace the s_i heading with $1 - s_i$ and change the sign of the resulting table values.

for $0.2 \leq s_i \leq 0.8$.

At first, it may appear that this linear approximation to the random delay derivative is overly simplified. However, Robertson points out that even when the degree of saturation, X_j, is as large as 0.9 and the offset is the best possible, typically the random delay is no more than half the total delay (R01). Thus this author considers this linear approximation adequate for the objectives of this research.

3.4 Near-Optimum Split

From Section 2.1, the objective function for each link j, was given as the weighted sum of the stops and delays or

$$F_j = KS_j + W_j(D_j + R_j), \tag{3.35}$$

and the total network objective function, F, as a summation of the link F_j's. This can also be written in terms of the node f_i's, namely

$$F = \sum_{j=1}^{\ell} F_j = \sum_{i=1}^{n} f_i , \tag{3.36}$$

where ℓ = the number of links in the network, and

n = the number of nodes within the network.

Assuming that the F_j's for the links terminating at any node, i, are dependent and those F_j's associated with any other node are independent of this set, results in:

$$F = \sum_{i=1}^{n} \sum_{j=1}^{\ell_i} [KS_j + W_j(D_j + R_j)] \ , \tag{3.37}$$

where ℓ_i = the number of links terminating at node i.

The equations for stops and uniform delay from Section 3.2 for each link j can be written in terms of the split as:

$$S_j = \begin{cases} (1 - s_i)Cc_j & \text{for } j \in \varphi_A \\ s_i Cc_j & \text{for } j \in \varphi_B, \end{cases} \tag{3.38}$$

$$D_j = \begin{cases} \frac{1}{2}(1 - s_i)^2 C^2 c_j & \text{for } j \in \varphi_A \\ \frac{1}{2} s_i^2 C^2 c_j & \text{for } j \in \varphi_B. \end{cases} \tag{3.39}$$

where all terms have been previously defined.

Thus, the total network objective function can be written as:

$$F = \sum_{i=1}^{n} \{KC[(1 - s_i) \sum_{j\in\varphi_A} c_j + s_i \sum_{j\in\varphi_B} c_j] + \frac{C^2}{2}[(1 - s_i)^2 \sum_{j\in\varphi_A} W_j c_j + s_i^2 \sum_{j\in\varphi_B} W_j c_j] + \sum_j W_j R_j \ . \tag{3.40}$$

where all the links are separated into two sets, namely those belonging to phase A, (φ_A) and phase B, (φ_B), respectively.

Now considering any node, i, the objective function f_i for all ℓ_i links feeding that node can be minimized with respect to its split, s_i, by the First Derivative Test (OL1) as follows:

$$0 = \frac{d}{ds_i}(f_i) \doteq KC[-\sum_{j\in\varphi_A} c_j + \sum_{j\in\varphi_B} c_j]$$
$$+ \frac{C^2}{2}[-2(1-s_i)\sum_{j\in\varphi_A} W_jc_j + 2s_i \sum_{j\in\varphi_B} W_jc_j]$$
$$+ s_i \sum_j \frac{W_jh_jK_{1j}}{m_j} + \sum_j \frac{W_jh_jK_{2j}}{m_j}\ . \qquad (3.41)$$

Then solving for the split s_i to provide a near minimization of the objective function for node i, gives:

$$\hat{s}_i = \frac{\sum_{j\in\varphi_A}(C^2W_jc_j + KCc_j - \frac{W_jh_jK_{2j}}{m_j}) - \sum_{j\in\varphi_B}(KCc_j + \frac{W_jh_jK_{2j}}{m_j})}{\sum_j(C^2W_jc_j + \frac{W_jh_jK_{1j}}{m_j})}. \qquad (3.42)$$

In order to be sure that $\hat{s}_i$ does indeed minimize the node objective function f_i, the second derivative with respect to the split must be positive or indicate convexity in an ε neighborhood about $\hat{s}_i$. Then by the Second Derivative Test (OL1),

$$\frac{d^2}{ds_i^2}(f_i) = C^2\sum_j W_jc_j + \sum_j \frac{W_jh_jK_{1j}}{m_j} > 0, \qquad (3.43)$$

since all terms are positive. Thus the near-optimum split $\hat{s}_i$ can be used for any two phase traffic signal where each phase may have numerous links.

The near-optimum normalized split has been plotted in Figure 3.3 for the case of a two phase signal located at the intersection of two one-way streets. The delay weighting factors, W_j, were assumed equal to unity, the stop factor equal to 4 and saturation flows of 4500 vehicles per hour. From Figure 3.3, it is observed that the split equals 0.5 for any situation having equal arrivals, IN_j, and saturation flows, G_j, on both phases. A more general statement can be made: the normalized split will equal 0.5 for any situation having equal c_j terms. These c_j terms were previously defined as the ratio of the product of the saturation flow and the arrival flow to their difference for the j^{th} link.

3.5 Two-Phase Double Cycling

Sections 3.1 through 3.4 of this chapter have covered the two-phase single cycling cases, however it may be advantageous to use double cycling in certain instances where the traffic flow rates are reasonably light or the cycle length is long. Figure 3.4 illustrates the double cycling timing of a two-phase signal and will constitute a reference for the following derivation. As a direct result of this diagram the following related timing variables are:

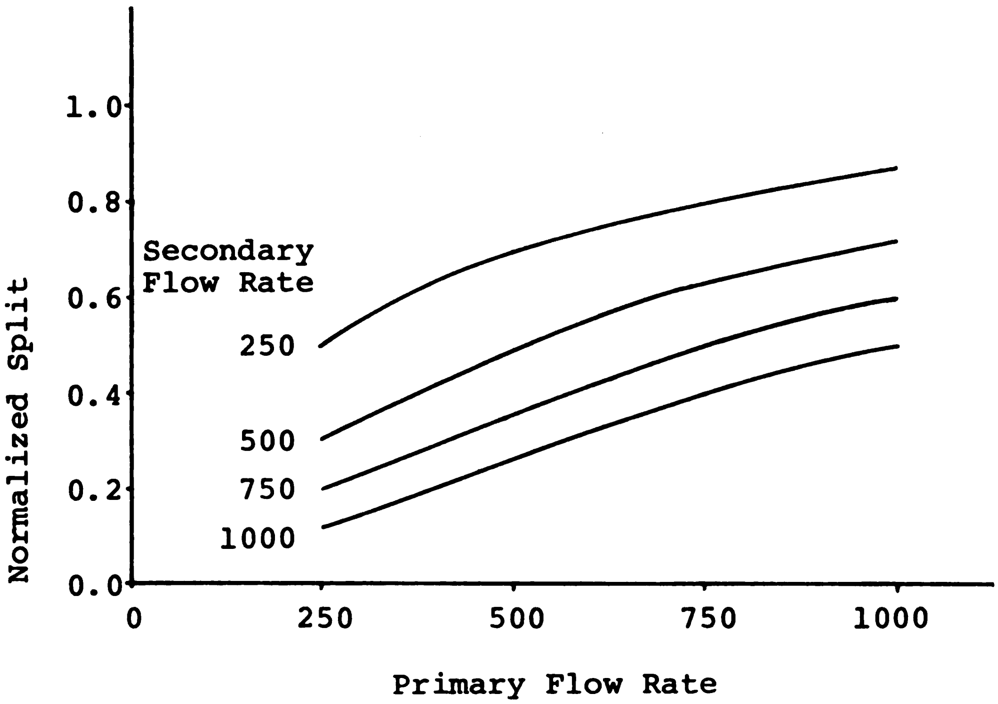

Figure 3.3 Normalized Split Relative to Arrivals

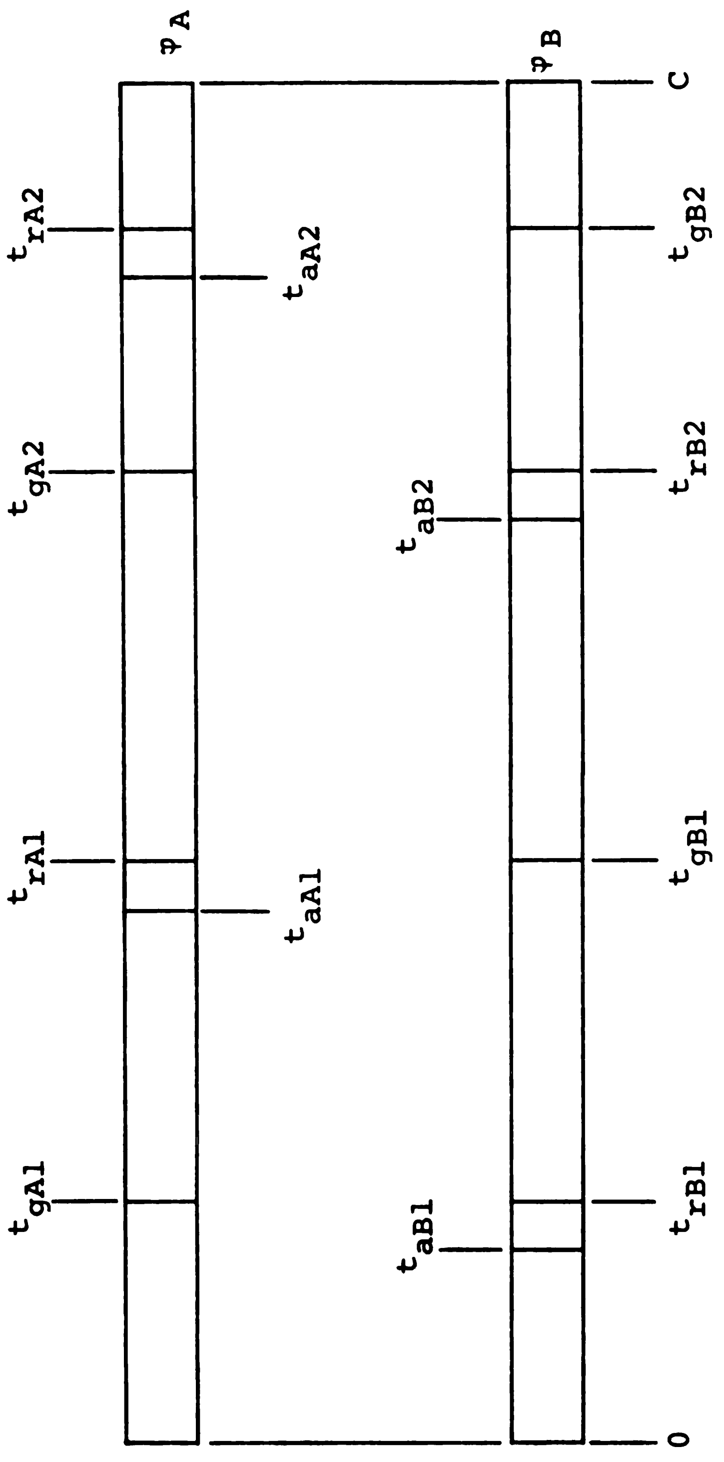

Figure 3.4 Double Cycled Timing of a Two-Phase Signal

$$\begin{aligned} t_{rB1} &= t_{gA1} \\ t_{gB1} &= t_{rA1} \\ t_{rB2} &= t_{gA2} \\ t_{gB2} &= t_{rA2}\,, \end{aligned} \tag{3.44}$$

where t_{ijk} = the cycle unit representing the start of the i^{th} time interval for the j^{th} phase during the k^{th} half cycle.

The signal split, s_i, is defined to be the sum of the two green intervals and two amber intervals normalized with respect to the cycle length. Alternately,

$$s_i = \frac{(t_{rA1} - t_{gA1}) + (t_{rA2} - t_{gA2})}{C}. \tag{3.45}$$

It is assumed that there exists half cycle symmetry of the timing parameters, that is

$$t_{ij2} = t_{ij1} + \frac{C}{2} \quad \text{for all} \quad i,j. \tag{3.46}$$

Thus, the split reduces to

$$s_i = \frac{2(t_{rA1} - t_{gA1})}{C}. \tag{3.47}$$

In double cycling, the queue can grow and decay twice during the cycle length, namely; once for each green interval. Thus by analogy to Section 3.2, the stops equation for the j^{th} link entering the subject intersection can be written as:

$$S_j = (t_{gj1} - t_{rj1})c_{j1} + (t_{qj2} - t_{rj2})c_{j2} \quad j = A,B. \tag{3.48}$$

Thus, substitution of the split term results in:

$$S_A = \frac{C}{2}(1 - s_i)(c_{A1} + c_{A2}),$$

and (3.49)

$$S_B = \frac{C}{2}(s_i)(c_{B1} + c_{B2}),$$

where

$$c_{jk} = \frac{G_j \quad IN_{jk}}{G_j - IN_{jk}} \tag{3.50}$$

and IN_{jk} = the uniform arrival rate for the j^{th} phase during the k^{th} half cycle. Again, similar to the derivation for single cycled signals, the uniform delay can be written as:

$$D_j = \frac{1}{2}(t_{gj1} - t_{rj1})^2 c_{j1} + \frac{1}{2}(t_{gj2} - t_{rj2})^2 c_{j2}, \quad j = A,B. \tag{3.51}$$

Then, by substitution

$$D_A = \frac{C^2}{8}(1 - s_i)^2 (c_{A1} + c_{A2}),$$

(3.52)

$$D_B = \frac{C^2}{8}(s_i)^2 (c_{B1} + c_{B2}),$$

and

$$\frac{dR_j}{ds_i} = \frac{h_j}{m_j}(K_{1j}s_i + K_{2j}) \quad j = A,B. \tag{3.53}$$

since the degree of saturation, X_j, is the same as for single cycled signals.

Then the near-optimum split $\hat{s}_i$ can be calculated analogously to that of single cycling by substitution into the node objective function. The final result after differentiation is:

$$\hat{s}_i = \frac{\sum\limits_{j\in\varphi_A}\left[\frac{C^2}{4}W_j(c_{j1}+c_{j2})+\frac{KC}{2}(c_{j1}+c_{j2})-\frac{W_jh_jK_{2j}}{m_j}\right]-\sum\limits_{j\in\varphi_B}\left[\frac{KC}{2}(c_{j1}+c_{j2})+\frac{W_jh_jK_{2j}}{m_j}\right]}{\sum\limits_{j}\left[\frac{C^2}{4}W_j(c_{j1}+c_{j2})+\frac{W_jh_jK_{1j}}{m_j}\right]}, \quad (3.54)$$

which is similar to the single cycling split except that the cycle length C is replaced with $C/2$ and c_j is replaced by $(c_{j1} + c_{j2})$.

3.6 Non-Overlapping Multiphase Single Cycling

Another important type of signalized intersection employs more than two phases operating in the single cycle mode. Left turn lanes handling heavy flow rates, pedestrian crosswalks and separate bus lanes are a few of the examples requiring multiphased signals. Figure 3.5 illustrates the single cycling of a four-phase traffic signal. From this diagram we note:

$$\begin{aligned} t_{gB} &= t_{rA} \\ t_{gC} &= t_{rB} \\ t_{gD} &= t_{rC} \\ t_{gA} &= t_{rD}, \end{aligned} \quad (3.55)$$

where t_{ij} = the cycle unit representing the start of the i^{th} time interval for the j^{th} phase.

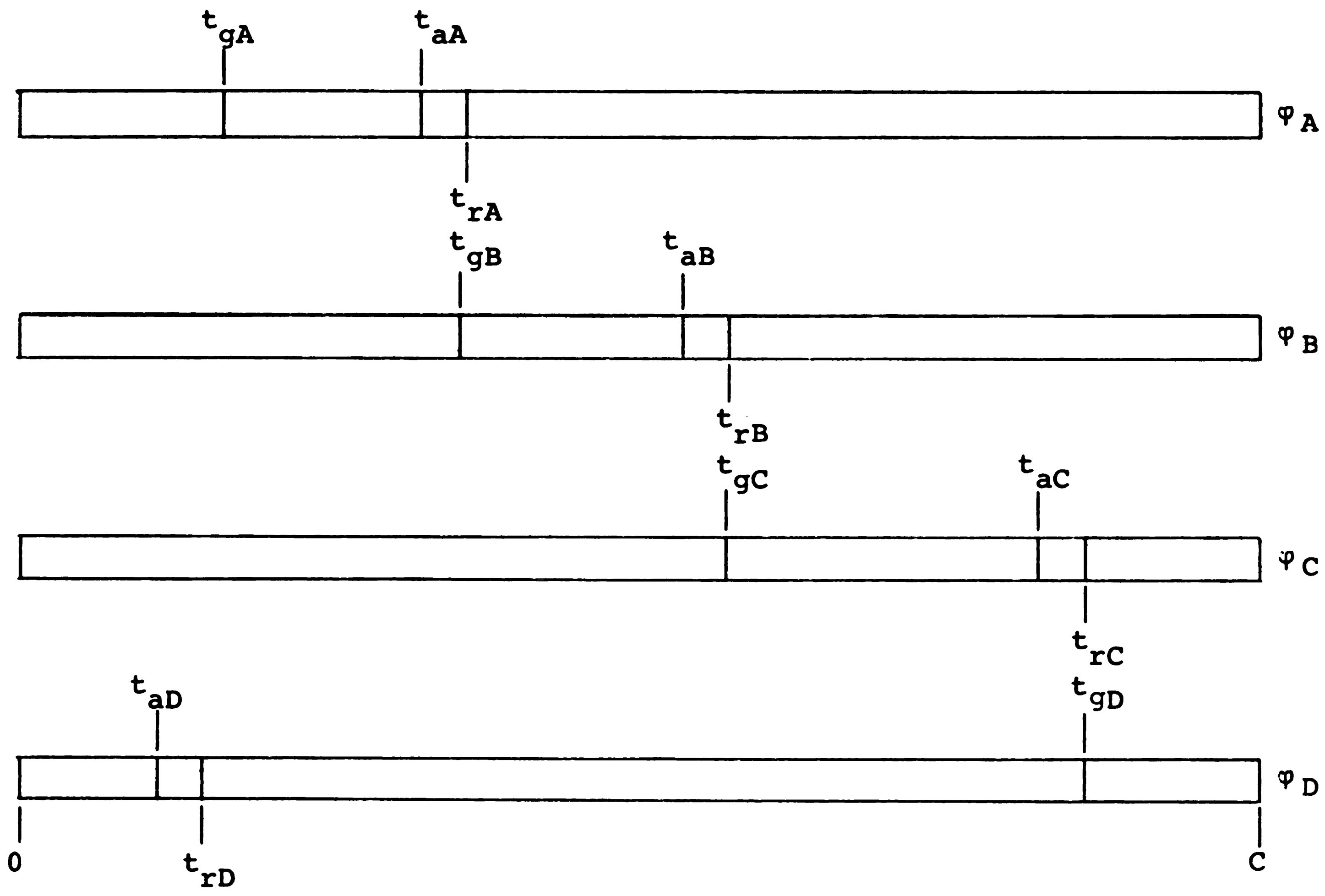

Figure 3.5 Single Cycled Timing of a Non-Overlapping Four-Phase Signal

For an N phase non-overlapping traffic signal, there are (N-1) split terms. Thus for our four phase example at the ith intersection,

$$s_{ij} = \frac{t_{rj} - t_{gj}}{C} \tag{3.56}$$

$$S_j = (t_{gj} - t_{rj})c_j \tag{3.57}$$

$$D_j = \frac{1}{2}(t_{gj} - t_{rj})^2 c_j \quad \text{where} \quad j = A,B,C \tag{3.58}$$

The stops and uniform delay equations are then written as:

$$S_j = (1 - s_{ij})Cc_j \qquad j = A,B,C \tag{3.59}$$

$$S_D = (s_{iA} + s_{iB} + s_{iC})Cc_D$$

$$D_j = \frac{1}{2}(1 - s_{ij})^2 C^2 c_j \qquad j = A,B,C \tag{3.60}$$

$$D_D = \frac{1}{2}(s_{iA} + s_{iB} + s_{iC})^2 C^2 c_D$$

Let $\overline{S}_i$, $\overline{D}_i$, and $\overline{R}_i$ represent the weighted sums of the stops, uniform and random delay terms for the i^{th} signal, respectively. Then take the first partial derivatives of $\overline{S}_i$, $\overline{D}_i$, and $\overline{R}_i$ with respect to the phase splits, s_{ij} to form:

$$\frac{\partial \overline{S}_i}{\partial s_{ij}} = KC(c_D - c_j)$$

$$\frac{\partial \overline{D}_i}{\partial s_{ij}} = C^2[(s_{iA} + s_{iB} + s_{iC})W_D c_D - (1 - s_{ij})W_j c_j] \tag{3.61}$$

$$\frac{\partial \overline{R}_i}{\partial s_{ij}} = \frac{W_j h_j}{m_j}(K_{1j}s_{ij} + K_{2j}) \quad , \quad j = A,B,C.$$

Then to insure that a minimum does exist for the objective function, f_i, for the i^{th} signal, from section 3.4,

$$f_i = \sum_{j=1}^{\ell_i} [KS_j + W_j(D_j + R_j)]$$

$$= \overline{S}_i + \overline{D}_i + \overline{R}_i \; . \qquad (3.62)$$

The second partial derivatives in turn appear as the forms:

$$L_{jj} = \frac{\partial^2 f_i}{\partial s_{ij}^2} = C^2(W_D c_D + W_j c_j) + \frac{W_j h_j K_{1j}}{m_j} > 0$$

$$L_{kj} = \frac{\partial^2 f_i}{\partial s_{ik} \partial s_{ij}} = C^2 W_D c_D > 0, \; j = A,B,C. \qquad (3.63)$$

By considering

$$L_{jj} = U + V_j > 0 \qquad (3.64)$$

$$L_{jk} = U > 0,$$

it is easily shown that

$$\Delta = \begin{vmatrix} L_{AA} & L_{BA} & L_{CA} \\ L_{AB} & L_{BB} & L_{CB} \\ L_{AC} & L_{BC} & L_{CC} \end{vmatrix}$$

$$= U(V_A V_B + V_A V_C + V_B V_C) + V_A V_B V_C > 0. \qquad (3.65)$$

Thus since the $L_{ij} > 0$ and $\Delta > 0$, the objective function for the i^{th} intersection has a relative minimum of $f_i\ (s_{iA}, s_{iB}, s_{iC})$ at the point $(\hat{s}_{iA}, \hat{s}_{iB}, \hat{s}_{iC})$.

Then by setting the first derivatives of the intersection's objective function with respect to the phase splits to zero, the general equation becomes:

$$0 = \frac{\partial \bar{S}_i}{\partial s_{ij}} + \frac{\partial \bar{D}_i}{\partial s_{ij}} + \frac{\partial \bar{R}_i}{\partial s_{ij}}$$

$$= KC(c_D - c_j) + C^2[(s_{iA} + s_{iB} + s_{iC})W_D c_D - (1 - s_{ij})W_j c_j]$$

$$+ \frac{W_j h_j}{m_j}(K_{1j} s_{ij} + K_{2j}) \qquad j = A, B, C. \tag{3.66}$$

By rearranging terms, we have the following set of equations:

$$KC(c_j - c_D) + (C^2 c_j - \frac{h_j K_{2j}}{m_j})W_j$$

$$= s_{ij}[C^2 W_D c_D + (C^2 c_j + \frac{h_j K_{1j}}{m_j})W_j]$$

$$+ (s_{ik} + s_{i\ell})C^2 W_D c_D$$

$$j, k, \ell = A, B, C \text{ and } j \neq k \neq \ell\ . \tag{3.67}$$

Let

$$y_j = KC(c_j - c_D) + (C^2 c_j - \frac{h_j K_{2j}}{m_j})W_j$$

$$w_j = C^2 W_D c_D + (C^2 c_j + \frac{h_j K_{1j}}{m_j})W_j \tag{3.68}$$

$$w = C^2 W_D c_D \qquad j = A, B, C.$$

Then the set of equations can be written in matrix form as:

$$\begin{bmatrix} y_A \\ y_B \\ y_C \end{bmatrix} = \begin{bmatrix} w_A & w & w \\ w & w_B & w \\ w & w & w_C \end{bmatrix} \begin{bmatrix} s_{iA} \\ s_{iB} \\ s_{iC} \end{bmatrix}$$

or

$$\underline{Y} = \underline{W} \cdot \underline{S}_i \qquad (3.69)$$

The set of splits for our multiphase situation can be determined by pre-matrix multiplication by $\underline{W}^{-1}$ or,

$$\underline{S}_i = \underline{W}^{-1} \cdot \underline{Y} \qquad (3.70)$$

The matrix $\underline{S}_i$ is a unique vector of phase splits for the i^{th} intersection provided $|\underline{W}| \neq 0$; a condition which can be shown true if $w_j \neq w \neq 0$ for all j.

This matrix representation can be used for any number of phases $(N \geq 2)$ constituting any signal's requirements. If there are N phases, then there will be $(N-1)$ phase splits and the $\underline{S}_i$, $\underline{W}^{-1}$, and $\underline{Y}$ matrices will have dimensions equal to $(N-1)$ by 1, $(N-1)$ by $(N-1)$, and $(N-1)$ by 1, respectively.

To extend this result to apply to situations where there are multiple links per phase, simply replace the y_j, and w_j with $\sum_j y_j$ and $\sum_j w_j$ respectively.

3.7 Overlapping Multiphase Single Cycling

The more general form of multiphase single cycling has some overlapping of green time intervals between the various signal phases.

Consider Figure 3.6 of a specific example of an overlapping four phase signal.

The respective red, green, and amber time intervals for this signal are illustrated in Figure 3.7. Note that there are only 2 independent phase split terms required, namely for phases A and C since the phase B green is an overlap of the greens of phases A and C. Phase D is a dependent phase.

Similar to Section 3.6, we can write:

$$\begin{aligned} t_{gB} &= t_{gA} = t_{rD} \\ t_{gC} &= t_{rA} \\ t_{gD} &= t_{rB} = t_{rC} \end{aligned} \tag{3.71}$$

Thus for an N phase traffic signal with M overlapping green time intervals, there are $(N - M - 1)$ split terms. These splits are

$$s_{ij} = \frac{t_{rj} - t_{gj}}{C} \quad \text{where} \quad j = A, C. \tag{3.72}$$

Then the stops and uniform delay terms can be written as:

$$S_j = \begin{cases} (1 - s_{ij})Cc_j \\ (1 - s_{iA} - s_{iC})Cc_B \\ (s_{iA} + s_{iC})Cc_D \end{cases} \quad j = A,C \tag{3.73}$$

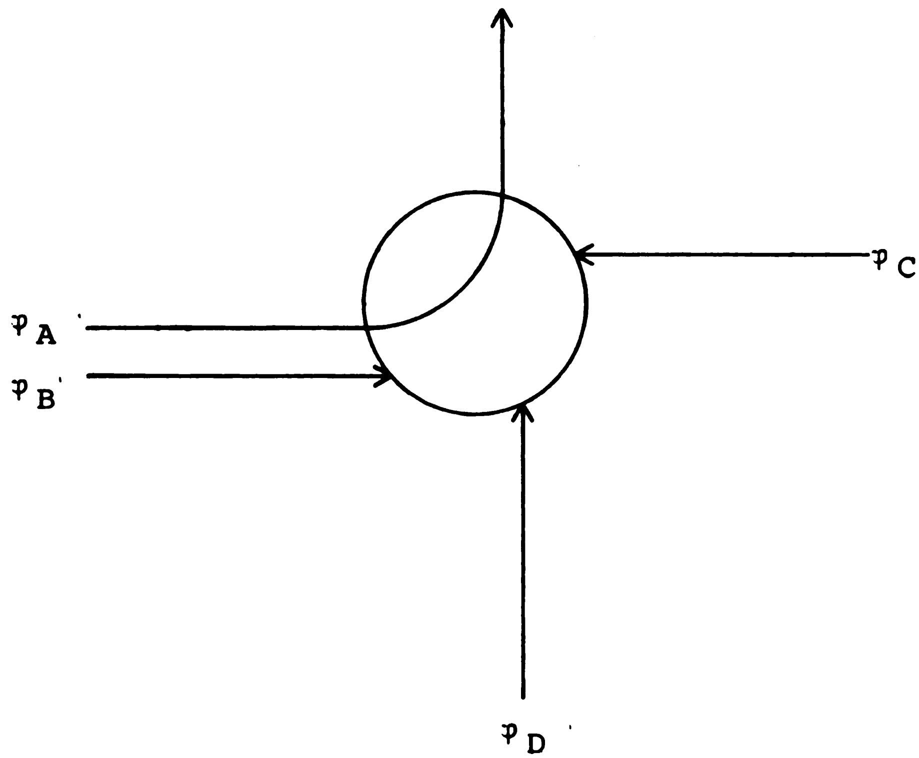

Figure 3.6 Four-Phase Overlapping Signal Model

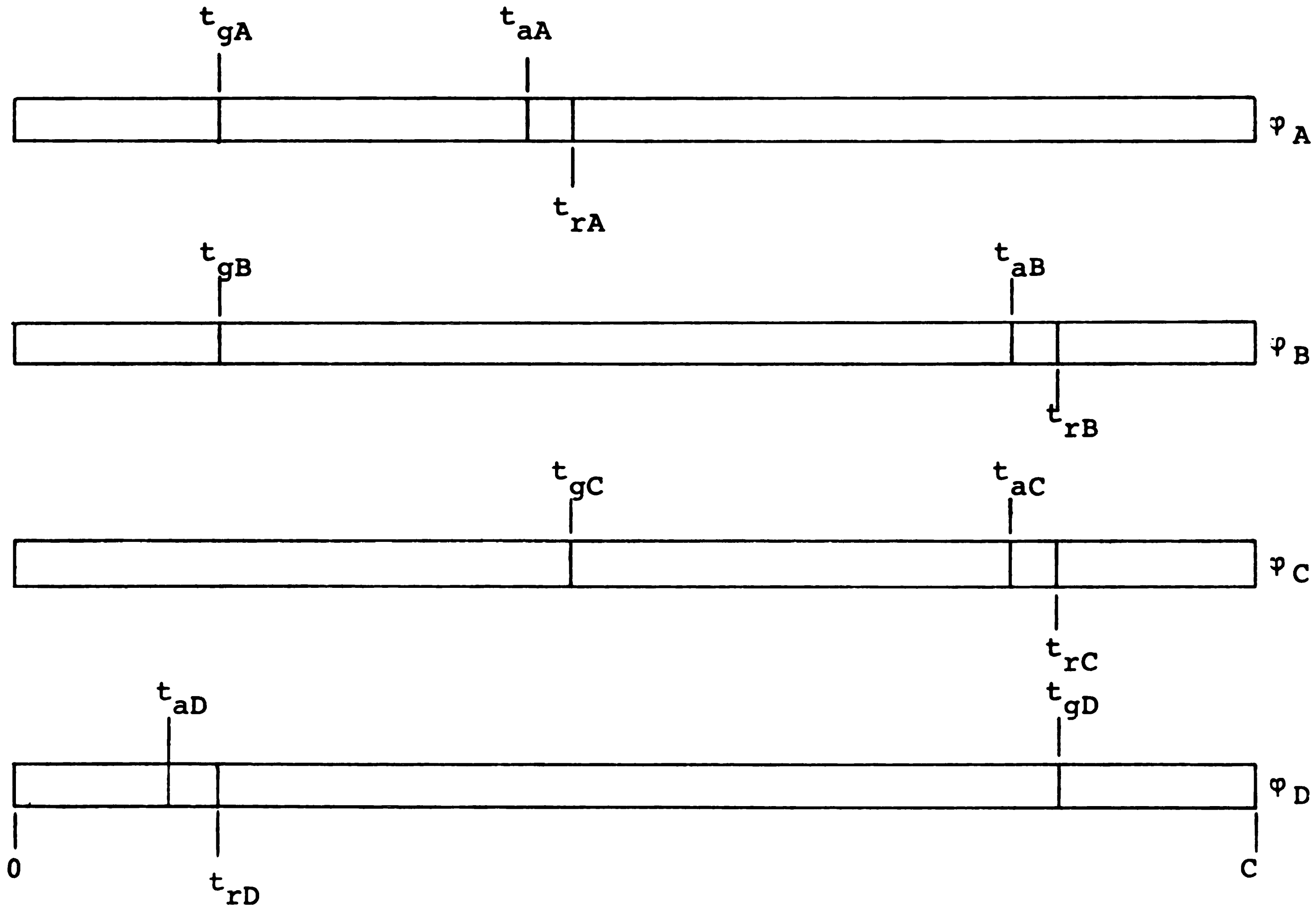

Figure 3.7 Single Cycled Timing of an Overlapping Four-Phase Signal

$$D_j = \begin{cases} \frac{1}{2}(1 - s_{ij})^2 C^2 c_j \\ \frac{1}{2}(1 - s_{iA} - s_{iC})^2 C^2 c_B \quad j = A,C. \\ \frac{1}{2}(s_{iA} + s_{iC}) C^2 c_D \end{cases} \tag{3.74}$$

In an analogous manner to the non-overlapping green's case of Section 3.6, it can be shown that:

$$\frac{\partial \bar{S}_i}{\partial s_{ij}} = KC(c_D - c_B - c_j)$$

$$\frac{\partial \bar{D}_i}{\partial s_{ij}} = C^2[(s_{iA} + s_{iC})W_D c_D - (1-s_{iA}-s_{iC})W_B c_B - (1-s_{ij})W_j c_j]$$

$$\frac{\partial \bar{R}_i}{\partial s_{ij}} = \frac{W_j h_j}{m_j}(K_{1j}s_{ij} + K_{2j}) \quad , \; j = A,C. \tag{3.75}$$

The minimum of the objective function, f_i, was obtained from examination of the second partial derivatives:

$$L_{jj} = \frac{\partial^2 f_i}{\partial s_{ij}^2} = C^2[W_D c_D + W_B c_B + W_j c_j] + \frac{W_j h_j K_{1j}}{m_j} > 0$$

$$L_{jk} = \frac{\partial^2 f_i}{\partial s_{ik} \partial s_{ij}} = C^2[W_D c_D + W_B c_B] > 0 \qquad j = A,C. \tag{3.76}$$

Then using equation set 3.64, it can be shown that

$$\Delta = \begin{vmatrix} L_{AA} & L_{CA} \\ L_{AC} & L_{CC} \end{vmatrix} = \begin{vmatrix} U + V_A & U \\ U & U + V_C \end{vmatrix}$$

$$= U(V_A + V_C) + V_A V_C > 0, \tag{3.77}$$

insures that the objective function has a relative minimum. This minimum $(\hat{s}_{iA},\hat{s}_{iC})$ results from

$$0 = \frac{\partial f_i}{\partial s_{ij}} = KC[c_D-c_B-c_j] + C^2[(s_{iA} + s_{iC})W_Dc_D -$$

$$(1-s_{iA}-s_{iC})W_Bc_B - (1-s_{ij})W_jc_j] + \frac{W_jh_j}{m_j}(K_{1j}s_{ij}+K_{2j})$$

$$j = A,C. \qquad (3.78)$$

Rearrangement of terms provides:

$$KC[c_j + c_B - c_D] + C^2(W_jc_j + W_Bc_B) - \frac{K_{2j}W_jh_j}{m_j}$$

$$= s_{ij}[C^2(W_Dc_D + W_Bc_B) + (C^2c_j + \frac{K_{1j}h_j}{m_j})W_j]$$

$$+ s_{ik}C^2(W_Dc_D + W_Bc_B)$$

$$j,k = A,C$$

$$j \neq k . \qquad (3.79)$$

The above equation can be set into matrix representation by letting

$$y_j = KC(c_j + c_B - c_D) + C^2(c_jW_j + c_BW_B) - \frac{K_{2j}W_jh_j}{m_j}$$

$$w_j = C^2(c_DW_D + c_BW_B) + (C^2c_j + \frac{h_jK_{1j}}{m_j})W_j \qquad (3.80)$$

$$w = C^2(c_DW_D + c_BW_B).$$

Then

$$\begin{bmatrix} y_A \\ y_C \end{bmatrix} = \begin{bmatrix} w_A & w \\ w & w_C \end{bmatrix} \begin{bmatrix} s_{iA} \\ s_{iC} \end{bmatrix} ,$$

or

$$\underline{Y} = \underline{W} \cdot \underline{S}_i \ . \qquad (3.81)$$

By comparing these results with those from Section 3.6, we can see that each overlapping green reduces the dimensions of the $\underline{W}$ matrix by 1.

3.8 Split Sensitivity

It has been shown in Kreer (KR1) that signal timing histograms developed by TRANSYT are insenitive to large volume changes within the network unless the volume changes cause one or more intersections to become saturated.

Knowledge of the sensitivity of the split equation will be of value to the traffic engineer when planning initial or changes to his traffic signal timing system. In order to determine the magnitude of the split sensitivity to cycle length, primary and secondary arrival flows, the split equation of Section 3.4 was used. For the i^{th} node, the following sensitivity equations were derived from the split equation by ordinary calculus methods:

$$\frac{\Delta\hat{s}_i}{\Delta C} \approx \frac{\partial\hat{s}_i}{\partial C} = \frac{2C[W_A c_A(1-\hat{s}_i) - W_B c_B \hat{s}_i] + K(c_A - c_B)}{\text{denom.}},$$

$$\frac{\Delta\hat{s}_i}{\Delta IN_A} \approx \frac{\partial\hat{s}_i}{\partial IN_A} = \frac{C[K + CW_A(1 - \hat{s}_i)]}{\text{denom.}}\left(\frac{c_A}{IN_A}\right)^2, \text{ and}$$

$$\frac{\Delta \hat{s}_i}{\Delta IN_B} \approx \frac{\partial \hat{s}_i}{\partial IN_B} = \frac{C[K + CW_B \hat{s}_i]}{\text{denom.}} \left(\frac{c_B}{IN_B}\right)^2 ,$$

where $\text{denom.} = C^2(W_A c_A + W_B c_B) + \frac{W_A h_A K_{1A}}{m_A} + \frac{W_B h_B K_{1B}}{m_B}$.

To illustrate these sensitivities, consider the intersection of two one-way streets controlled by a two phase signal with the following values:

1. Cycle length, $C = 60$ seconds, divided into 60 cycle units,
2. Delay weighting factors, $W_A = W_B = 1$,
3. Stop penalty factor, $K = 4$,
4. Saturation flows, $G_A = G_B = 4500$ vehicles/hour,
5. Random delay terms, $h_A/m_A = h_B/m_B = 50$.

These sensitivity equations are then solved for the ΔC, ΔIN_A, and ΔIN_B values which can be tolerated without varying the split, s_i, by $\pm$ 1 cycle units. For example, consider the situation where the primary and secondary flow rates are initially equal to 500 and 250 vehicles/hour respectively. The primary flow rate can increase by 6% to 530 vehicles/hour before the integer valued split estimate will increase by one cycle unit (0.0167 for the normalized split). A number of other variations in the cycle length, primary and secondary flow rates have been evaluated and summarized in Table 3.3.

Table 3.3: Split Sensitivity

Arrival Flow Rates IN_A (vehicles/hour)	IN_B (vehicles/hour)	Normalized Split s_i	Variation for a Split Change of $\pm$ 1 Cycle Unit: ΔC (seconds)	ΔIN_A (vehicles/hour)	ΔIN_B (vehicles/hour)
250	250	.500	∞	± 13.9	± 13.9
500	250	.704	∓ 40.6	± 30.0	± 15.9
750	250	.809	∓ 27.0	± 52.3	± 19.7
1000	250	.873	∓ 22.5	± 80.8	± 24.5
250	500	.296	± 40.6	± 15.9	± 30.0
500	500	.500	∞	± 26.1	± 26.1
750	500	.631	∓ 64.1	± 38.8	± 27.6
1000	500	.722	∓ 37.9	± 54.0	± 30.9
250	1000	.127	± 22.5	± 24.5	± 80.8
500	1000	.278	± 37.9	± 30.8	± 54.0
750	1000	.400	± 84.2	± 37.9	± 47.2
1000	1000	.500	∞	± 45.7	± 45.7

One can conclude that the sensitivity of the split equation is dependent upon the actual magnitude of the cross flow rates in addition to their relative values.

CHAPTER IV

ARTERIAL OFFSET CALCULATION

4.1 Time-Space Diagrams

For years, traffic engineers have used time-space diagrams as a visual aid in studying the behavior of vehicle movement on an arterial. These diagrams illustrate the split for each signalized intersection along an arterial as well as the offsets between the signals. It should be noted that the vehicle speeds between any two adjacent signals can be different from those for any other set of adjacent signals. This results in the outbound and inbound green bands taking on a zig-zag slope (Figure 4.1) instead of the constant slope bands for constant velocity along the entire street (Figure 4.2).

4.2 Maximal Arterial Bandwidth

Now consider an urban bidirectional roadway with a number of signalized intersections all with a common cycle time. The widths of the outbound and inbound progression green bands, shown in Figures 4.1 and 4.2, are the outbound and inbound maximal bandwidths, respectively. A progression is determined by the splits, the offsets, and the cycle length.

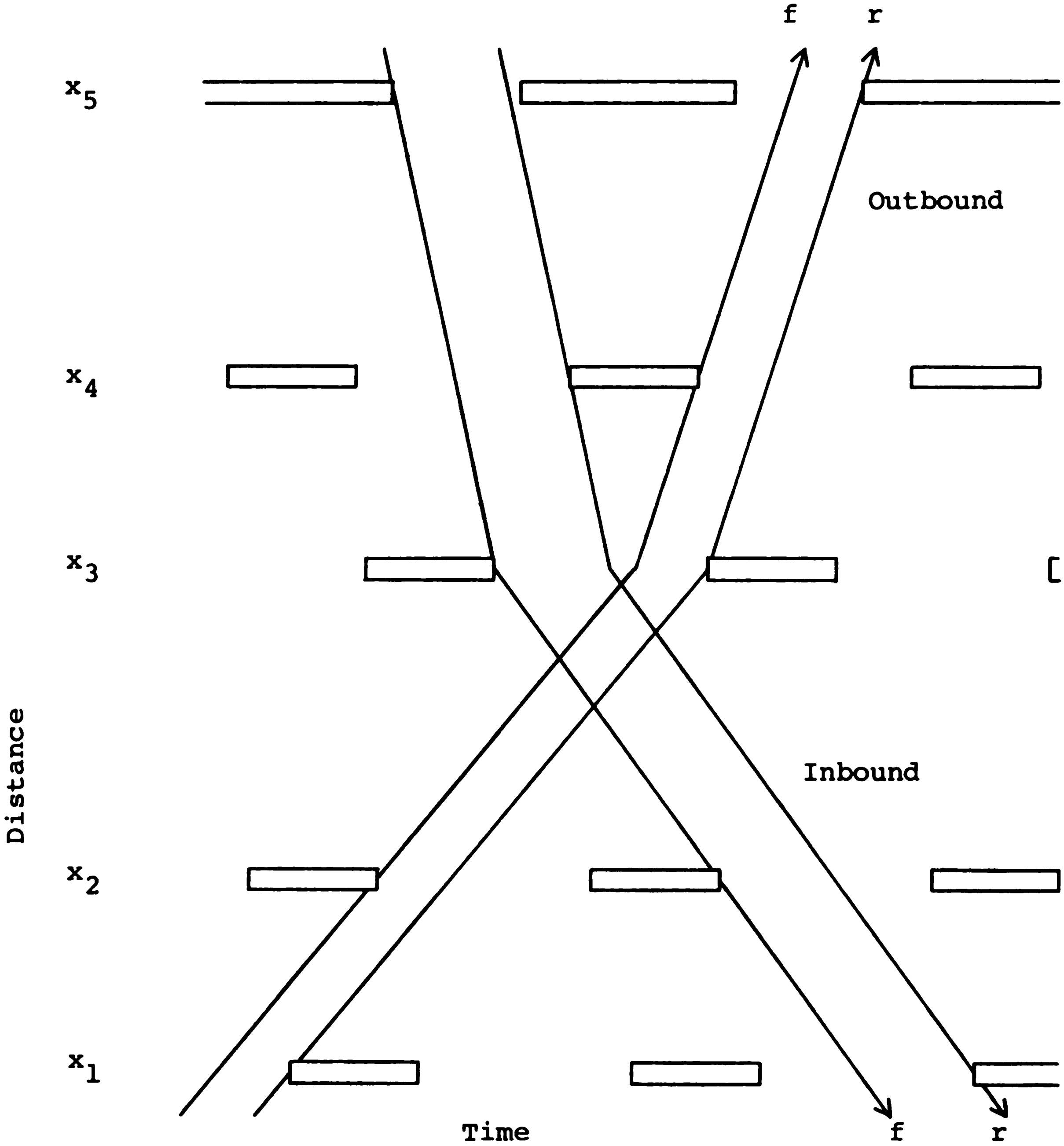

Figure 4.1 Typical Time-Space Diagram

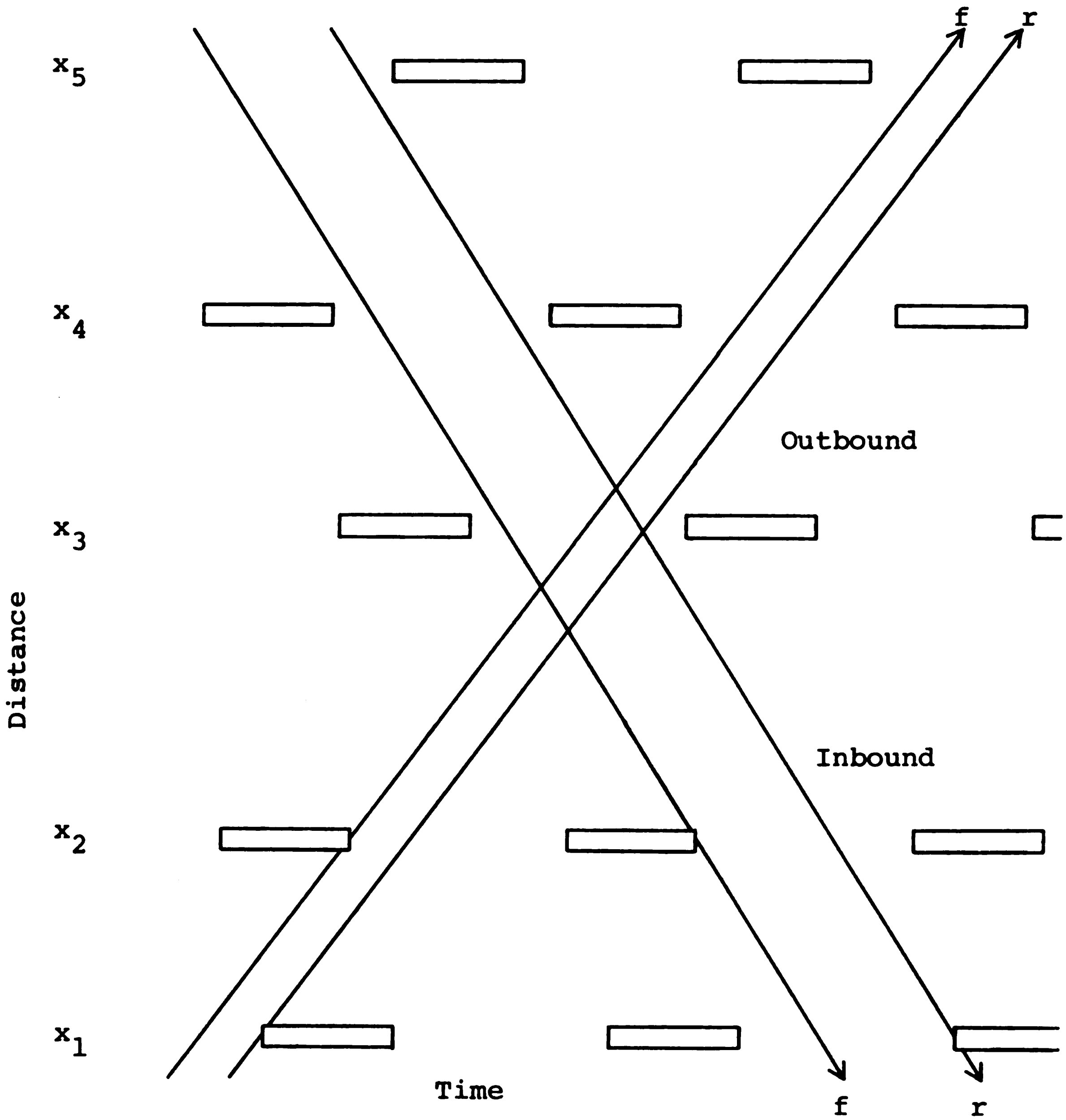

Figure 4.2 Typical Constant Velocity Time-Space Diagram

The objective function for an arterial is sometimes chosen as the maximization of bandwidth. Morgan and Little (LM1) have developed an algorithm based upon this concept where they offer solutions to the following two problems:

1. Given a common cycle length, splits for each signal, the vehicle speeds between adjacent signals, determine the set of offsets which will produce bandwidths which are equal in each direction and as large as possible, and

2. Adjust the set of offsets to increase one of the two bandwidths, when possible, while giving the other direction the largest bandwidth then possible.

Before proceeding, a set of terms need to be defined for the remainder of the maximal bandwith discussion. These are:

r_j = red time for node j on the street being studied (cycles),

$b(\bar{b})$ = outbound (inbound) directional bandwidth (cycles),

x_j = location of node j downstream from the reference point (feet),

$v_j(\overline{v_j})$ = outbound (inbound) vehicle speed along link j (feet/sec.),

$\tau_{ij}(\overline{\tau_{ij}})$ = travel time from node i to node j in the outbound (inbound) direction (cycles), C = cycle length (sec./cycle),

θ_{ij} = relative offset from node i to node j measured between the center of the red intervals of the two nodes (cycles),

g = minimum green of all nodes along the arterial (cycles),

α_j = offset shift of node j for unequal bandwidth (cycles),

$p(\bar{p})$ = outbound (inbound) platoon length (seconds),

m = number of nodes or signals along the arterial.

By convention, $0 \leq \theta_{ij} < 1$ and the set $\{\theta_{ij} | j = 1,\ldots,m\}$ for any i is called a synchronization of the m signals along the street in question.

The travel times between the i^{th} and j^{th} signals are determined from

$$\tau_{ij} = \begin{cases} \sum_{k=i}^{j-1} \tau_{k,k+1} & j > i \\ 0 & j = i \\ -\sum_{k=j}^{i-1} \tau_{k,k+1} & j < i \end{cases} \tag{4.1}$$

and the $\bar{\tau}_{ij}$ are obtained by replacing each τ with $\bar{\tau}$. Then for two sequential intersections, namely i and (i + 1),

$$\tau_{i,i+1} = \frac{x_{i+1} - x_i}{v_i C}$$
$$\bar{\tau}_{i,i+1} = \frac{x_i - x_{i+1}}{\bar{v}_i C} \quad (4.2)$$

By definition, a signal is called 'critical' if one side of its red touches the green band in one direction and the other side touches the green band in the other direction. Morgan and Little's approach was to maximize the directional bandwidths b and $\bar{b}$. It was determined that all critical signals must fall into at least one of the two groups defined as follows:

a) Group 1: consist of signals with reds touching the front of the outbound and the rear of the inbound, and

b) Group 2: where reds touch the front of the inbound and the rear of the outbound.

With the aid of Figures 4.3, 4.4, and 4.5 for the various combinations of Group 1 and 2 signals the offset relations can be written as:

$$0 \le \theta_{ij} = \frac{1}{2}(\tau_{ij} + \bar{\tau}_{ij}) + \frac{1}{2}(\text{integer}) < 1. \quad (4.3)$$

This leads to two possible solutions (0 and 1/2) and is 'half-integer synchronization' for the maximal equal bandwidth case.

By defining man $(\cdot)$ = mantissa of $(\cdot)$; obtained by dropping the integer portion and adding unity if the result is negative; and $d_{ij} = 0, 1/2$, we have

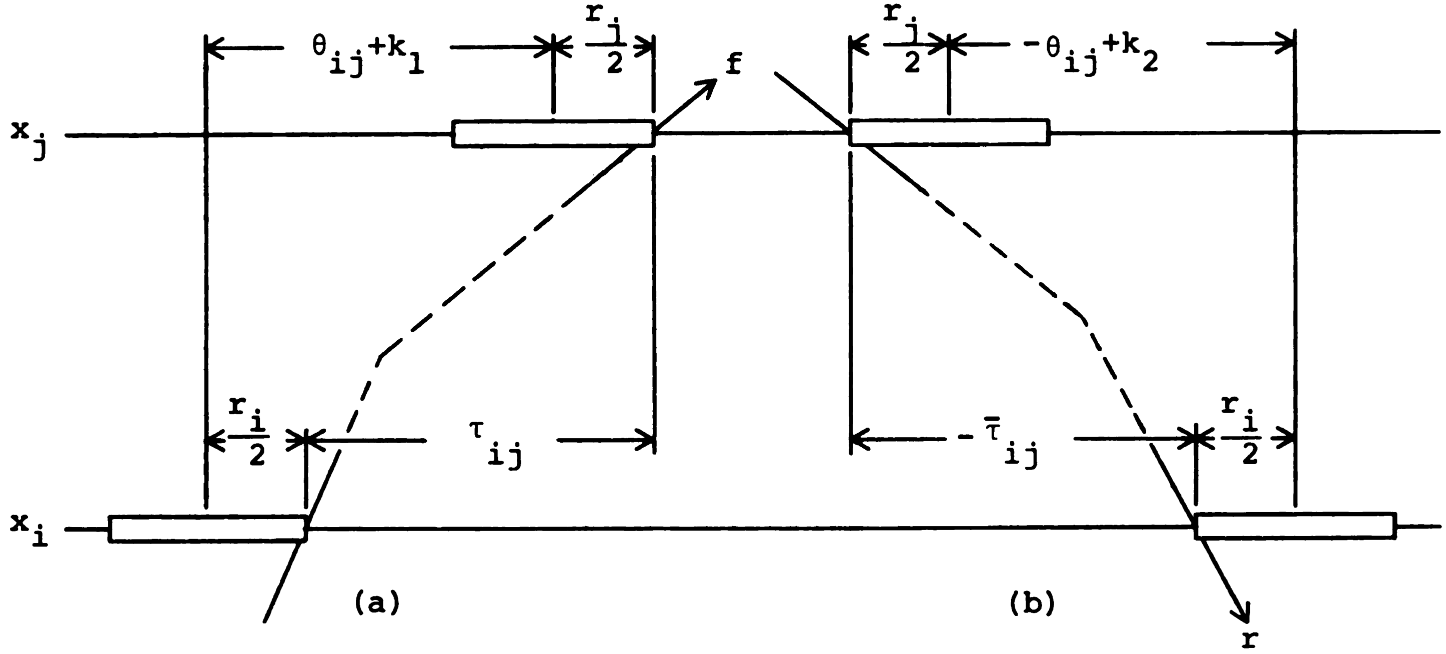

Figure 4.3 Two Group 1 Signals Limiting the Green Band

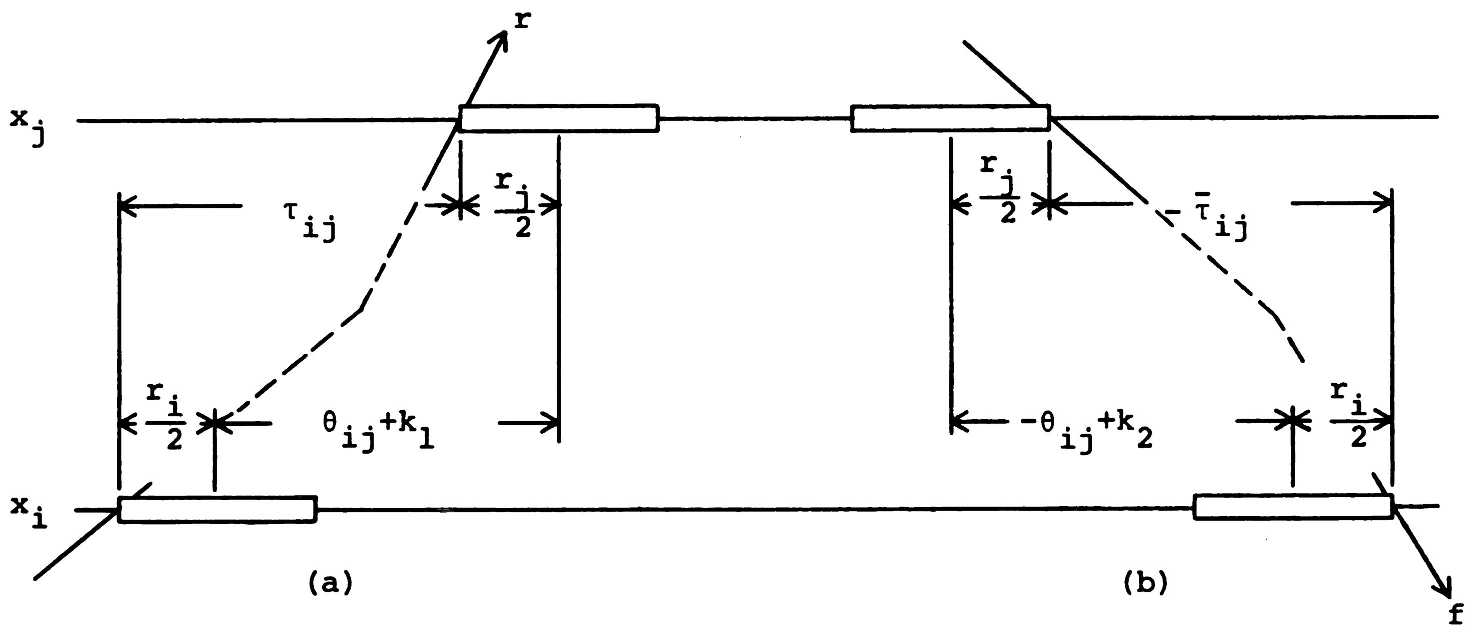

Figure 4.4 Two Group 2 Signals Limiting the Green Band

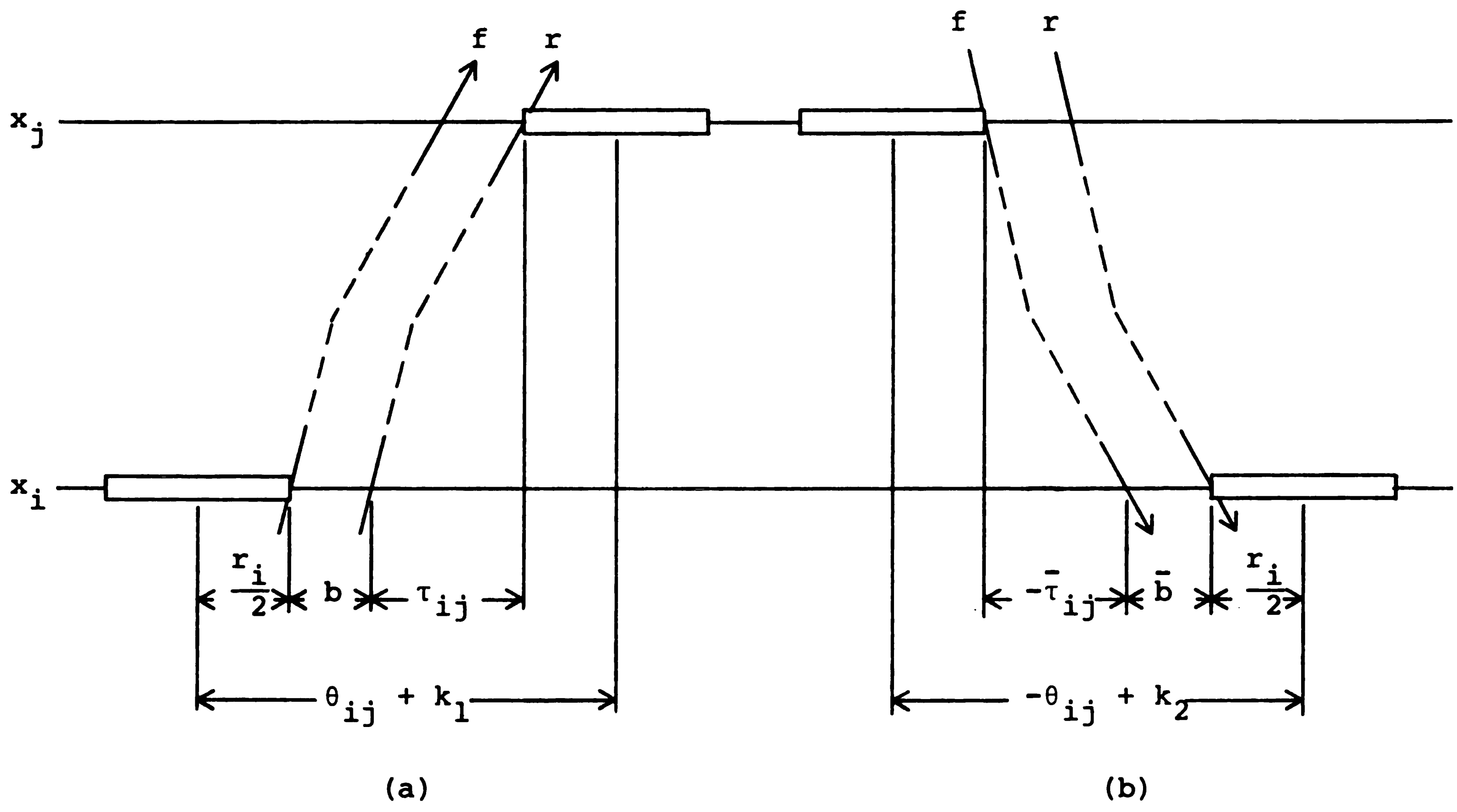

Figure 4.5 A Group 1 Signal and a Group 2 Signal Limiting the Green Band

$$\theta_{ij} = \text{man}[\tfrac{1}{2}(\tau_{ij} + \bar{\tau}_{ij}) + d_{ij}]. \tag{4.4}$$

If the i^{th} signal's red touches the front of the outbound green band, it appears as shown in Figure 4.3a. By taking the right side of the i^{th}'s red as the origin, the trajectory (not shown) touching the right side of the j^{th}'s red passes the i^{th} signal at a point in time:

$$u_{ij} = 1 - \text{man}[\tfrac{1}{2}(r_i - r_j) + \tfrac{1}{2}(\tau_{ij} - \bar{\tau}_{ij}) - d_{ij}] \ . \tag{4.5}$$

The trajectory touching the left of the j^{th} red passes the i^{th} signal at $u_{ij} - r_j$. Thus since $d_{ij} = 0$ or $1/2$ and the i^{th} red must touch the front, we get the main result of Morgan and Little's paper, namely:

$$B = \max\{\max_i \min_j \max_{d_{ij}}[u_{ij}(d_{ij}) - r_j],\ 0\}, \tag{4.6}$$

and a maximal equal bandwidth synchronization, $\{\theta_{c1},\ldots,\theta_{cm}\}$.

Now in an effort to summarize the Morgan-Little offset method for equal bandwidths, the next five steps are listed.

1. Calculate the set $Y = (y_j | j \in [1,m])$ from $y_1 = 0$

$$y_j = y_{j-1} - \tfrac{1}{2}(r_j - r_{j-1})$$

$$+ \frac{1}{2C}(x_j - x_{j-1})\left(\frac{1}{v_{j-1}} + \frac{1}{\bar{v}_{j-1}}\right). \tag{4.7}$$

2. Calculate the set $Z = (z_j | j \in [1,m])$

from $z_1 = 0$

$$z_j = z_{j-1} + \frac{1}{2C}(x_j - x_{j-1})\left(\frac{1}{v_{j-1}} - \frac{1}{\bar{v}_{j-1}}\right). \quad (4.8)$$

3. Calculate the set $U = (u_{ij} | i,j \in [1,m])$

from $u_{ij}(d) = 1 - \mathrm{man}(y_j - y_i - d_{ij})$,

$$d_{ij} = 0, 1/2. \quad (4.9)$$

4. After completing the previous three steps, we have the maximum equal directional bandwidths

$$B = \max\{\max_i \min_j \max_{d_{ij}} (u_{ij}(d_{ij}) - r_j),\ 0\}. \quad (4.10)$$

5. Then a two-way synchronization $(\theta_{c1}, \ldots, \theta_{cm})$ for maximal bandwidths is determined from

$$\theta_{cj} = \mathrm{man}(z_j - z_c + d_{cj}). \quad (4.11)$$

In general, either the outbound or the inbound flow is greater; very seldom will they be exactly equal. This unequal flow condition is a function of the time of day and relative locations of residential, work, and recreational areas in any given geographical setting. The resulting morning and afternoon peak traffic flows may dictate different bandwidths as a function of time during the day or week.

Morgan and Little suggested dividing the total available bandwidth, 2B, between the two directions on the basis of platoon lengths p and $\bar{p}$, where they defined platoon length (in seconds) as the hourly volume times the vehicle headway divided by 3,600. The shifting procedure used to obtain the unequal directional bandwidths, b and $\bar{b}$, was developed from Figure 4.6. To shift the front of the outbound band from f to f' in order to obtain the directional bandwidth b, we have

$$\alpha_j = \max[(u_{cj} - 1) - (B - b), 0] \tag{4.12}$$

for

$$\max[0,B] \le b \le g .$$

To obtain the inbound bandwidth $\bar{b}$, the shift of the rear of the inbound band from r to r' is achieved by

$$\alpha_j = \max[\bar{b} - (u_{cj} - r_j), 0] \tag{4.13}$$

for

$$\max[0,B] \le \bar{b} \le g.$$

An important point to remember is that only one of these bandwidth shifts can be made for any one arterial since the second is dependent on the other and the total available bandwidth.

Summarizing the unequal directional flow cases, we take the following steps.

The total bandwidth can be divided between the two opposing directions by first calculating the minimum green time band.

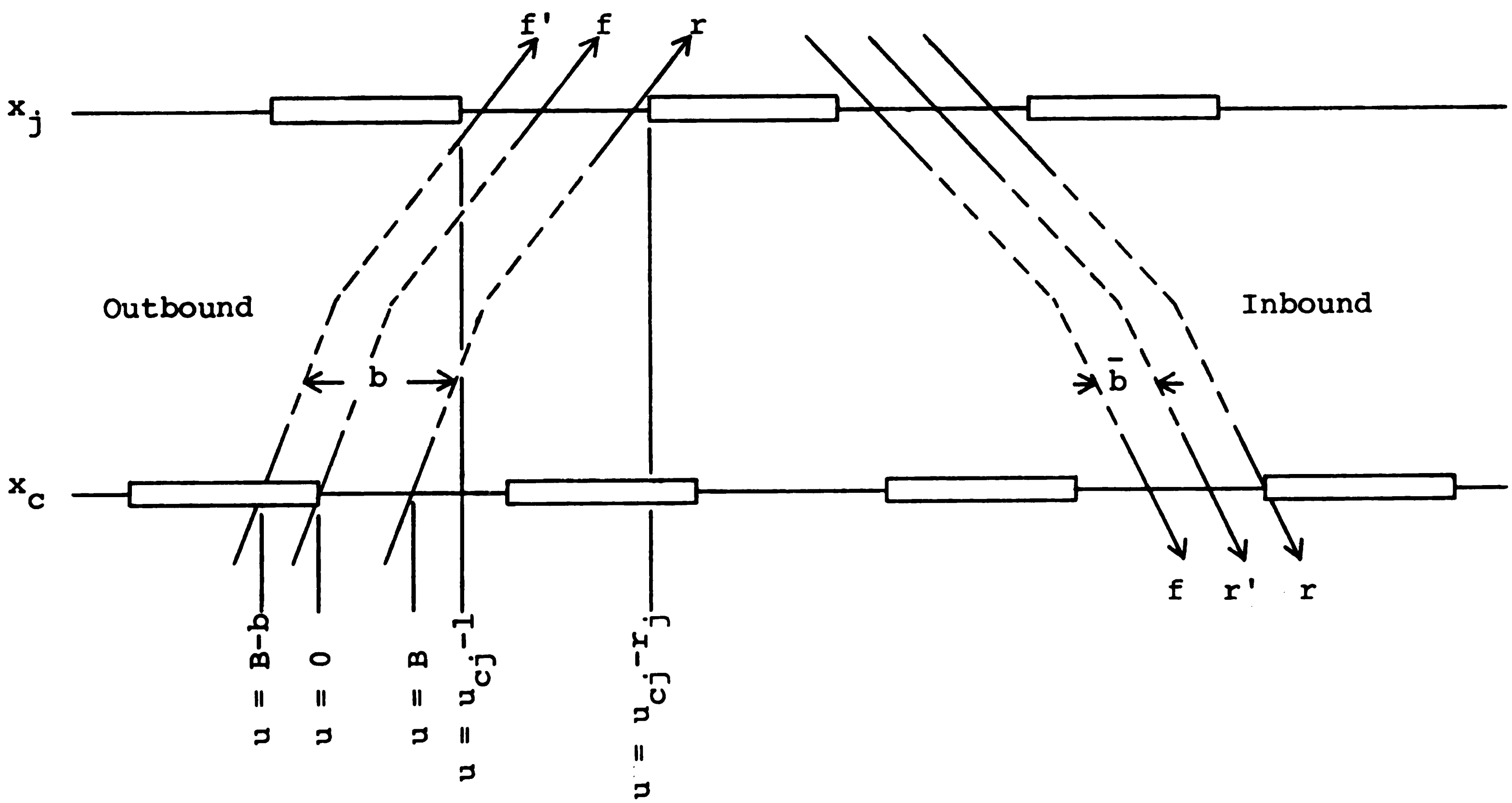

Figure 4.6 Adjustment of the Green Bands

$$g = \min_i(1 - r_i) = 1 - \max_i(r_i). \qquad (4.14)$$

Then for the inbound arrivals less than the outbound $(\bar{p} < p)$.

1. Calculate the larger bandwidth from

$$b = \begin{cases} \min(g, 2B\ p/(p + \bar{p})) & \text{if} \quad p+\bar{p} \leq 2B \\ g & p \geq 2B \\ \min(g,p) & \text{other} \end{cases} \qquad (4.15)$$

2. Calculate the adjustment set $(\alpha_1,\ldots,\alpha_m)$ from

$$\alpha_j = \max(u_{cj} - 1 + b - B,\ 0), \qquad (4.16)$$

where the u_{cj}'s were a result of step 3 above.

3. Calculate the smaller bandwidth from

$$\bar{b} = \max(2B - b,\ 0). \qquad (4.17)$$

4. Then an adjusted two-way synchronization $(\theta_{c1},\ldots,\theta_{cm})$ is obtained from

$$\theta_{cj} = \text{man}(z_j - z_c + d_{cj} - \alpha_j). \qquad (4.18)$$

If the opposite case exists $(\bar{p} > p)$, then

1. Calculate the larger directional bandwidth from

$$\bar{b} = \begin{cases} \min(g,\ 2B\ \bar{p}/(p + \bar{p})) & \text{if} \quad p+\bar{p} \leq 2B \\ g & \bar{p} \geq 2B \\ \min(g,\bar{p}) & \text{other} \end{cases} \qquad (4.19)$$

2. Calculate the adjustment set $(\alpha_1,\ldots,\alpha_m)$ from

$$\alpha_j = \max(\bar{b} + r_j - u_{cj}, 0). \qquad (4.20)$$

3. Calculate the smaller directional bandwidth from

$$b = \max(2B - \bar{b}, 0). \qquad (4.21)$$

4. Then an adjusted two-way synchronization $(\theta_{c1},\ldots,\theta_{cm})$ is obtained from

$$\theta_{cj} = \mathrm{man}(z_j - z_c + d_{cj} - \alpha_j). \qquad (4.22)$$

CHAPTER V

TRANSYT/G OFFSET CALCULATION

Now that the maximal arterial bandwidth concept of Morgan and Little has been described in Chapter IV, several modifications will be presented. Even though the basic maximal bandwidth procedure has appeal for non-iterative offset calculations, this author considers this algorithm to have several disadvantages, namely:

1. The criterion given for the apportionment of unequal bandwidths does not include turning movements,
2. Queue growth and decay are ignored, and
3. The arterial concept needs to be extended to networks

Because of these disadvantages, the set of Morgan-Little offsets may or may not minimize the previously defined objective function of stops and delays for a network.

A reasonably good set of signal offsets may be obtained provided that the effects of these above mentioned detriments are sufficiently minimized. This author feels that an optimization procedure such as the hillclimbing method is not required. In its place, Morgan and Little's method was used as a base from which the TRANSYT/G offsets were determined.

In addition to the terms defined in Chapter IV, several terms pertaining to the TRANSYT/G offset adjustments are listed below.

β_{cj} = the offset shift of node j relative to the critical node for queue clearance (cycles),

$\gamma_{cj}(\bar{\gamma}_{cj})$ = the excess green to the right of the rear edge of the outbound (inbound) bandwidth for node j relative to the critical node (cycles),

$\mu(\bar{\mu})$ = the outbound (inbound) average cumulative arrivals, and

ϕ_{cj} = the TRANSYT/G offset for node j relative to the critical node (cycles).

5.1 Unequal Bandwidth Apportionment

In the opinion of this author, Morgan and Little's definition of platoon length does not reflect the dependence upon turning movements and thus is not responsive enough to the vehicle flow rates within the system. Therefore it is suggested that the total bandwidth should be apportioned between the two directions of flow on the basis of the cumulative number of arrivals, $I_j(t_{rj} + C)$, for each direction of flow. The turning movements are taken into account in the definitions of the average arrival demand, μ. The cumulative arrivals averaged over all the links comprising the outbound direction of flow is

$$\mu = \frac{1}{m} \sum_{j=1}^{m} I_j (t_{rj} + C) . \tag{5.1}$$

There exists a similar relation $\bar{\mu}$ for the inbound direction. Since the cumulative arrival terms are reasonably estimated in the TRANSYT/G flow model, the turning movements can exert their influence upon the offset determinations.

As an illustration of this total bandwidth apportionment, consider the two three-signal arterials of Figure 5.1. In both cases, (a) and (b), Morgan and Little would apportion the total bandwidth equally since

$$p = \bar{p} = \frac{1000}{3600} = 0.277 \; . \tag{5.2}$$

This author would apportion the total bandwidth unequally for both cases. In case (a) where $\mu < \bar{\mu}$,

$$\begin{aligned} \mu &= \frac{1000 + 300 + 300}{3} = 533., \text{ and} \\ \bar{\mu} &= \frac{1000 + 1000 + 1000}{3} = 1000. \end{aligned} \tag{5.3}$$

For case (b), $\mu > \bar{\mu}$ and

$$\begin{aligned} \mu &= \frac{1000 + 1500 + 1500}{3} = 1333., \\ \bar{\mu} &= \frac{1000 + 1000 + 1000}{3} = 1000. \end{aligned} \tag{5.4}$$

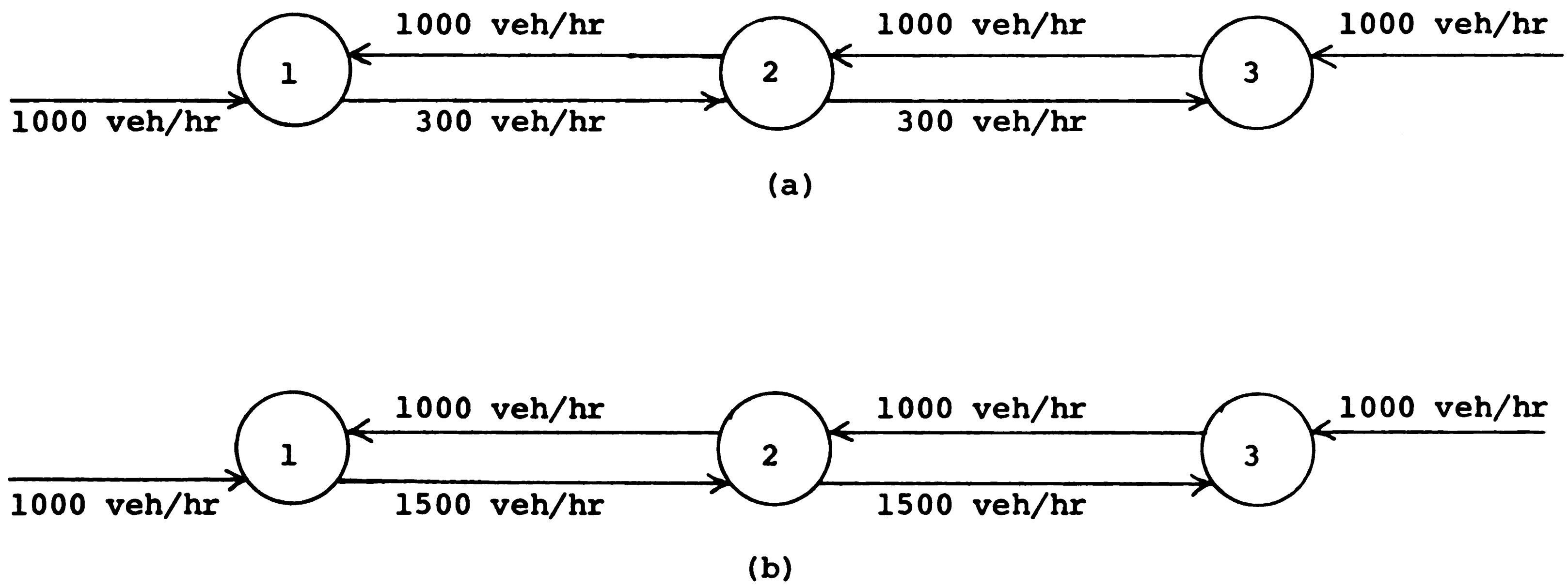

Figure 5.1 Total Bandwidth Apportionment as a Function of Cumulative Arrivals

With the aid of Figure 5.1, it is obvious that unequal bandwidths are called for, thus the use of $\mu(\bar{\mu})$ is preferred to $p(\bar{p})$ for apportionment.

5.2 Excess Green Adjustment

Now the second shortcoming of Morgan and Little's offset method will be alleviated, namely the consideration of the requirements imposed on the offsets by the need to start the clearing of queues prior to the arrival of the next platoon.

Panyan (PA1) describes the situation where the progression band occupies the total green time of the signal having the minimum green. He suggests shifting <u>all</u> the excess green of the remaining signals to the left, earlier in time, to allow the queues to start decaying prior to the arrival of the next platoon. This queue clearance shift of excess green time can be derived from Figure 5.2 by taking a reference point at the center of the Group 1 critical signal's red time interval. For signal j, we have:

$$\begin{aligned} \gamma_{cj} &= \text{man}[\theta_{cj} - \tfrac{1}{2}(r_c + r_j) - b - \tau_{cj}\text{sgn}(j - c)] \\ \bar{\gamma}_{cj} &= \text{man}[\theta_{cj} + \tfrac{1}{2}(r_c - r_j) + \bar{\tau}_{cj}\text{sgn}(j - c)] \end{aligned} \tag{5.5}$$

where these excess green times lie within the following bounds:

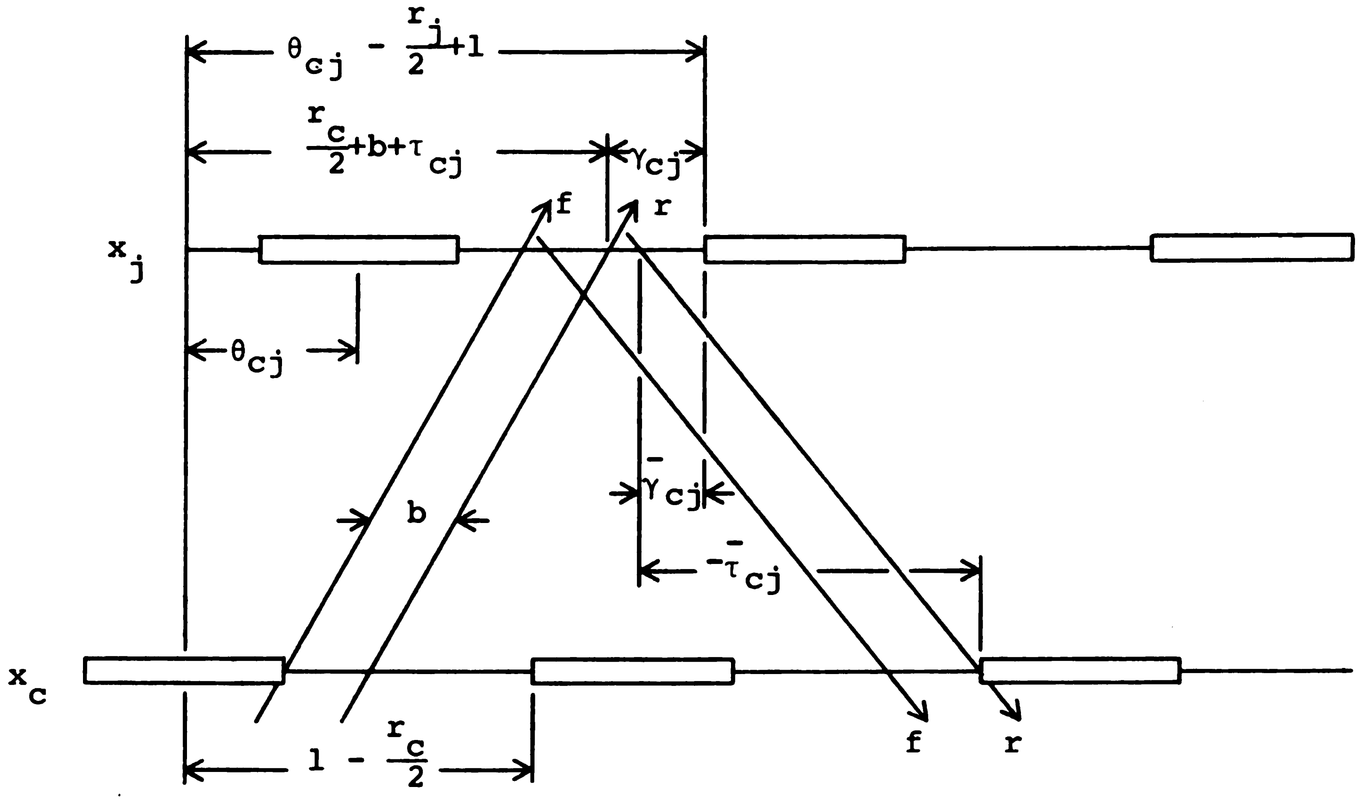

Figure 5.2 Shifting of Excess Green Time for Queue Clearances

$$
\begin{aligned}
&0 \le \gamma_{cj} \le 1 - r_j - b, \\
&0 \le \bar{\gamma}_{cj} \le 1 - r_j - \bar{b} \;.
\end{aligned}
\qquad (5.6)
$$

Since the magnitude of γ_{cj} and $\bar{\gamma}_{cj}$ are unequal for the unequal bandwidth cases, one only wants to shift the excess green of the j^{th} signal by the smaller of the γ_{cj} and $\bar{\gamma}_{cj}$ quantities so as not to restrict either directional bandwidth. Thus the shift of the j^{th} offset relative to the critical node, c, would be

$$\beta_{cj} = \min(\gamma_{cj}, \bar{\gamma}_{cj}) \ge 0. \qquad (5.7)$$

This queue clearance shift would be applied to all signals other than the critical signals resulting in the start of all red times touching the rear of the progression green bands.

There is one important drawback to Panyan's shift of all the available excess green time, namely: that none of the excess green is available to the right of the progression band for stragglers at the end of the platoon. Thus Panyan's 100% excess green shift may not be the optimum choice. This author proposes that the excess green shift should be some intermediate value between Panyan's 100% shift and the 0% shift inherent in the Morgan-Little method. This proposed shift for the j^{th} signal is made relative to the Morgan-Little offsets, θ_{cj}, described in Chapter IV. The resulting TRANSYT/G offsets are:

$$\phi_{cj} = \text{man}[\theta_{cj} - k_j\beta_{cj}\text{sgn}(j - c)] \qquad (5.8)$$

where the multiplicative shift terms, k_j, range between 0.0 and 1.0 and are determined during the initial check-out of each network application.

Again referring to Figure 5.2, consider the possibility that the j^{th} signal is also critical, $j = c'$, along our selected street. Two possibilities exist: c' belongs to either Group 1 or to Group 2. It is noted that for $c \in$ Group 1, and

$$\begin{array}{ll} & c' \in \text{Group 1}, \ \gamma_{cc'} \neq 0 \ \text{ and } \ \bar{\gamma}_{cc'} = 0, \\ \text{or} & \\ & c' \in \text{Group 2}, \ \gamma_{cc'} = 0 \ \text{ and } \ \bar{\gamma}_{cc'} \neq 0. \end{array} \qquad (5.9)$$

In either situation, $\beta_{cc'} = 0$ and is the expected shift between two critical signals along the same street.

5.3 Network Considerations

Now that the author's offsets have been developed for arterials, an extension to networks requires the proper interface of signal timings between the arterials and cross streets.

The offsets for a general network are determined by applying the author's arterial offset concept to a subset of all the possible streets within the network according to the following constraints. Each signalized street selected will be referred to as a vein. When constructing a vein-interconnection model:

1. Each intersection must be included in one of the veins,
2. All veins after selection of the first must begin at an intersection belonging to a previously selected vein to insure proper relative timing,
3. No closed loops are to be formed when selecting these veins,
4. Attempt to select streets with the heavier traffic flows as veins first, and
5. Attempt to select as few veins as possible.

The vein-interconnection model is simply an overlay of the general network such that no set of veins form a closed loop. It forms the sequential order in which the offsets are estimated.

The first three rules are inherent in this author's offset method while rules 4 and 5 generally help one construct a vein-interconnection model having a lower final objective function value.

The actual equations for the start of the green and red time intervals can be visualized from Figures 5.2 and 5.3. By definition, let

δ = the relative shift due to the phasing at the interconnecting node between two veins, such as at node j in Figure 5.3.

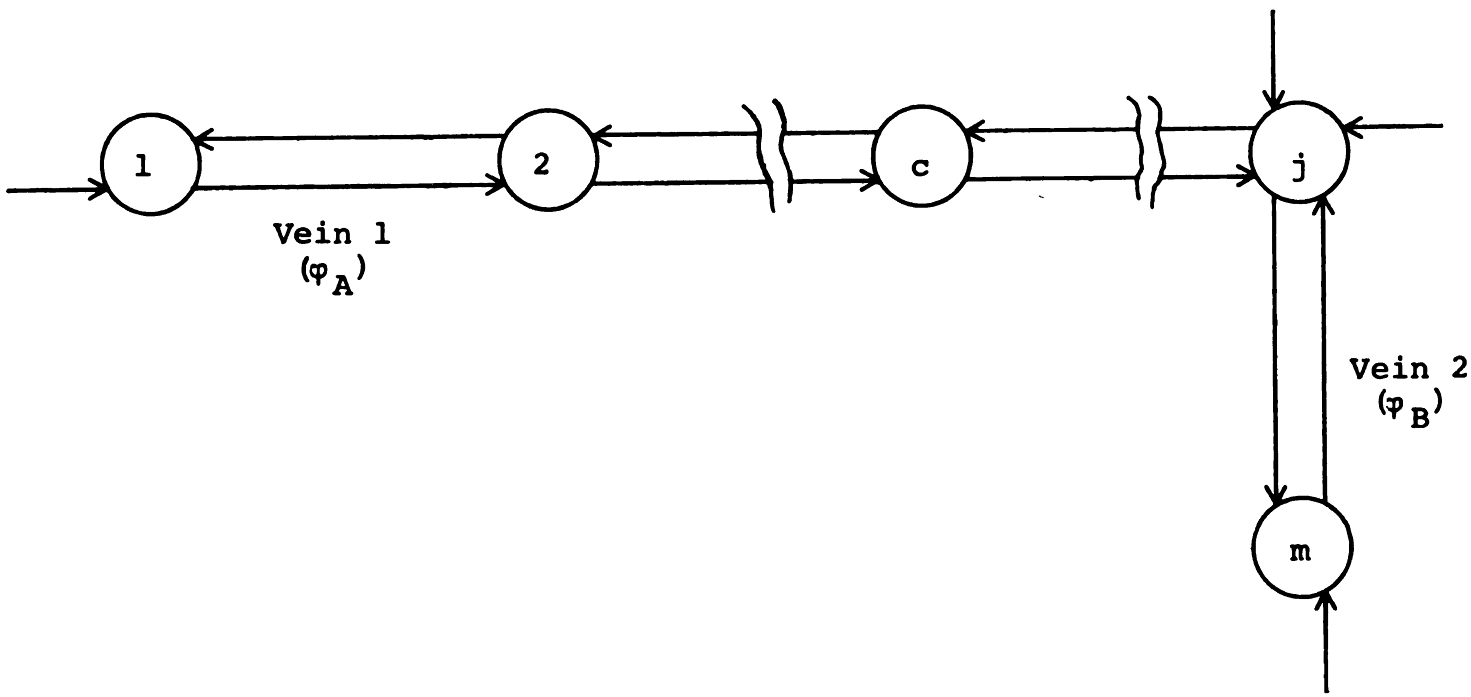

Figure 5.3 Interconnection of Two, Two-Way Veins

Since node 1 is the first to be considered in our example, we can select $\delta = 0$, or any other convenient value. Thus for $\delta = 0$ on vein 1, the φ_A green for node 1 will start at zero. Next, the φ_A green for node 2 starts at $\text{man}[\frac{1}{2}(r_2 - r_1) + \phi_{c2} - \phi_{c1}]$. For vein 2, belonging to φ_B here, δ equals the newly calculated φ_A node j starting green time minus its red time interval. In summary, the green and red time intervals on a two-way vein are shifted according to:

$$t'_{gj} = \text{man}[\tfrac{1}{2}(r_j - r_1) + \phi_{cj} - \phi_{c1} + \delta] \qquad (5.6)$$

where

$$\delta = \begin{cases} 0 & \text{for vein 1} \\ t'_{gi} - r_i & \text{for all other veins where } i \text{ is the cross phase at the interconnecting node} \end{cases}$$

and

$$t'_{rj} = t'_{gj} + (t_{rj} - t_{gj}) \quad \text{for} \quad 1 \le j \le n \qquad (5.7)$$

The primed and unprimed symbols represent the new and previous values respectively.

If the vein is a one-way, there is only one bandwidth and it equals the minimum green of all the nodes associated with that particular vein. In this case, equation 5.6 is replaced by

$$t'_{gj} = \text{man}[r_j - r_1 + \tau_{1j} + (1 - k_j)(1 - r_j - g) + \delta] \qquad (5.8)$$

In the next chapter, two applications to general urban traffic networks will be illustrated in detail.

CHAPTER VI

NETWORK APPLICATIONS

Now that this author's signal timing method has been developed in the previous chapters, two applications to actual urban areas will be illustrated. First, a 21 intersection portion of the Ft. Wayne, Indiana downtown area was selected for comparison of TRANSYT/G versus the standard hillclimbing TRANSYT. Certain non-critical modifications of the network configuration were made. Vehicle volumes, speeds, turning movements and physical dimensions were supplied by Ft. Wayne officials.

The second application consisted of a modified 38 intersection portion of Washington, D.C. This location was selected due to availability of geometric and traffic data similar to the Ft. Wayne data.

To evaluate the effectiveness of the new signal timing method proposed by this author, data from the above mentioned example areas were used in two computer programs, namely; TRANSYT and TRANSYT/G.

6.1 Link Numbering System

The link numbering system is keyed to the node numbers such that node number i becomes the first part of the link number. The last digit of the link number takes on a value from 0 to 7 depending upon the direction of flow into the i^{th} node. Links entering the node from the north, east, south, west, northeast, southeast, southwest, and northwest are assigned the values 0,...,7, respectively for their last digit (Figure 6.1a). Figure 6.1b illustrates this technique for an intersection of two two-way streets at node number 9.

6.2 Selection of Networks

In Ft. Wayne, an area bounded by Main Street on the north, Jefferson on the south, Fairfield on the west, and Lafayette on the east was selected. The node-link model selected for this region consists of 21 nodes, one for each signalized intersection, and 56 links, one for each directional flow including 6 dummy links required to break loops for the TRANSYT calculations. Main and Harrison Streets are two-way while the other eight streets are one-way, as indicated in Figure 6.2.

Using the guidelines outlined in Chapter V, a vein interconnection model required for TRANSYT/G was selected and is illustrated as heavy black in Figure 6.3. Since this vein interconnection model is not unique, other suitable models could have been selected.

In Washington, D.C., the node-link model selected consisted of 38 nodes and 134 links including 21 dummy

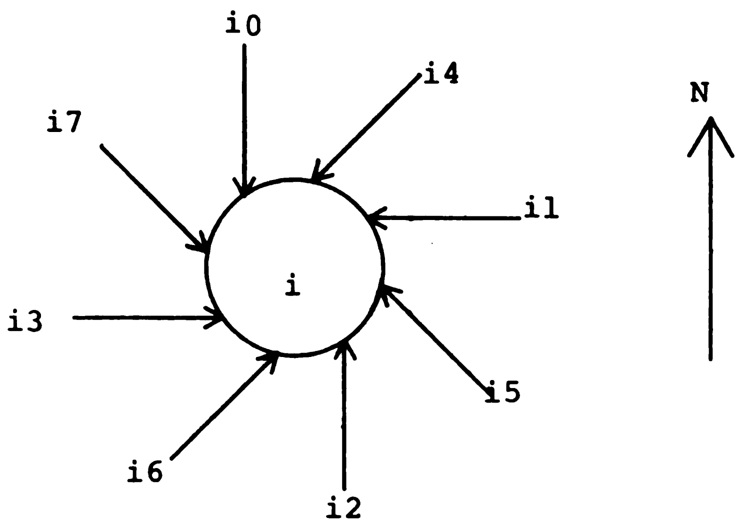

(a)

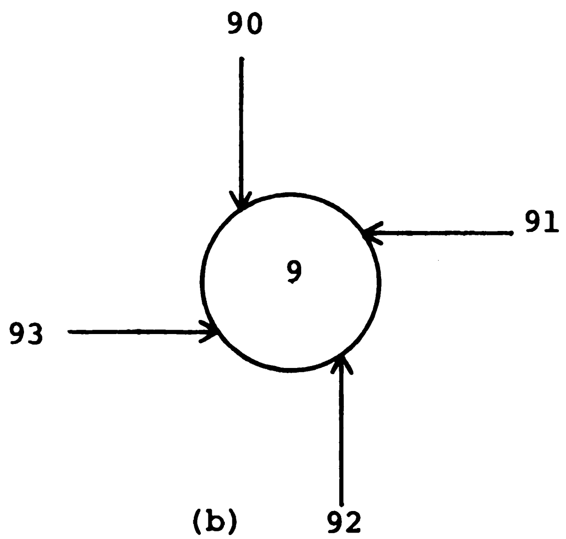

(b)

Figure 6.1 General Link Numbering System and a Specific Example

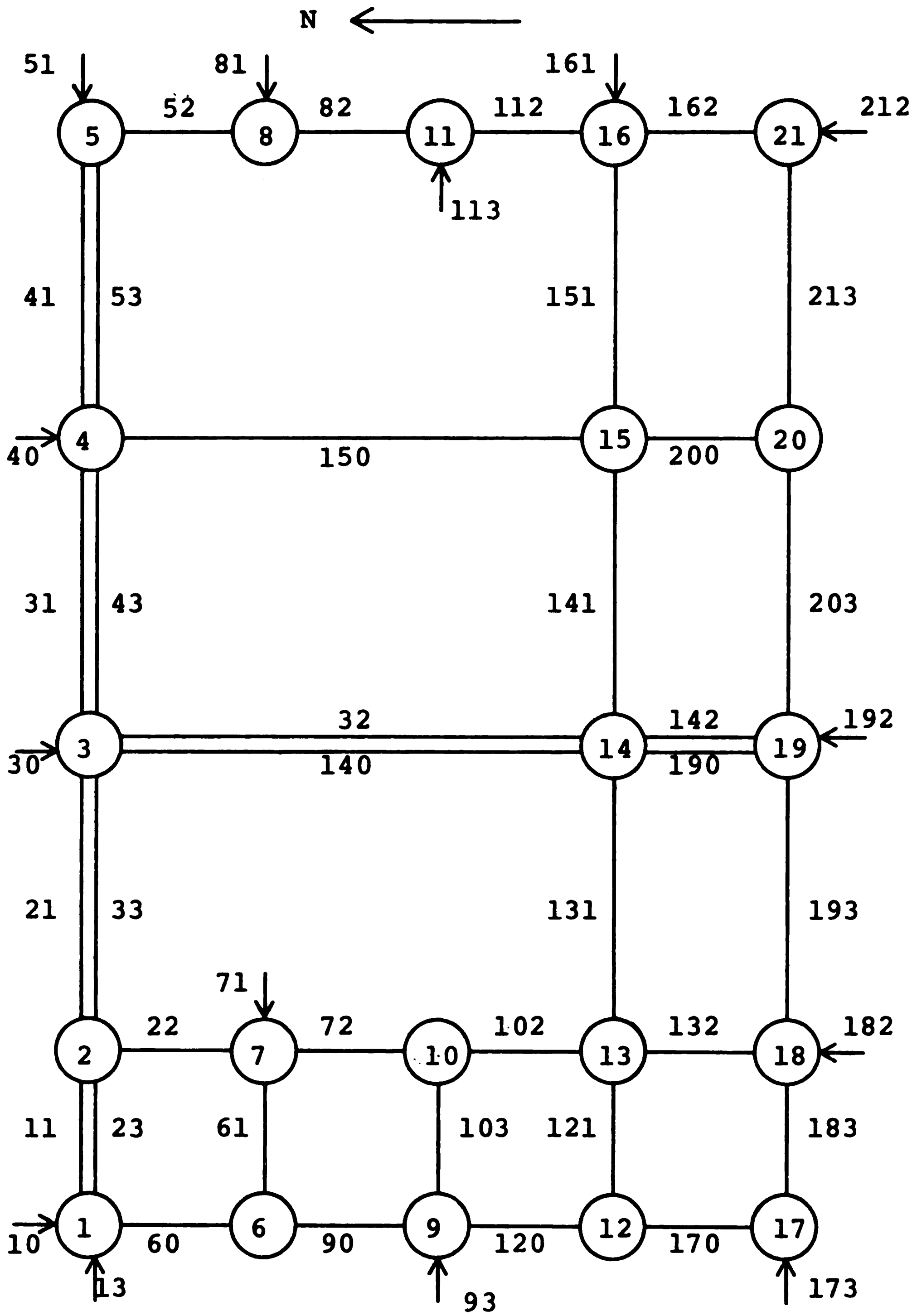

Figure 6.2 Node-Link Model of Modified Ft. Wayne, Indiana Area

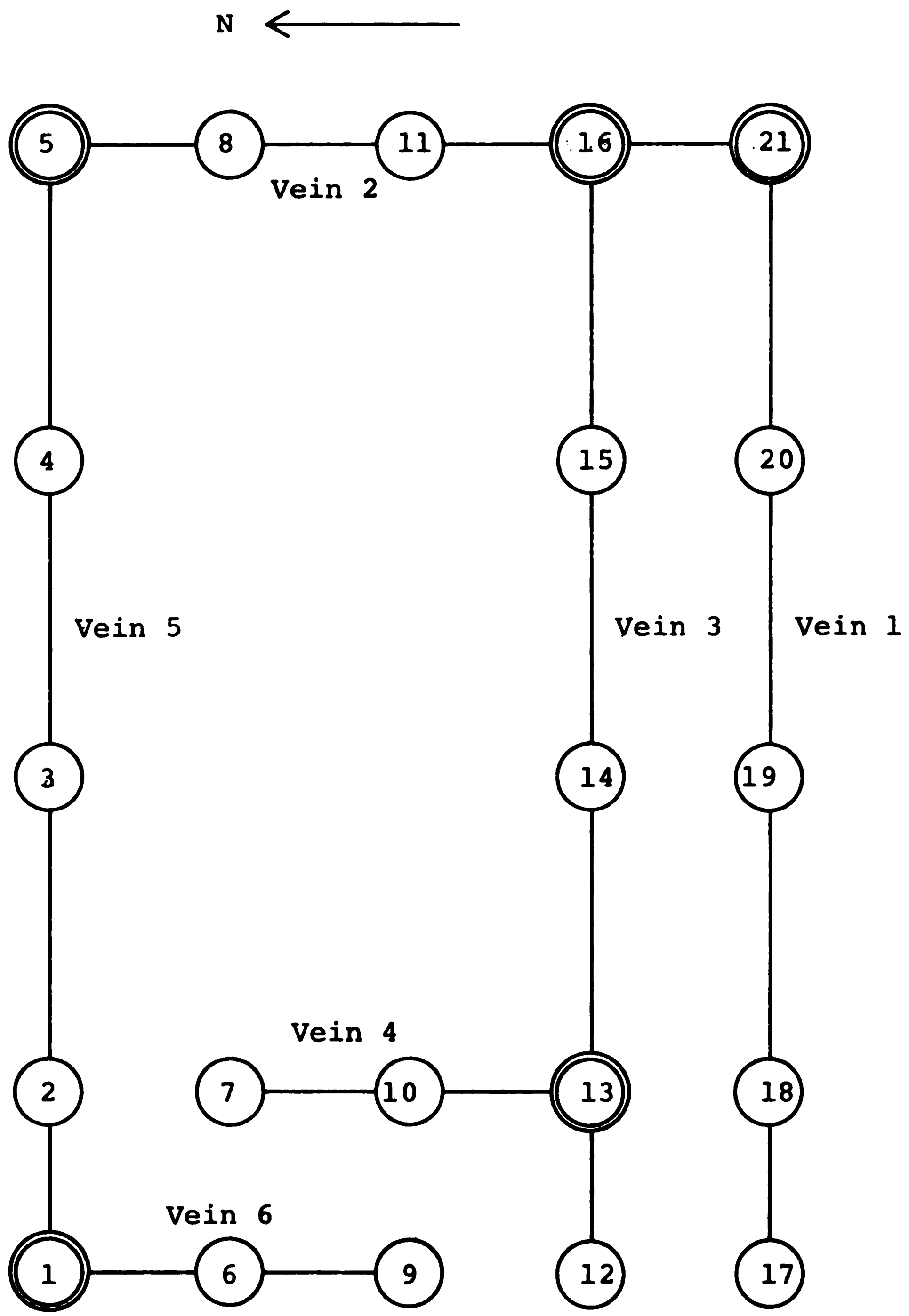

Figure 6.3 Vein Interconnection Model of Figure 6.2

links. The area includes nine two-way and six one-way streets (Figure 6.4).

Similar to the Ft. Wayne example, a vein-interconnection model was selected for TRANSYT/G (Figure 6.5).

6.3 Input Data

The input data required for TRANSYT is described in detail in Robertson's User's Manual (RO2) and will not be reprinted here due to its length. The same data set used for TRANSYT can be used for TRANSYT/G with one exception; the type 4 hillclimbing step size card has been replaced by the new type 4 vein list cards. One card or file line is required for each vein. The format consists of right justified quantities in the standard five column field widths used in TRANSYT. Field 1 contains a 4. Field 2 contains the direction of flow indicator per the following code:

bbbb1 for one-way flow going east,
bbbb2 for one-way flow going north,
bbbb3 for one-way flow going west,
bbbb4 for one-way flow going south,
bbbb5 for two-way flow going east and west,
bbbb6 for two-way flow going north and south,

assuming north at the top of the vein interconnection model diagram. Fields 3 - 16 contain the node numbers comprising the vein and are in the order in which they are encountered in the vein model.

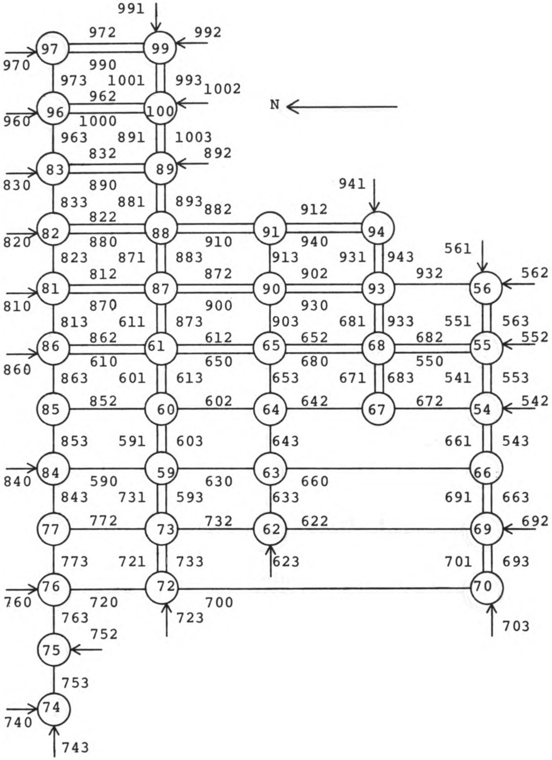

Figure 6.4 Node-Link Model of Modified Washington, D.C. Area

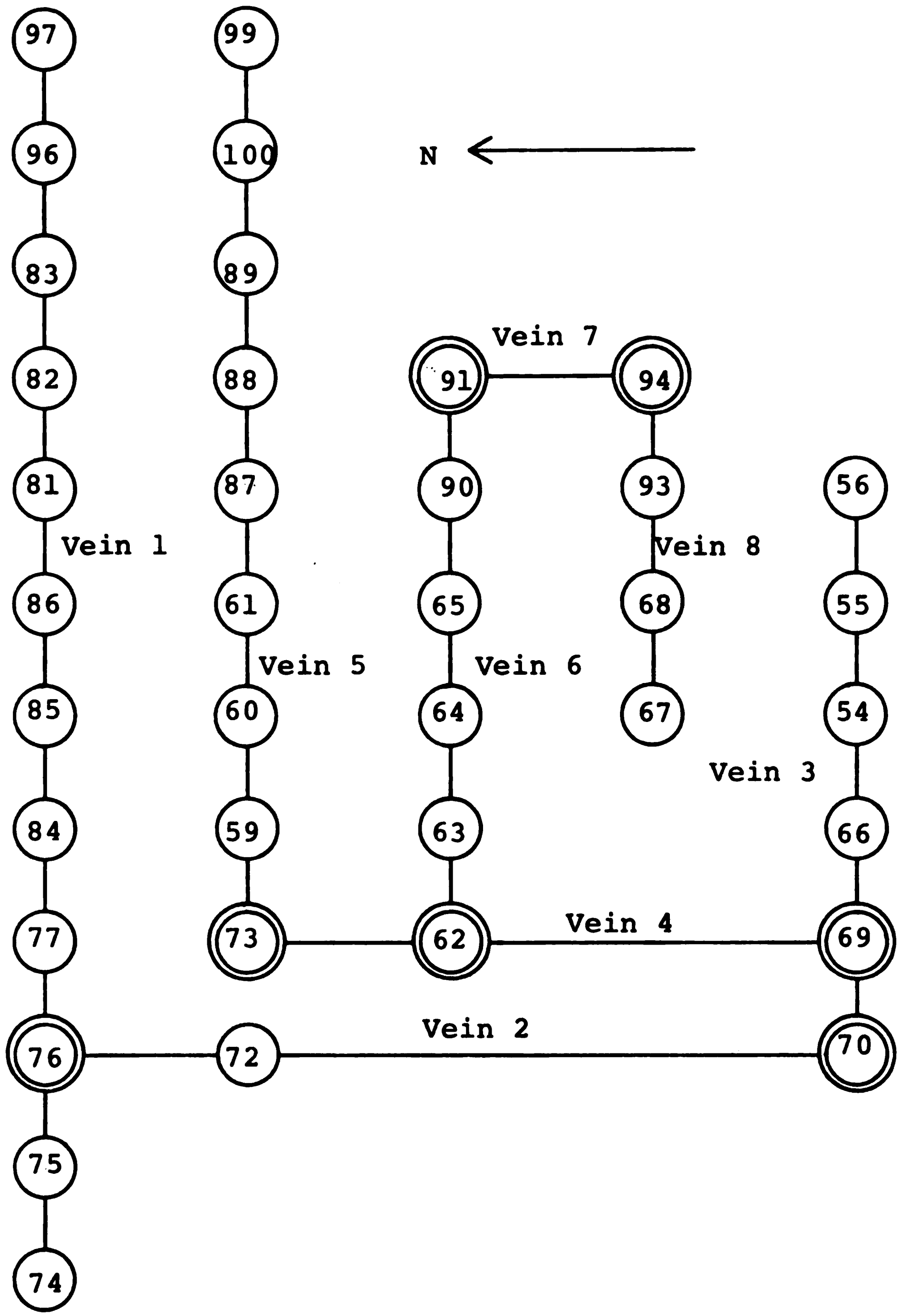

Figure 6.5 Vein Interconnection Model of Figure 6.4

6.4 Comparison of TRANSYT/G versus TRANSYT

To compare the new split and offset calculations of TRANSYT/G to the previous hillclimbing TRANSYT method, the following computer runs were made for both the Ft. Wayne and the Washington data on a Burroughs B7700 system:

1. Initial conditions with equal splits and zero offsets,
2. TRANSYT (STAR1) splits without hillclimbing on offsets,
3. TRANSYT/G (SPLIT) splits without offset calculations,
4. 7-Step hillclimbing TRANSYT with STAR1 splits,
5. 7-Step hillclimbing TRANSYT with SPLIT splits,
6. TRANSYT/G with no excess green shift,
7. TRANSYT/G with full excess green shift, and
8. TRANSYT/G with partial excess green shift.

These results are summarized in Table 6.1.

By comparing run numbers 3 to 2 and also 5 to 4 for each data set, one can conclude that this author's split calculation method (SPLIT) is superior to Robertson's (STAR1). This is evidenced by that fact that the use of SPLIT produced lower objective function and higher system speed values than those produced by STAR1. Another observation can be made concerning runs 4 and 5. This author's split estimation method produces a better set of initial conditions for the hillclimbing procedure.

Table 6.1 Comparison of TRANSYT/G to TRANSYT - Part I

Run	Use of subroutine SUBPT No. of Entries	No. of Links Processed	CPU Run Time (sec.)	Total Uniform Delay (veh-hr /hr)	Total Random Delay (veh-hr /hr)	Total Stops (veh./ sec.)	Objective Function (——)	System Speed (mi/hr)
Example 1: Ft. Wayne, Indiana (21 nodes)								
1	1	56	*	122.89	4.54	5.86	150.86	16.34
2	1	56	*	118.38	4.28	5.93	146.40	16.65
3	1	56	*	115.38	6.18	5.76	144.58	16.73
4	363	13,451	115.6	78.69	4.28	4.83	102.29	19.77
5	360	12,351	114.6	74.73	6.18	4.99	100.87	19.96
6	2	112	3.1	80.33	6.18	5.10	106.91	19.44
7	2	112	3.1	86.88	6.18	5.32	114.35	18.87
8	2	112	3.1	78.98	6.18	5.09	105.51	19.57
Example 2: Washington, D.C. (38 nodes)								
1	1	134	*	221.37	7.70	11.67	275.74	14.21
2	1	134	*	204.93	6.65	11.23	256.50	14.74
3	1	134	*	198.88	9.06	11.74	254.91	14.85
4	636	53,624	452.3	167.42	6.65	11.15	218.66	16.01
5	632	52,413	444.3	161.05	9.06	11.00	214.09	16.15
6	2	268	6.2	182.19	9.06	11.93	238.97	15.40
7	2	268	6.2	175.46	9.06	12.55	234.72	15.63
8	2	268	6.2	170.01	9.06	11.75	226.07	15.83

* - Not available for partial runs.

In both examples, fewer total number of calculations were required and lower objective functions were obtained.

Run numbers 6, 7 and 8 are similar in nature except for the amount of excess green shift adjustment to the offsets. The shift values for runs 6, 7 and 8 were zero (Morgan-Little), full (Panyan) and partial (Grove) respectively. Comparison of these runs indicate lower objective function and higher system speed values for this author's partial shift for both examples. Thus, the partial shift is preferred. It should be emphasized that the partial shift varies from one network to another and is determined from several trial runs during either the preliminary checkout of a new signal timing system or during on-line system operation.

Finally, comparison of runs 8 to 4 points out the potential use of TRANSYT/G versus TRANSYT (Table 6.2). In the opinion of this author, the benefit of TRANSYT/G's extremely fast computer running time relative to TRANSYT's far outshadows its slightly higher objective function (about 3%) and lower system speed (about 1%) values. In fact, from runs 4 and 8, the improvement in running time can be estimated from the CPU times as follows:

a) the Ft. Wayne data ran $\frac{115.6}{3.1} = 37.3$ times faster, and

b) the Washington data ran $\frac{452.3}{6.2} = 73.0$ times faster

Table 6.2 Comparison of TRANSYT/G to TRANSYT - Part II

Example Data Set	No. of Nodes	TRANSYT/G (Run 8) - TRANSYT (Run 4) Differences					
		Objective Function		System Speed		CPU Run Time	
		(——)	(%)	(mi/hr)	(%)	(Sec)	Ratio (——)
Ft. Wayne	21	+3.22	+3.15	-0.20	-1.01	-112.5	1:37.3
Washington	38	+7.41	+3.39	-0.18	-1.12	-446.1	1:73.0

on TRANSYT/G than on TRANSYT. Although the CPU run times on the B7700 computer vary slightly as a function of the system load, general comparisons such as these can be made. Similar comparisons should result for other computers.

Another estimation of relative computer speed of TRANSYT/G versus TRANSYT can be inferred by comparing the number of links processed by the subroutine SUBPT. This produces even higher ratios in favor of TRANSYT/G.

As an aside, comparison of the CPU times for run number 4 of both data sets supports Robertson's general statement (RO1) that the run time of TRANSYT increases as the square of the number of nodes in the data set. Washington's 38 nodes versus Ft. Wayne's 21 nodes produced a CPU ratio of $\frac{452.3}{115.6} = 3.9$. Since TRANSYT/G is a non-iterative program, its run time increases approximately linearly with the number of network nodes.

CHAPTER VII

CONCLUDING REMARKS

7.1 Conclusions

The primary objective of this research was to use Robertson's basic TRANSYT traffic flow model and replace his time consuming hillclimbing optimization process with a non-iterative split and offset estimation technique. This resulted in a much faster and thus less costly running TRANSYT/G computer program yielding sub-optimal signal timings.

Based upon the results of testing the Ft. Wayne, Indiana and the Washington, D.C. data sets, it was concluded that:

1) This author's split estimation method is superior to Robertson's in terms of lower objective function and higher system speed values. This is true for its use in both TRANSYT/G for on-line control applications and in TRANSYT for more accurate off-line signal timing optimization studies, and,

2) TRANSYT/G's vastly lower computer running time and sub-optimal signal timings makes it a potential candidate for an on-line signal timing control method.

A secondary result of this research was the development of a finite traffic queue dispersion model (Appendix A) for use in off-line simulation studies requiring a more accurate model than the infinite queue version presently being used in TRANSYT.

7.2 Suggested Future Research

Further research should be undertaken to determine other refinements in calculating near optimal splits and offsets. For example, by relaxing the assumption of uniform arrivals (Figure 3.2) in the stops and uniform delay models, a better near-optimum split set may result. Also, inclusion of secondary interdependencies of nearby nodes and links may improve the offset calculations.

Secondly, the partial excess green shift used in the offset predictions should be investigated as to its dependence upon the various network geometries and traffic parameters.

And thirdly, the finite queue dispersion model should be extensively field tested in many urban areas culminating in an improved TRANSYT/G program.

APPENDICES

APPENDIX A

TRAFFIC QUEUES AND THEIR DISPERSION

Queueing theory was originated by Erlang in 1909 in order to solve a congestion problem in a telephone system. It was developed to describe the behavior of a system providing a service for random demands. Since this general description applies to both discrete and continuous flows, queueing theory is a logical portion of any present day traffic flow model. For more detail, Drew (DR1) is one of the many authors covering queueing processes as applied to traffic systems.

In order to specify a queueing system, the following items must be given:

1. the distribution of arrivals,
2. the source finiteness,
3. the queue discipline,
4. the channel configuration, and
5. each channel's service time distribution.

The collection of arrivals waiting to be served is defined as the queue and the actual number of arrivals waiting for service at time t is called the queue length.

A queueing system is considered to be in state n if it contains exactly n items where $n > 0$, including all items in line and those being served. If the arrival rate, a, is less than the service rate, b, the queueing system is said to be stable and there exists a finite time independent probability of the queue being in any state n. On the other hand, if the ratio $(\frac{a}{b}) > 1$, the queue length continues to grow with time.

When considering the idea of the queue length (number of vehicles in a queue) for an urban traffic network, first consider a directional traffic stream having Poisson arrivals and an exponential service rate.

Let $P_n(t + \Delta t)$, $n > 0$ represent the probability that the queueing system contains n vehicles at time $(t + \Delta t)$. Let Δt be such that only one vehicle can arrive or depart during the Δt time interval. Then there are only three ways in which this queueing system can reach state n during the time t to $t + \Delta t$, i.e.,

1. the system remains in state n, or
2. the system changed from state $(n - 1)$ to state n, or
3. the system changed from state $(n + 1)$ to state n.

If the probability of one arrival in Δt is $(a \Delta t)$ and the probability of one departure in Δt is $(b \Delta t)$, the corresponding probabilities of no arrivals or departures are $(1 - a \Delta t)$ and $(1 - b \Delta t)$.

Since traffic signals are spaced some finite distance apart in an urban network, the queue lengths must be restricted to some finite value of N vehicles, where N is a function of signal separation distance, split, offset, and cycle length. Thus, if the maximum number of vehicles in the queueing system is limited to N such that vehicles arriving when $n > N$ will not be able to join the queue, we have, neglecting higher order terms:

$$\begin{aligned}
P_n(t + \Delta t) &= P_n(t)[1 - (a+b)\Delta t] \\
&\quad + P_{n-1}(t)[a \Delta t] + P_{n+1}(t)[b \Delta t], \quad 0 < n < N \\
P_0(t + \Delta t) &= P_0(t)[1 - a \Delta t] + P_1(t)[b \Delta t], \quad n = 0 \\
P_N(t + \Delta t) &= P_N(t)[1 - b \Delta t] + P_{N-1}(t)[a \Delta t], \quad n = N.
\end{aligned} \tag{A.1}$$

Passing to the limit with respect to Δt results in:

$$\begin{aligned}
\dot{P}_n(t) &= -(a+b)P_n(t) + aP_{n-1}(t) + bP_{n+1}(t) \quad 0 < n < N, \\
\dot{P}_o(t) &= -aP_o(t) + bP_1(t) \quad n = 0, \\
\dot{P}_N(t) &= -bP_N(t) + aP_{N-1}(t) \quad n = N.
\end{aligned} \tag{A.2}$$

Setting the time derivatives equal to zero and eliminating time results in:

$$\begin{aligned}
(1 + \lambda)P_n &= P_{n+1} + \lambda P_{n-1} \quad && 0 < n < N \\
P_1 &= \lambda P_o && n = 0 \\
P_N &= \lambda P_{N-1} && n = N.
\end{aligned} \tag{A.3}$$

where $\lambda = \frac{a}{b}$ is the ratio of the arrival rate to the service rate. P_n is the steady state time-independent probability of n vehicles being in the system.

For a finite length queue, all of the individual probabilities sum to unity,

$$\sum_{n=0}^{N} P_n = 1 = P_0 + P_1 + \ldots + P_N$$

$$= P_0 + \lambda P_0 + \ldots + \lambda^N P_0$$

$$= P_0 \left(\frac{1 - \lambda^{N+1}}{1 - \lambda}\right) , \tag{A.4}$$

thus giving

$$P_0 = \frac{1 - \lambda}{1 - \lambda^{N+1}} . \tag{A.5}$$

Then the discrete distribution for a finite maximum allowable queue length N is,

$$P_n = \lambda^n P_0 = \frac{\lambda^n (1 - \lambda)}{1 - \lambda^{N+1}}. \tag{A.6}$$

Next the probability-generating function (pgf) for this distribution is derived from the definition

$$Z_n(\theta) = E(\theta^n) \equiv \sum_{n=0}^{\infty} \theta^n P_n$$

$$= \frac{1 - \lambda}{1 - \lambda^{N+1}} \sum_{n=0}^{N} (\lambda\theta)^n$$

$$= \left(\frac{1 - \lambda}{1 - \lambda^{N+1}}\right) \frac{1 - (\lambda\theta)^{N+1}}{1 - \lambda\theta} . \tag{A.7}$$

The expected number of vehicles in a queue, $E(n)$, for which the maximum allowable is N is obtained from the first derivative of the pgf with respect to θ,

$$Z_n'(1) = \left.\frac{dZ_n(\theta)}{d\theta}\right|_{\theta = 1} .$$

After some algebraic manipulation, we have

$$E(n) = Z_n'(1) = \left(\frac{\lambda}{1-\lambda}\right) \frac{1 - (N+1)\lambda^N + N\lambda^{N+1}}{1 - \lambda^{N+1}} . \tag{A.8}$$

The limiting case is the non-truncated queue where the expected number of vehicles in the queue is

$$\lim_{N\to\infty} E(n) = \frac{\lambda}{1-\lambda} , \tag{A.9}$$

as expected.

Table A.1 illustrates the relation between the expected queue length, $E(n)$, as a function of the ratio of the arrival rate to the service rate for several finite length queues and the limiting non-truncated queue. From Table A.1, we can see that the expected queue length becomes increasingly dependent upon the maximum queue length N as the arrival to service rates ratio approaches unity.

In an analogous manner, the variance for this distribution can be calculated from the first and second derivatives of the pgf by

$$\sigma^2 = Z_n''(1) + Z_n'(1) - [Z_n'(1)]^2 \tag{A.10}$$

TABLE A.1

EXPECTED QUEUE LENGTH, E(n)

Ratio of Arrival Rate to Service Rate, λ	Maximum Queue Length					
	N=5	N=10	N=15	N=20	N=25	N=∞
0.00	0.000	0.000	0.000	0.000	0.000	0.000
0.05	0.053	0.053	0.053	0.053	0.053	0.053
0.10	0.111	0.111	0.111	0.111	0.111	0.111
0.15	0.176	0.176	0.176	0.176	0.176	0.176
0.20	0.250	0.250	0.250	0.250	0.250	0.250
0.25	0.332	0.333	0.333	0.333	0.333	0.333
0.30	0.424	0.429	0.429	0.429	0.429	0.429
0.35	0.527	0.538	0.538	0.538	0.538	0.538
0.40	0.642	0.666	0.667	0.667	0.667	0.667
0.45	0.768	0.816	0.818	0.818	0.818	0.818
0.50	0.905	0.995	1.000	1.000	1.000	1.000
0.55	1.051	1.207	1.221	1.222	1.222	1.222
0.60	1.206	1.460	1.495	1.500	1.500	1.500
0.65	1.368	1.760	1.841	1.855	1.857	1.857
0.70	1.533	2.111	2.280	2.322	2.331	2.333
0.75	1.701	2.515	2.838	2.950	2.985	3.000
0.80	1.868	2.966	3.537	3.805	3.921	4.000
0.85	2.034	3.456	4.383	4.951	5.281	5.667
0.90	2.195	3.969	5.361	6.420	7.204	9.000
0.95	2.351	4.490	6.422	8.155	9.697	19.000

where it can be shown that

$$Z_n''(1) = \frac{2\lambda}{1-\lambda} Z_n'(1) - \frac{N(N+1)\lambda^{N+1}}{1 - \lambda^{N+1}} \quad . \tag{A.11}$$

Therefore by substitution, the variance for our finite queue is

$$\sigma^2 = E(n)[\frac{1 + \lambda}{1 - \lambda} - E(n)] - \frac{N(N+1)\lambda^{N+1}}{1 - \lambda^{N+1}} \; . \tag{A.12}$$

The variance for the limiting queue is well known (DR1) and serves as a check for our finite case, namely

$$\lim_{N\to\infty} \sigma^2 = \frac{\lambda}{(1-\lambda)^2} \; . \tag{A.13}$$

Table A.2 is a tabulation of the variance as a function of λ and N.

Now that the basics for queueing processes as applied to urban traffic models with Poisson arrivals and exponential departures have been discussed, the dispersion of moving queues will be covered.

Consider the placement of an observer near a signalized intersection and given the task of determining the effect of the signal's phase changes upon a stream of traffic. He would note that the headway between successive vehicles would decrease as they approached the signal, tending to form a grouping or compression of vehicles during the red phase. After the start of the green phase the vehicle headway would then increase as vehicle speeds increased, thus spreading out this group of vehicles.

TABLE A.2

QUEUE LENGTH VARIANCE, σ^2

Ratio of Arrival Rate to Service Rate, λ	Maximum Queue Length					
	N=5	N=10	N=15	N=20	N=25	N=∞
0.00	0.000	0.000	0.000	0.000	0.000	0.000
0.05	0.055	0.055	0.055	0.055	0.055	0.055
0.10	0.123	0.123	0.123	0.123	0.123	0.123
0.15	0.207	0.208	0.208	0.208	0.208	0.208
0.20	0.310	0.312	0.312	0.312	0.312	0.312
0.25	0.436	0.444	0.444	0.444	0.444	0.444
0.30	0.586	0.612	0.612	0.612	0.612	0.612
0.35	0.762	0.827	0.828	0.828	0.828	0.828
0.40	0.962	1.106	1.111	1.111	1.111	1.111
0.45	1.184	1.469	1.487	1.488	1.488	1.488
0.50	1.420	1.941	1.996	2.000	2.000	2.000
0.55	1.662	2.547	2.698	2.714	2.716	2.716
0.60	1.902	3.308	3.678	3.740	3.749	3.750
0.65	2.130	4.229	5.046	5.254	5.297	5.306
0.70	2.338	5.288	6.921	7.531	7.714	7.778
0.75	2.518	6.429	9.382	10.946	11.618	12.000
0.80	2.666	7.561	12.371	15.856	17.945	20.000
0.85	2.779	8.572	15.598	22.242	27.601	37.778
0.90	2.858	9.357	18.529	29.161	40.081	90.000
0.95	2.903	9.842	20.550	34.629	51.573	380.000

As traffic volumes increase on a given roadway, the vehicles generally bunch-up forming moving queues or platoons.

Robertson (RO1) developed his version of the smoothing factor empirically by making many observations of vehicle travel times along several different roadways during various times of the day. He then approximated his field data with the equation,

$$A = \frac{1}{1 + 0.5t} , \tag{A.14}$$

where t and A are the vehicle travel time and smoothing factor, respectively.

Another approach was taken by Seddon (SE1) in which, based upon a geometric distribution of travel times, he derived the same smoothing factor to be,

$$A = \frac{1}{1 + 0.25t} . \tag{A.15}$$

Seddon concluded that his result was larger than Robertson's due to taking his summation of the geometric distribution over the complete set of positive non-zero real integers. Seddon indicated that a truncated summation might be more appropriate but it would not lead to a straightforward solution.

This author then proceeded to obtain such a solution by considering this to be a finite process. First, consider a vehicle that leaves a traffic signal stopline and travels along a roadway such that it passes an observation point downstream. Define the random variables

$$X_k = \begin{cases} 1 & \text{if the vehicle is observed downstream in the } k^{th} \text{ interval} \\ 0 & \text{otherwise,} \end{cases}$$

where the X_k are independent random variables and their probabilities are

$$P(X_k = 1) = A,$$

and

$$P(X_k = 0) = 1 - A \;. \tag{A.16}$$

Consider the event where the vehicle that leaves the signal stopline in the 1^{st} interval passes the downstream observation point in the i^{th} interval, t time interval units later. The probability of this event is given by:

$$P(i+t) = [\prod_{k=1}^{i-1} P(X_k = 0)]P(X_k = 1) = (1-A)^{i-1}A, \qquad i = 1,2,... \tag{A.17}$$

The average value of travel times past the observation point in the interval $(i+t)$ is given by

$$t_{ave} = \tfrac{1}{2}[(i + t - 1) - (1) + (i + t) - (2)]$$

$$= i + t - 1, \tag{A.18}$$

provided that the departure time at the stopline and the arrival time at the observation point are randomly distributed within the appropriate intervals. Then the expected travel time, E(T), for this vehicle over a finite number of intervals, N, is

$$E(T) = \sum_{i=1}^{N} t_{ave} P(i + t) / \sum_{i=1}^{N} P(i + t)$$

$$E(T) = \sum_{i=1}^{N} (i + t - 1)(1 - A)^{i-1}A / \sum_{i=1}^{N} (1 - A)^{i-1}A$$

$$= (t - 1) + \sum_{i=1}^{N} i(1 - A)^{i-1}A / \sum_{i=1}^{N} (1 - A)^{i-1}A. \tag{A.19}$$

The denominator summation is a truncated geometric series having the closed form $1 - (1 - A)^N$. By equating the definition of expected value to the result derived from the probability generating function, the numerator summation can be shown to have the closed form $[1 - (N + 1)A(1 - A)^N - (1 - A)^{N+1}]/A$. Thus

$$E(T) = (t-1) + [1 + (N+1)A(1-A)^N - (1-A)^{N+1}]/A[1-(1-A)^N]. \tag{A.20}$$

The desired result is to have the smoothing factor, A, expressed explicitly in terms of the travel time, t, and queue length, N. This is not easily done for general values of N. However this function can be solved for t in terms of A and N.

Both Robertson and Seddon have confirmed that the expected travel time $E(T) = 1.25t$. Substitution into the previous equation leads to,

$$t = \frac{1-A - NA(1-A)^{N} - (1-A)^{N+1}}{0.25A[1 - (1-A)^{N}]} . \tag{A.21}$$

In the limit for infinite queues, we have

$$\lim_{N\to\infty} [t] = \frac{4(1 - A)}{A}, \tag{A.22}$$

which is exactly equal to Seddon's result and twice Robertson's empirical form. Figure A.1 was constructed from Table A.3 which is a tabulation of this author's, Seddon's and Robertson's travel time equations for comparison.

Although Robertson's result was accurate enough for this author's split and offset calculations, a more sophisticated model of urban traffic flow may require a smoothing factor which is a function of the maximum allowed queue length, N. It is for this reason that these results have been included.

TABLE A.3

TRAVEL TIME, t

Smoothing Factor	Maximum Queue Length N=5	N=10	N=20	N=50	N=∞*	Robertson's
0.05	7.590	16.315	31.295	59.328	76.000	38.000
0.10	7.161	14.586	24.928	34.964	36.000	18.000
0.15	6.714	12.861	19.441	22.607	22.667	11.333
0.20	6.252	11.188	15.067	15.997	16.000	8.000
0.25	5.777	9.613	11.745	12.000	12.000	6.000
0.30	5.293	8.171	9.269	9.333	9.333	4.667
0.35	4.803	6.883	7.414	7.429	7.429	3.714
0.40	4.314	5.757	5.997	6.000	6.000	3.000
0.45	3.829	4.787	4.888	4.889	4.889	2.444
0.50	3.355	3.961	4.000	4.000	4.000	2.000
0.55	2.897	3.259	3.273	3.273	3.273	1.636
0.60	2.460	2.662	2.667	2.667	2.667	1.333
0.65	2.048	2.153	2.154	2.154	2.154	1.077
0.70	1.666	1.714	1.714	1.714	1.714	0.857
0.75	1.314	1.333	1.333	1.333	1.333	0.667
0.80	0.994	1.000	1.000	1.000	1.000	0.500
0.85	0.704	0.706	0.706	0.706	0.706	0.353
0.90	0.444	0.444	0.444	0.444	0.444	0.222
0.95	0.211	0.211	0.211	0.211	0.211	0.105
1.00	0.000	0.000	0.000	0.000	0.000	0.000

*Limiting case is same as Seddon's result.

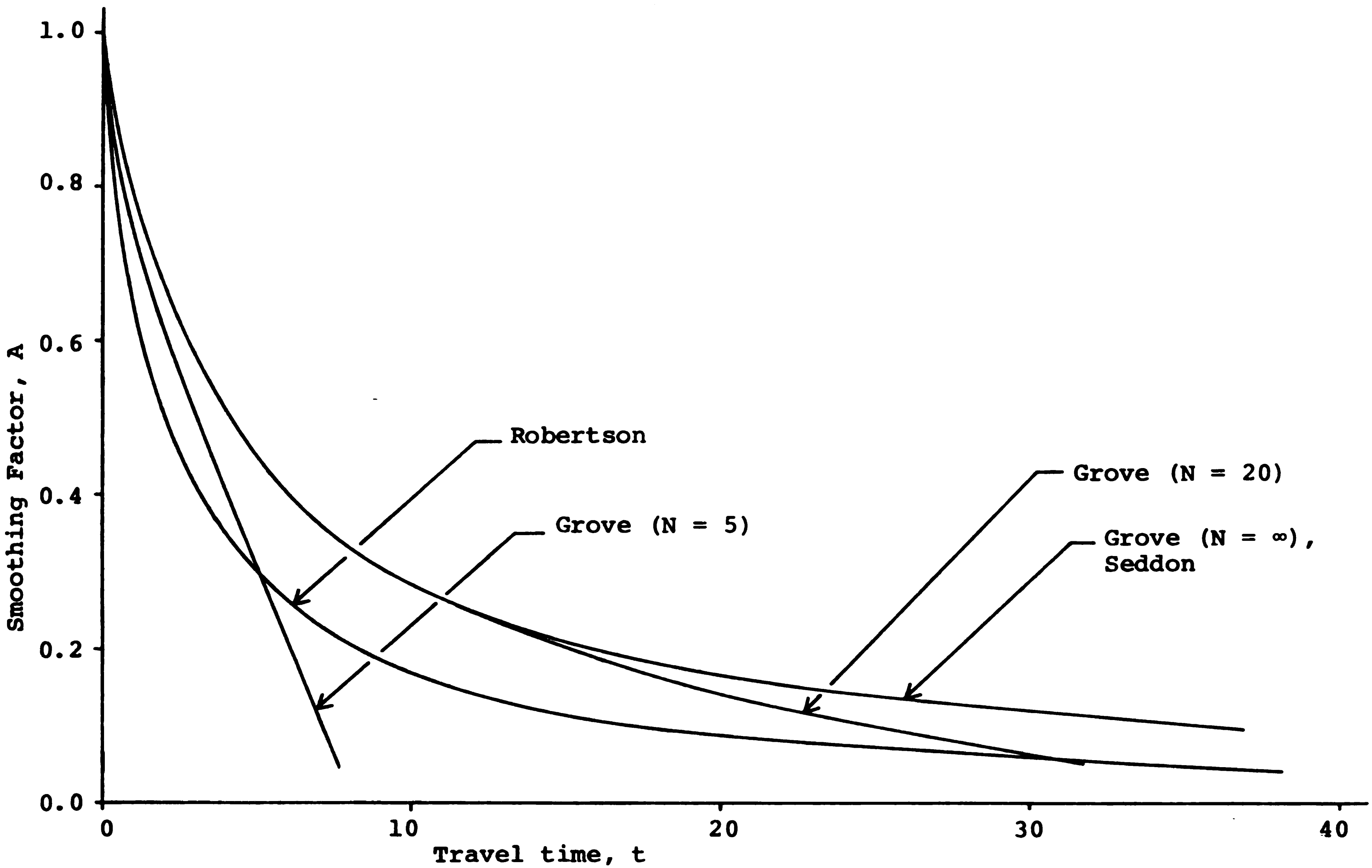

Figure A.1 Smoothing Factor Versus Travel Time

APPENDIX B

This appendix contains a general flow diagram of Robertson's TRANSYT signal timing program and this author's modified version, TRANSYT/G, illustrated in Figure B.1. Due to the length of these two computer programs, only listings of the following portions of TRANSYT/G will be included:

1) the Type 4 Vein Card Section of TINPUT (Figure B.2),
2) the complete SPLIT subroutine (Figure B.3), and
3) the complete OFFSET subroutine (Figure B.4).

A general description of the function of the various other subroutines called by TRANSYT and TRANSYT/G is as follows:

TINPUT - reads all the input data and checks for appropriate order and boundedness,

STAR1 - an optional calculation of the splits based upon equal saturation of cross phases (TRANSYT only),

HILLCL - performs Robertson's hillclimbing optimization of splits (optional) and offsets (TRANSYT only), SUBPT - calculates the delays, stops, and objective function for a given set of signal settings,

TOUTP - outputs the previously calculated information for each node and link along with their totals, and

SPLOT - plots out the link flow histograms.

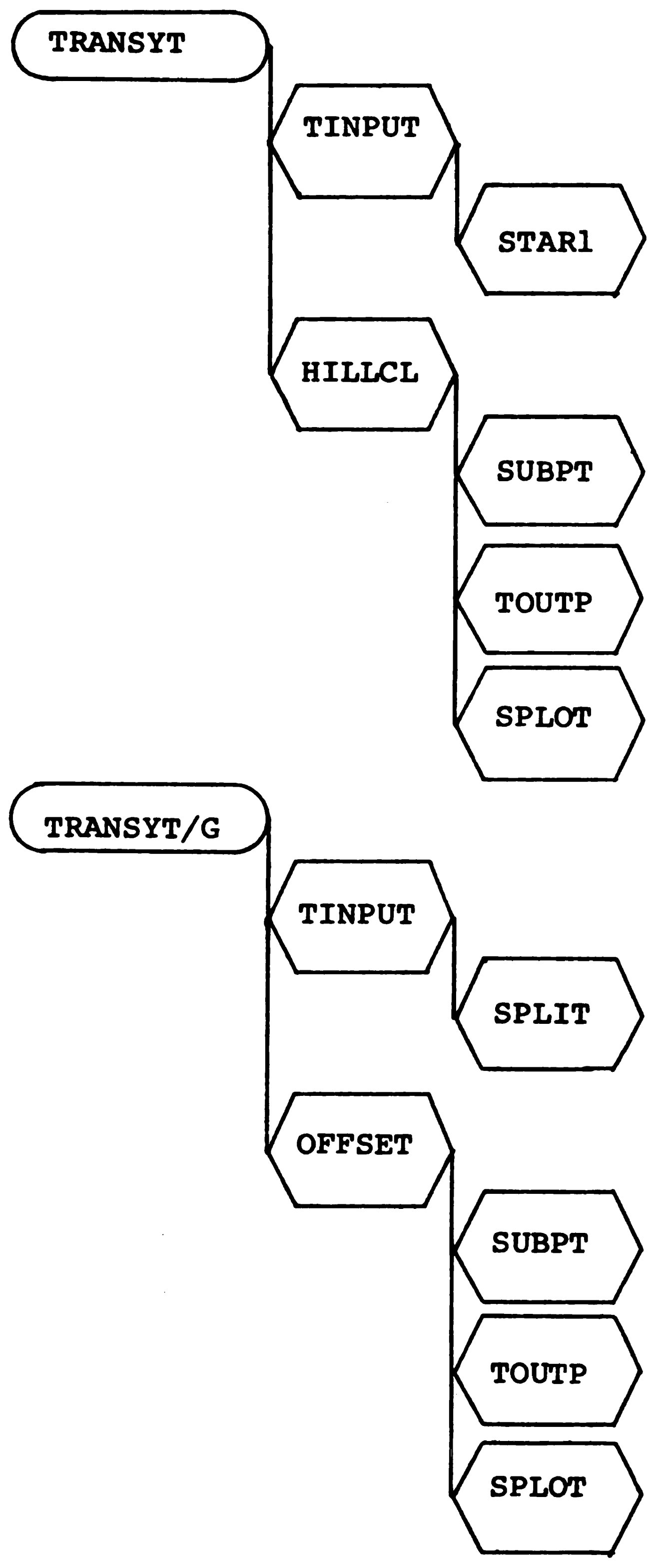

Figure B.1 TRANSYT and TRANSYT/G General Flow Diagrams

```
      SUBROUTINE TINPUT(ICL40)
C-
C-     MISSING SECTION (SEE ORIGINAL TRANSYT LISTING).
C-
C-     THE NEXT SECTION PROCESSES A TYPE 4 CARD(A VEIN CARD)
C-
  240 IF(IPCARD.LT.3.OR.IPCARD.GT.4)GO TO 110
      IF(WR11.EQ.3)GO TO 246
      IF(IPCARD.EQ.4)GO TO 245
      WRITE( 6,5110)
      IF(WR11.NE.0) WRITE(11,5110)
 5110 FORMAT("0CARD",4X,"CARD",38X,"NODE/VEIN  LIST"/
     1"  NO.     TYPE")
  245 WRITE( 6,5040)ICRNO,(ICARD(I),I=1,16)
      IF(WR11.NE.0) WRITE(11,5040)ICRNO,(ICARD(I),I=1,16)
  246 NART=NART+1
      LO(NART)=ICARD(2)
      NN(NART)=0
      DO 250 I=3,16
      J=ICARD(I)
      IF(J.EQ.0)GO TO 250
      IF(J.GT.0)GO TO 247
      NFAULT=1
      IFAULT(I)=IMINUS
  247 IF(NN(NART).GE.15)GO TO 255
      NN(NART)=NN(NART)+1
      LN(NART,I-2)=J
  250 CONTINUE
      GO TO 258
  255 WRITE( 6,5120)
      IF(WR11.NE.0) WRITE(11,5120)
 5120 FORMAT('0TOO MANY NODES PER VEIN IN LIST - LIMIT 14'/)
      NFAULT=1
  258 DO 256 I=1,16
      IF(IFAULT(I) .EQ. IMINUS) GO TO 257
  256 CONTINUE
      GO TO 100
  257 WRITE(  6,5050) IFAULT
      WRITE(  6,2000)
      WRITE(  6,2003)
      IF(WR11.EQ.0) GO TO 100
      WRITE(11,5050) IFAULT
      WRITE(11,2000)
      WRITE(11,2003)
      GO TO 100
C-
C-     MISSING SECTION (SEE ORIGINAL TRANSYT LISTING).
C-
      RETURN
      END
```

Figure B.2 TINPUT Type 4 Card Input Section Listing

```
      SUBROUTINE SPLIT
      REAL*4 STPEN(200),RUNTIM(200),VEHKMS(200),WGHT(200)
     1      ,RKA(200),RKB(200),RKC(200),RKD(200),RKE(200)
      INTEGER NLIST(50),LNUM(200),ICARD(16),IFAULT(16)
     1         ,NORD(7,11),NUMAX(7),KNBIAS(7),NOOMAX(7)
     2         ,ITLE(20)
      INTEGER NLINK(50),NBIAS(7,50),NMIN(7,50),LOUTN(200)
     1         ,LBSTRT(2,200),LBFNSH(2,200),LDSTRT(2,200)
     2         ,LFSTRT(2,200),LFFNSH(2,200),LVEHC(200)
     3         ,LTOTF(200),LUNIF(200),LLNO(4,200)
     4         ,LJT(4,200),LNUMO(200),NNUMO(50),ISIZES(15)
     5         ,NSTAGE(50),KLIST(50),LPLOT(240),LFUDG(4,200)
     6         ,IN(50),NK(50,11),NDSAT(200),NTSAT(200)
     7         ,IPTOUT(12000),IMARK(11)
     8         ,LDFNSH(2,200),LSATF(200),LENTF(4,200)
      COMMON STPEN,RUNTIM,VEHKMS,WGHT,CONV1,CONV5,CONV6
     1      ,CONV7,CONV8,CONVA,CONVB,CONVC,DST,DFN,STOPP
     2      ,TIM,OLDPI,PINDEX,PA,PB,PC,TOTRT,TVK,BUSRT
     3      ,BVK,NLIST,LNUM,ICARD,IFAULT,ITLE,NPN,MFAULT
     4      ,NFAULT,IEND,IL,IP,ISTEPS,INODES,ILINKS
     5      ,ISTLST,INODC,IV,NOSE,NOSL,NPLTS,ICYCLE
     6      ,NLINK,NBIAS,NMIN,LOUTN,LBSTRT,LBFNSH
     7      ,LDSTRT,LDFNSH,LFSTRT,LFFNSH,LVEHC,LSATF
     8      ,LTOTF,LUNIF,LLNO,LENTF,LJT,LNUMO,NNUMO
     9      ,ISIZES,IMARK,NSTAGE,KLIST,LPLOT,LFUDG,WR11
      COMMON/BLKA/NR1(200),NART,LO(20),NN(20),LN(20,16)
      IP=1
      IL=1
      NOSE=0
      NOSL=0
      IF(WR11.EQ.4)GO TO 199
C-     THE TRAFFIC PATTERNS, DELAYS, ETC FOR THE
C-     INITIAL SETTINGS ARE CALCULATED AND THE
C-     SIGNAL AND LINK DETAILS ARE OUTPUT(OPTIONAL).
      J=IMARK(6)
      IF(J.EQ.0)GO TO 5
      MFAULT=0
      IL=0
      CALL SUBPT(IPTOUT,RKA,RKB,RKC,RKD,RKE)
      IF(J.EQ.1)GO TO 5
      IV=1
      IF(WR11.EQ.3)IV=3
      NFAULT=0
      CALL TOUTP(RKA,RKB,RKC,RKD,RKE)
    5 NOSE=0
      NOSL=0
      MFAULT=0
      CALL SUBPT(IPTOUT,RKA,RKB,RKC,RKD,RKE)
      IV=1
      IF(WR11.EQ.3)IV=3
```

Figure B.3 SPLIT Listing

```
      NFAULT=0
      CALL TOUTP(RKA,RKB,RKC,RKD,RKE)
C-     THIS VERSION WILL ADJUST SPLITS FOR UNGROUPED
C-     SIGNALS HAVING 2 STAGES, 1 GREEN/STAGE ONLY;
C-     OTHERS LEFT AS IS.
C-     SET UP NK(*,*) LINK TERMINATION MATRIX.
  199 DO 200 I=1,INODES
  200 IN(I)=0
      DO 210 J=1,ILINKS
      I=LOUTN(J)
      IF(I.LT.0)GO TO 210
      IN(I)=IN(I)+1
      KON=IN(I)
      NK(I,KON)=J
      NK(I,11)=IN(I)
  210 CONTINUE
C-     FOR EACH NODE I, CALC NEW SPLIT AND ADJUST
C-     GREEN BAND FOR EACH LINK EXITING FROM NODE I.
      IX=ISTEPS
      XC=IX
      CL=ICYCLE
      I=0
  211 I=I+1
C-     IF NODE I HAS MORE THAN 2 STAGES OR IS TO
C-     BE GROUPED WITH A LATTER NODE, LEAVE
C-     SPLIT AS IS.
      NNK=NK(I,11)
      IF(NSTAGE(I).GT.2.OR.NLIST(I).LT.0)GO TO 230
      CA=0.;CB=0.
      WKA=0.;WKB=0.
      WCA=0.;WCB=0.
      WKKA=0.;WKKB=0.
      K=0
  181 K=K+1
      NA=NK(I,K)
      JB=LBSTRT(1,NA)
      NS=NBIAS(JB,I)
      JBB=LBFNSH(1,NA)
      NF=NBIAS(JBB,I)
      IF(NF.LT.NS)NF=NF+IX
      NG1=NF-NS
      IF(NG1.GT.IX)NG1=NG1-IX
      NR1(NA)=IX-NG1
      IF(LNUM(NA).LT.0)GO TO 189
      A=LTOTF(NA)
      B=LSATF(NA)
      C=B*A/(B-A)
      D=0.5*TIM*A
      NNN=1.25*A*XC/B+0.5
      NMIN(JB,I)=MAX0(NMIN(JB,I),NNN)
```

Figure B.3 (cont'd.)

```
      IF(JB.NE.1)GO TO 186
      CA=CA+C
      WKA=WKA+WGHT(NA)*41.66*D
      WKKA=WKKA-WGHT(NA)*33.33*D
      WCA=WCA+WGHT(NA)*C
      GO TO 187
  186 CB=CB+C
      WKB=WKB+WGHT(NA)*41.66*D
      WKKB=WKKB-WGHT(NA)*8.33*D
      WCB=WCB+WGHT(NA)*C
  187 CONTINUF
  189 IF(K.LT.NNK)GO TO 181
      AIC=(CL*CL*WCA)-(WKKA+WKKB)+STOPP*CL*(CA-CB)
      IC=XC*AIC/(CL*CL*(WCA+WCB)+WKA+WKB)+.5
      NA=NK(I,1)
      JB=LBSTRT(1,NA)
      JBB=LBFNSH(1,NA)
      KX=LNUM(NA)/2
      KX=2*KX
      KK=1
  184 KK=KK+1
      NB=NK(I,KK)
      KXB=LNUM(NB)/2
      KXB=2*KXB
      KIJ=2
      IF(KXB.EQ.LNUM(NB))KIJ=1
      KIK=2
      IF(KX.EQ.LNUM(NA))KIK=1
      IF(KIK.NE.KIJ)GO TO 188
      IF(KK.LT.NNK)GO TO 184
  188 KJB=LBSTRT(1,NB)
      KJBB=LBFNSH(1,NB)
      IC=MIN0(MAX0(IC,NMIN(JB,I)),IX-NMIN(KJB,I))
      KXX=LNUM(NA)
      IF(JB.EQ.1)GO TO 171
      LX=NBIAS(KJBB,I)+IC-NR1(NA)
      MA=KJBB
      GO TO 172
  171 LX=NBIAS(JBB,I)+IC-NR1(NB)
      MA=JBB
  172 NBIAS(MA,I)=SCAL(LX,ISTEPS)
  192 K=0
  191 K=K+1
      NA=NK(I,K)
      JB=LBSTRT(1,NA)
      NS=NBIAS(JB,I)
      JBB=LBFNSH(1,NA)
      NF=NBIAS(JBB,I)
      NG1=SCAL(NF-NS,ISTEPS)
      NR1(NA)=IX-SCAL(NG1,ISTEPS)
```

Figure B.3 (cont'd.)

```
      IF(K.LT.NNK)GO TO 191
  230 IF(I.LT.INODES)GO TO 211
C-     OUTPUT FOR NEW SPLITS.
      MFAULT=0
      IL=1
      CALL SUBPT(IPTOUT,RKA,RKB,RKC,RKD,RKE)
      IV=1
      IF(WR11.EQ.3)IV=3
      NFAULT=2
      CALL TOUTP(RKA,RKB,RKC,RKD,RKE)
      RETURN
      END
```

Figure B.3 (cont'd.)

```
      SUBROUTINE OFFSET
C-     THIS SUBROUTINE IS ENTERED FROM THE MAIN PROGRAM
C-     AND PERFORMS THE ESTIMATION SEQUENCE NECESSARY TO
C-     FIND THE OFFSET SETTINGS. TWO SUBROUTINES ARE
C-     ENTERED FROM "OFFSET" - "SUBPT" TO CALCULATE
C-     DELAYS ETC AFTER EACH SIGNAL CHANGE AND "TOUTP" TO
C-     OUTPUT RESULTS TO THE LINE PRINTER.
      REAL*4 STPEN(200),RUNTIM(200),VEHKMS(200),WGHT(200)
     1       ,RKA(200),RKB(200),RKC(200),RKD(200),RKE(200)
     2       ,PIN(15)
      INTEGER NLIST(50),LNUM(200),ICARD(16),IFAULT(16)
     1          ,NOS(15),ILL(15),NOD(15),NP(15),KS(15)
     2          ,ITLE(20)
      INTEGER NLINK(50),NBIAS(7,50),NMIN(7,50),LOUTN(200)
     1          ,LBSTRT(2,200),LBFNSH(2,200),LDSTRT(2,200)
     2          ,LFSTRT(2,200),LFFNSH(2,200),LVEHC(200)
     3          ,LTOTF(200),LUNIF(200),LLNO(4,200)
     4          ,LJT(4,200),LNUMO(200),NNUMO(50),ISIZES(15)
     5          ,NSTAGE(50),KLIST(50),LPLOT(240),LFUDG(4,200)
     6          ,IPTOUT(12000),IMARK(11)
     7          ,LDFNSH(2,200),LSATF(200),LENTF(4,200)
      COMMON STPEN,RUNTIM,VEHKMS,WGHT,CONV1,CONV5,CONV6
     1       ,CONV7,CONV8,CONVA,CONVB,CONVC,DST,DFN,STOPP
     2       ,TIM,OLDPI,PINDEX,PA,PB,PC,TOTRT,TVK,BUSRT
     3       ,BVK,NLIST,LNUM,ICARD,IFAULT,ITLE,NPN,MFAULT
     4       ,NFAULT,IEND,IL,IP,ISTEPS,INODES,ILINKS
     5       ,ISTLST,INODC,IV,NOSE,NOSL,NPLTS,ICYCLE
     6       ,NLINK,NBIAS,NMIN,LOUTN,LBSTRT,LBFNSH
     7       ,LDSTRT,LDFNSH,LFSTRT,LFFNSH,LVEHC,LSATF
     8       ,LTOTF,LUNIF,LLNO,LENTF,LJT,LNUMO,NNUMO
     9       ,ISIZES,IMARK,NSTAGE,KLIST,LPLOT,LFUDG,WR11
      COMMON/BLKA/NR1(200),NART,LO(20),NN(20),LN(20,16)
      COMMON/BLKB/EGS
      DIMENSION Y(15),Z(15),T(15),TB(15),R(15)
      DIMENSION DLC(15),UC(15),TH(15),AL(15),EGS(15)
      WRITE(11,789)
      DO 777 J=1,NART
      EGS(J)=0.0
      READ(12,/)EGS(J)
  777 CONTINUE
  789 FORMAT(" INSERT 0.0--1.0 EXCESS GREEN SHIFT FOR"/
     1"EACH VEIN 1 LINE AT A TIME")
      IP=1
      IL=1
      NOSE=0
      NOSL=0
      XC=ISTEPS
      CL=ICYCLF
      IF(IMARK(1).NE.10)GO TO 400
C-     THE TRAFFIC PATTERNS, DELAYS, ETC FOR THE INITIAL
```

Figure B.4 OFFSET Listing

```
C-      SETTINGS ARE CALCULATED AND THE SIGNAL AND LINK
C-      DETAILS ARE OUTPUT.
      J=IMARK(6)
      IF(J.EQ.0)GO TO 5
      MFAULT=0
      IL=0
      CALL SUBPT(IPTOUT,RKA,RKB,RKC,RKD,RKE)
      IF(J.EQ.1)GO TO 5
      IV=1
      IF(WR11.EQ.3)IV=3
      NFAULT=0
      CALL TOUTP(RKA,RKB,RKC,RKD,RKE)
    5 NOSE=0
      NOSL=0
      MFAULT=0
      CALL SUBPT (IPTOUT,RKA,RKB,RKC,RKD,RKE)
      IV=1
      IF(WR11.EQ.3)IV=3
      NFAULT=0
      CALL TOUTP (RKA,RKB,RKC,RKD,RKE)
  400 CONTINUE
C-      CALC NEW OFFSETS FOR EACH NODE & ADJUST LINK GREENS.
      M=0
      IND=0
  509 M=M+1
      N=NN(M)
      TN=1800*N
      P=0
      PBR=0
      IF(LO(M).GE.5)GO TO 550
C-      SET UP FOR ONE-WAY STREET.
      I=5-LO(M)
      J=0
  520 J=J+1
      NLN=LN(M,J)
      NA=10*NLN+I-1
      DO 521 IA=1,ILINKS
      IF(NA.EQ.LNUM(IA))GO TO 522
  521 CONTINUE
  522 IF(J.EQ.N)GO TO 524
      NA2=10*LN(M,J+1)+I-1
      DO 523 IB=1,ILINKS
      IF(NA2.EQ.LNUM(IB))GO TO 526
  523 CONTINUE
  526 T(J)=CONV1*AVE(LJT,IB)
  524 RR=NR1(IA)
      R(J)=RR*CONVA
      IF(J.LT.N)GO TO 520
      G=1.-R(1)
      DO 41 J=2,N
```

Figure B.4 (cont'd.)

```
      XG=1.-R(J)
      IF(G.GT.XG)G=XG
   41 CONTINUE
      N2=N-1
      GO TO 916
C-     SET UP FOR TWO-WAY STREET.
  550 I=7-LU(M)
      J=0
  610 J=J+1
      NLN=LN(M,J)
      IF(J.EQ.1.AND.LN(M,J).GT.LN(M,J+1))I=I+2
      NAP=10*NLN+I-1
      IF(J.EQ.1)KI=ISIGN(2,LN(M,J+1)-LN(M,J))
      DO 611 IA=1,ILINKS
      IF(NAP.EQ.LNUM(IA))GO TO 612
  611 CONTINUE
  612 PBR=PBR+LTOTF(IA)
      NA=NAP+KI
      DO 613 IB=1,ILINKS
      IF(NA.EQ.LNUM(IB))GO TO 614
  613 CONTINUE
  614 P=P+LTOTF(IB)
      NA2=0
      IF(J.EQ.N)GO TO 615
      NA2=10*LN(M,J+1)+KI+I-1
      DO 616 IE=1,ILINKS
      IF(NA2.EQ.LNUM(IE))GO TO 617
  616 CONTINUE
  617 T(J)=CONV1*AVE(LJT,IE)
      TB(J)=CONV1*AVE(LJT,IA)
  615 RR=NR1(IB)
      R(J)=RR*CONVA
      IF(J.LT.N)GO TO 610
      PBR=PBR/TN
  621 P=P/TN
      N2=N-1
C-     CALC Y(I) & Z(I) FOR EACH SIGNAL.
      Y(1)=0.
      Z(1)=0.
      DO 10 I=2,N
      IF(LU(M).LE.4)TB(I-1)=0.
      DX=.5*(T(I-1)+TB(I-1))/CL
      Y(I)=Y(I-1)+DX-.5*(R(I)-R(I-1))
      DXX=.5*(T(I-1)-TB(I-1))/CL
   10 Z(I)=Z(I-1)+DXX
C-     CALC MAX EQUAL BANDWIDTH.
      CB=-1.1
      DO 20 I=1,N
      SB=1.1
      J=0
```

Figure B.4 (cont'd.)

```
   30 J=J+1
      YY=Y(J)-Y(I)
      U0=1.-SCAL(YY,1.)
      YY=Y(J)-Y(I)-.5
      U5=1.-SCAL(YY,1.)
      U0R=U0-R(J)
      U5R=U5-R(J)
      IF(U0R.LT.U5R)GO TO 3
      TH(J)=0.
      AL(J)=U0
      D=U0R
      GO TO 4
    3 TH(J)=0.5
      AL(J)=U5
      D=U5R
    4 IF(D.LT.SB)SB=D
      IF(J.LT.N)GO TO 30
      IF(SB.LE.CB)GO TO 20
      CB=SB
      KC=I
      DO 21 J=1,N
      DLC(J)=TH(J)
   21 UC(J)=AL(J)
   20 CONTINUE
      IF(CB.LT.0)CB=0.
      CB2=2.*CB
      BS=CB
      BBS=CB
C-     CALC MAX EQUAL BANDWIDTH SYNCHRONIZATION.
      DO 35 J=1,N
      ZZ=Z(J)-Z(KC)+DLC(J)
   35 TH(J)=SCAL(ZZ,1.)
C-     CALC MIN GREEN.
      G=1.-R(1)
      DO 40 I=2,N
      XG=1.-R(I)
      IF(G.GT.XG)G=XG
   40 CONTINUE
      PPB=P+PBR
      IF(PBR-P)45,105,70
C-     CALC ADJUSTMENTS FOR INBOUND LT OUTBOUND.
   45 IF(PPB.GT.CB2)GO TO 50
      BS=AMIN1(G,CB2*P/PPB)
      GO TO 60
   50 IF(P.GE.CB2)GO TO 55
      BS=AMIN1(G,P)
      GO TO 60
   55 BS=G
   60 DO 65 J=1,N
   65 AL(J)=AMAX1(UC(J)-1.+BS-CB,0.)
```

Figure B.4 (cont'd.)

```
      BBS=AMAX1(CB2-BS,0.)
      IF(LU(M).LE.4)BBS=0.
      GO TO 95
C-     CALC ADJUSTMENTS FOR INBOUND GT OUTBOUND.
   70 IF(PPB.GT.CB2)GO TO 75
      BBS=AMIN1(G,CB2*PBR/PPB)
      GO TO 85
   75 IF(PBR.GE.CB2)GO TO 80
      BBS=AMIN1(G,PBR)
      GO TO 85
   80 BBS=G
   85 DO 90 J=1,N
   90 AL(J)=AMAX1(BBS+R(J)-UC(J),0.)
      BS=AMAX1(CB2-BBS,0.)
   95 AL(KC)=0.
      DO 100 J=1,N
      YY=TH(J)-AL(J)
  100 TH(J)=SCAL(YY,1.)
  105 CONTINUE
C-     MAKE EXCESS GREEN ADJUSTMENTS TO OFFSETS.
      DO 880 J=1,N
      AJ=J-KC
      TC=0.
      J1=J
      J2=KC-1
      IF(J-KC)883,879,884
  884 J1=KC
      J2=J-1
  883 DO 882 JJ=J1,J2
  882 TC=TC+I(JJ)
  879 TC=TC/CL
      GC=TH(J)-.5*(R(KC)+R(J))-BS-SIGN(TC,AJ)
      GCU=1.-R(J)-BS
      GC=SCAL(GC,1.)
      TCB=0.
      IF(J.EQ.KC)GO TO 878
      DO 832 JJ=J1,J2
  832 TCB=TCB-TB(JJ)
  878 TCB=TCB/CL
      GCB=TH(J)+.5*(R(KC)-R(J))+SIGN(TCB,AJ)
      GCBU=1.-R(J)-BBS
      GCB=SCAL(GCB,1.)
      BC=AMIN1(GC,GCB)
      TH(J)=TH(J)-EGS(M)*SIGN(BC,AJ)
      IF(TH(J).LT.0.)TH(J)=TH(J)+1.
  880 TH(J)=TH(J)*XC+.5
C-     SET UP INTERFACE FROM OFFSETS TO NBIAS(*,*).
  916 T1=0.
      DO 907 J=1,N
      IF(M.EQ.1.AND.J.EQ.1)DEL=0.
```

Figure B.4 (cont'd.)

```
      IF(J.GT.1)GO TO 926
      IF(M.GT.1)GO TO 907
      NS=DEL+.5
      GO TO 901
  926 IF(LO(M).GE.5)GO TO 927
      T1=T1+T(J-1)/CL
      ES=(1.-EGS(M))*(1.-R(J)-G)
      NS=(T1+R(J)-R(1)+DEL+ES)*XC+.5
      GO TO 901
  927 YY=TH(J)-TH(1)
      NS=YY+(.5*(R(J)-R(1))+DEL)*XC+.5
  901 NS=SCAL(NS,ISTEPS)
      NLN=LN(M,J)
      DO 770 KKK=1,INODES
      IF(NLN.EQ.NLIST(KKK))GO TO 771
  770 CONTINUE
  771 IF(LO(M).LE.4)GO TO 911
      I=1
      IF(LO(M).EQ.5)I=2
  911 NA=10*NLN+I-1
      DO 908 IA=1,ILINKS
      IF(NA.EQ.LNUM(IA))GO TO 909
  908 CONTINUE
  909 JB=LBSTRT(1,IA)
      JBB=LBFNSH(1,IA)
      NF=NBIAS(JBB,KKK)-NBIAS(JB,KKK)
      NBIAS(JB,KKK)=NS
      A=NS
      NF=NF+NS
      NF=SCAL(NF,ISTEPS)
      NBIAS(JBB,KKK)=NF
      IF(M.EQ.NART)GO TO 907
      IF(NLN.EQ.LN(M+1,1))XG=A*CONVA-R(J)
      IF(M.EQ.NART-1)GO TO 907
      DO 887 L=2,NART-M
      IF(NLN.NE.LN(M+L,1))GO TO 887
      XG2=A*CONVA-R(J)
      IND=M+L
      GO TO 907
  887 CONTINUE
  907 CONTINUE
      DEL=XG
      IF(IND.EQ.0)GO TO 700
      IF(M.EQ.IND-1)DEL=XG2
  700 IF(M.LT.NART)GO TO 509
C-     OUTPUT FOR NEW SIGNAL TIMINGS.
      MFAULT=0
      IL=1
      CALL SUBPT(IPTOUT,RKA,RKB,RKC,RKD,RKE)
      IV=1
```

Figure B.4 (cont'd.)

```
      IF(WR11.EQ.3)IV=3
      ISTLST=2
      NFAULT=ISTLST
      CALL TOUTP(RKA,RKB,RKC,RKD,RKE)
C-     FURTHER COPIES OF THE FINAL OUTPUT ARE PRINTED
C-     IF SPECIFIED BY THE CONTENTS OF IMARK(9).
      IF(IMARK(9).LT.2.OR.IMARK(9).GT.6)GO TO 201
      IY=IMARK(9)-1
      DO 309 IZ=1,IY
      CALL TOUTP (RKA,RKB,RKC,RKD,RKE)
  309 CONTINUE
  201 IF(NPLIS.EQ.0)GO TO 202
      CALL SPLOT (IPTOUT)
  202 RETURN
      END


      FUNCTION SCAL(A,X)
C-     THIS FUNCTION SCALES (A) BY (X) SUCH THAT
C-     (A) LIES BETWEEN 0.0 AND (X).
      SCAL=A
   11 IF(SCAL.GE.0.)GO TO 12
      SCAL=SCAL+X
      GO TO 11
   12 IF(SCAL.LT.X)RETURN
      SCAL=SCAL-X
      GO TO 12
      RETURN
      END


      FUNCTION AVE(X,K)
C-     THIS FUNCTION AVERAGES THE X(*,K) VECTOR COMPONENTS.
      DIMENSION X(4,200)
      COUNT=0.
      AVE=0.
      DO 1 I=1,4
      IF(X(I,K).EQ.0.)GO TO 1
      COUNT=COUNT+1.
      AVE=AVE+X(I,K)
    1 CONTINUE
      IF(AVE.EQ.0.)RETURN
      AVE=AVE/COUNT
      RETURN
      END
```

Figure B.4 (cont'd.)

BIBLIOGRAPHY

BIBLIOGRAPHY

(AL1) Allsop, R.E., "Selection of Offsets to Minimize Delay to Traffic in a Network Controlled by Fixed-Time Signals," Transportation Science, 1 (1967), 1-13.

(AL2) Allsop, R.E., Optimization Techniques for Reducing Delay to Traffic in Signalized Road Networks, Ph.D. Thesis, University College, London, 1970.

(CR1) Cronk, D.L., "Modern Highways News Report," Rural and Urban Roads, (February 1974), 9.

(DR1) Drew, D.R., Traffic Flow Theory and Control, McGraw-Hill, Inc., 1968.

(GA1) Gartner, N., "Microscopic Analysis of Traffic Flow Patterns for Minimizing Delay on Signal-Controlled Links," Highway Research Board, Record No. 445, (1973), 12-23.

(GL1) Gartner, N., Little, J.D.C., "Generalized Combination Method for Area Traffic Control," Transportation Research Board, Record No. 531, (1975), 58-69.

(GW1) Gerlough, D.L., Wagner, F.A., "Improved Criteria for Traffic Signals at Individual Intersections," National Cooperative Research Program, 32(1967).

(HI1) Hillier, J.A., "Appendix to Glasgow's Experiment in Area Traffic Control," Traffic Engineering and Control, 7, 9, (1966), 569-571.

(IN1) Inose, H., Fujisaki, H., Hamada, T., "A Road Traffic Control Theory Based on a Macroscopic Traffic Model," J.I.E.E., 87, 8, (1967), 55-67.

(KP1) Kaplan, J.A., Powers, L.D., "Results of SIGOP-TRANSYT Comparison Studies," Traffic Engineering, (September 1973), 17-23.

(KR1) Kreer, J.B., "Factors Affecting the Relative Performance of Traffic Responsive and Time-of-Day Traffic Signal Control," Transportation Research, Vol. 10, (1976), 75-81.

(LM1) Little, J.D.C., Martin, B.V., and Morgan, J.T., "Synchronizing Traffic Signals for Maximal Bandwidth," Highway Research Board, Record No. 118, (1966), 21-47.

(LW1) Lieberman, Edward B., Woo, James L., "SIGOP II: A New Computer Program for Calculating Optimal Signal Timing Patterns," Transportation Research Record, Record No. 596, (1976), 16-21.

(MH1) Munjal, P.K., Hsu, Y.S., "Comparative Study of Traffic Control Concepts and Algorithms," Highway Research Board, Record No. 409, (1972), 64-80.

(MW1) Messer, Carroll J., Whitson, Robert H., Dudek, Conrad L., and Romano, Elio J., "A Variable-Sequence Multiphase Progression Optimization Program," Transportation Research Board, Record No. 445, (1973), 24-33.

(OL1) Olmstead, J.M.H., Advanced Calculus, New York: Appleton-Century-Crafts, Inc., 1961.

(PA1) Panyan, W.D., Urban Traffic System Simulation and Control, Ph.D. Thesis, Michigan State University, 1969.

(RO1) Robertson, D.I., "TRANSYT: A Traffic Network Study Tool," Transport and Road Research Laboratory, TRRL Report LR-253, (1969).

(RO2) Robertson, D.I., "TRANSYT Method for Area Control Program-Manual," Transport and Road Research Laboratory, NTIS PB-224 084, (August 1972).

(SE1) Seddon, P.A., "The Prediction of Platoon Dispersion in the Combination Methods of Linking Traffic Signals," Transportation Research, 6, (June 1972), 125-130.

(TR1) "SIGOP: Traffic Signal Optimization Program, A Computer Program to Calculate Optimum Coordination in a Grid Network of Synchronized Traffic Signals," Traffic Research Corp., New York, (1966).

(WA1) Wagner, F.A., et al., "Improved Criteria for Traffic Signal Systems on Urban Arterials," National Cooperative Research Program, 73, (1969).

(WE1) Webster, F.V., "Traffic Signal Settings," Road Research Laboratory, Technical Paper 39, London, (1958).